

The University of Maine

DigitalCommons@UMaine

Electronic Theses and Dissertations

Fogler Library

Fall 12-16-2022

Operation and Preliminary Energy Balance of a Portable Kelp Dryer in Maine

Tuqa Al-Asadi

University of Maine, tuqa86h@gmail.com

Follow this and additional works at: <https://digitalcommons.library.umaine.edu/etd>



Part of the [Process Control and Systems Commons](#), [Thermodynamics Commons](#), and the [Transport Phenomena Commons](#)

Recommended Citation

Al-Asadi, Tuqa, "Operation and Preliminary Energy Balance of a Portable Kelp Dryer in Maine" (2022). *Electronic Theses and Dissertations*. 3739.

<https://digitalcommons.library.umaine.edu/etd/3739>

This Open-Access Thesis is brought to you for free and open access by DigitalCommons@UMaine. It has been accepted for inclusion in Electronic Theses and Dissertations by an authorized administrator of DigitalCommons@UMaine. For more information, please contact um.library.technical.services@maine.edu.

**OPERATION AND PRELIMINARY ENERGY BALANCE OF A PORTABLE KELP
DRYER IN MAINE**

By

Tuqa H. Al-Asadi

B.S. University of Basrah, 2008

A THESIS

Submitted in Partial Fulfillment of the

Requirements for the Degree of

Master of Science

(in Chemical Engineering)

The Graduate School

The University of Maine

December 2022

Advisory Committee:

Peter van Walsum, Associate Professor of Chemical Engineering, Advisor

Adriaan R. P. van Heiningen, Professor, J. Larcom Ober Chair of Chemical Engineering

Jennifer J. Perry, Associate Professor of Food Microbiology

THESIS ACCEPTANCE STATEMENT

On behalf of the Graduate Committee for Tuqa H. Al-Asadi I affirm that this manuscript is the final and accepted thesis. Signatures of all committee members are on file with the Graduate School at the University of Maine, 42 Stodder Hall, Orono, Maine.

Peter van Walsum, Professor of Chemical Engineering , 2022

© 2022 Tuqa H. Al-Asadi

All Rights Reserved

LIBRARY RIGHTS STATEMENT

In presenting this dissertation in partial fulfillment of the requirements for an advanced degree at The University of Maine, I agree that the Library shall make it freely available for inspection. I further agree that permission for "fair use" copying of this dissertation for scholarly purposes may be granted by the Librarian. It is understood that any copying or publication of this dissertation for financial gain shall not be allowed without my written permission.

Signature: _____

Date: _____

OPERATION AND PRELIMINARY ENERGY BALANCE OF A PORTABLE KELP DRYER IN MAINE

By Tuqa Al-Asadi

Thesis Advisor: Dr. Peter van Walsum

An Abstract of the Thesis Presented
In Partial Fulfillment of the Requirements for the
Master of Science
(in Chemical Engineering)
December 2022

Seaweed (macroalgae) is a marine resource that has a high economic value. Seaweeds are important commodities as raw material for food or additives and as a source of biomass. One popular species of seaweed is Sugar kelp (*Saccharina latissima*) – a brown algae that is native to the Maine coast and also a commonly farmed species. It is a rich source of fibers, vitamins, minerals, and antioxidants. Seaweeds are highly perishable due to their high moisture content and will spoil quickly if not preserved, therefore a common practice is to dry the product to prolong storage life and to minimize the cost for transportation. A drying method using warm (not hot) air will extend seaweed shelf life and also retain many of the valuable bioactive components that are heat and/or UV sensitive. Thus, a controlled drying environment can best retain product and nutritional value and prevent degradation of the food quality.

A first of a kind drying system with controlled temperature, air flow and exit humidity has been developed and assembled in the advanced manufacturing center (AMC) at the University of Maine. The drying system is built within a 40-foot-long shipping container.

Inside the container, the seaweed is suspended from an oval shaped overhead conveyor system, where it slowly rotates around the length of the chamber. A utility room at one end of the container houses two parallel propane powered heaters with integral blowers, an exhaust fan and a control system.

My project is looking at examining the drying time, the temperature and humidity within the drying process, the drying rate, and energy efficiency of the process. Several experiments were run during early and late springtime 2020 using wet towels or fresh Sugar kelp in the dryer. The drying system is equipped with five temperature and humidity sensors which logged data every 0.5 seconds. Examination of the drying runs shows that as air passes through the drying chamber it decreases in temperature and gains humidity, as expected. It became apparent that partial recycling of the air was important for achieving high exit humidity and lower energy cost. In early runs, the data showed that air was short circuiting through the dryer and circumventing the hanging material being dried. This flaw was partly resolved by adding some sheeting at the top of the conveyor and partially blocking two ventilation ports. We also noted that the temperature measurement of the incoming air was being affected by the level of recycle and furnace activity. It can also be seen that through the duration of the drying work, the exiting air shows a steady trend of rising temperature and decreasing RH.

Analysis of the energy dynamics for the system shows that more data are needed to consistently close the energy balance, particularly with respect to metering the propane used, determining the temperatures of different surfaces of the dryer, the rate of air flow into and out of the system, as well as weather conditions, insolation rate and orientation to the sun. Estimated values for these variables suggest that insulating the walls of the container, except on bright sunny days, will likely be cost effective.

DEDICATION

I dedicate this work to my wonderful husband and deepest love, Firas Mahyob, who has been a constant source of support and encouragement during the challenges of this journey.

Also, I would like to dedicate my work to my three angels Malath, Zulfa and Mousa who give me the courage and power to succeed.

ACKNOWLEDGMENT

First and foremost, I would like to express my deep and sincere gratitude to my research supervisor, Peter Van Walsum, for giving me the opportunity to do research and providing invaluable guidance throughout this research. It was a great privilege and honor to work under his guidance. I am grateful for the help and care during the pandemic time, without his guidance and perseverance my thesis would not have been possible.

I would like to express my thanks to my committee members Dr. Adriaan van Heiningen and Dr. Jennifer Perry for their encouragement and support. Also, I would like to thank Dr. Bousfield for accepting and welcoming me through the graduate program.

Furthermore, I would like to thank the AMC team, especially Bradly, for their support. Also, I would like to thank my friends and colleagues who helped me through my studies.

I would like to thank Dr. Hemant Pendse for financial support during this journey.

I would like to thank the OIP staff, especially Sarah, Orlina and Mireille, for their love, care, and support through this hard work.

I would like to thank my teachers at Eastern Maine Community College (EMCC) for guiding me through this path.

I would like to express my deepest appreciation to our wonderful friends the Hasbrouck family, Hildebrand family, Quirk family and Stoner family for all the love, kindness, and support throughout our journey. You were truly friends during the tough time.

Furthermore, I am extremely grateful to my friend Nancy for the wonderful friendship. I really appreciate all the messages that were sent to me asking about me and my family. Thank you for sharing the beautiful time with me.

I am deeply indebted to my closest friend Sally. Sally, there is no word that can describe you and what you have done for me and my family. Sally, you are more than our friend. Thank you for all the kindness, love, encouragement, and support. Thank you for all the advice. Thank you for taking care of my children during my giving birth. Thank you for being a part of our family.

I am also grateful to my parents (mom, dad, and brothers), who have always loved me unconditionally and for supporting me through this journey. Also, a special thanks to my wonderful second family, (my father-in-law, my mother-in-law and my sister-in-law) for all love, care, and support.

Most importantly, I am extremely grateful to the person who makes me to be in now my sweet and loving husband Firas Mahyob who supported me emotionally and psychologically with motivating words during my tough time. Thank you for being my shoulder to lean. Thank you for making my dreams come true. Thank you for all the beautiful time, for taking care of the children during my studies and during my pregnancy. Thank you for making me believe in myself. Thank you for all the love, patience, care, and trust during this journey. Also, a special thanks to my sweet, wonderful children Malath, Zulfa and Mousa for being such good children and self-dependent and helping me through the house cleaning. I am sorry that I did not spend too much time with you during my studies, but I promise you I will give you more time in the next chapter of my life.

Above all, I thank Allah for making everything possible.

TABLE OF CONTENTS

DEDICATION	vii
ACKNOWLEDGEMENTS	viii
LIST OF TABLES	xiii
LIST OF FIGURES	xiv
Chapter	
1 INTRODUCTION	1
1.1 Motivation and Project Objectives.....	1
1.2 Seaweed	2
1.3 History of Seaweed, Health Beneficial Effects and Industry Uses.....	4
1.4 History of Drying of Seaweed	7
1.5 Effect of Drying Treatments on Nutrient Composition and Properties of Seaweed	10
1.6 Seaweed Drying Kinetics.....	12
1.7 Simulation and Modeling of Seaweed Drying (Energy Balances)	13
2 METHODOLOGY	14

2.1 Parameters for a Seaweed Dryer: Size, Internal Configuration, Unit Mobility, Energy Sources	14
2.2 Dryer Design.....	16
2.2.1 The Drying Chamber	16
2.2.2 The Control Room	19
2.2.3 The PLC Logic and Data Logging.....	22
2.3 Seaweed Handling	23
2.4 Hanger Types	28
2.4.1 Regular Clothes Hangers	28
2.4.2 Custom Seaweed Hangers.....	28
2.5 Seaweed Drying Process.....	30
2.6 Energy Balance Calculations	32
2.6.1 Heating and Evaporation Calculations.....	33
2.6.2 Fan and Air Flow Calculation.....	34
2.6.2.1 Mass Balance Results	34
2.6.2.2 Energy Balance Results	35
2.6.3 Heat Loss Through the Walls of Dryer Calculations.....	36
2.6.4 Solar Energy Calculations.....	37
2.6.5 Energy Modeling of The Dryer Using Aspen Plus.....	38

2.6.5.1 Aspen Simulation of Seaweed Throughput prediction and Energy Cost	38
2.6.5.2 Furnaces and Fans Effects on Energy Balance	40
2.6.5.3 Weather Effects (Temperature and RH of Ambient Air and Solar Energy)	41
3 RESULTS AND DISCUSSIONS	43
3.1 Design and Assembly of The Dryer.....	43
3.1.1 Temperature	43
3.1.2 Mobile Unit.....	44
3.1.3 Avoiding Stickiness of Seaweed.....	45
3.1.3.1 Hanger System	45
3.1.3.2 Conveyor.....	45
3.1.3.3 Hanger Design	46
3.1.4 Loading and Unloading.....	48
3.1.5 Solar Energy.....	48
3.1.6 Insulation.....	49
3.1.7 Heat Pump vs Furnace	50
3.1.8 Air Flow Velocity	51
3.1.9 Recycling Air.....	51

3.1.10 Dryer Control System	52
3.1.11 Volume of the Cabinet and The Dryer.....	53
3.2 Initial Test Run Results.....	54
3.3 Modifications to Control Logic Simulation and Modeling.....	57
3.4 Mass of water evaporated calculation.....	57
3.5 Seaweed Drying Runs.....	60
3.6 Seaweed Drying Data	62
3.6.1 EasyLog USB Data	62
3.6.2 Infrared (IR) Camera Data	68
3.7 Aspen Simulation of The Dryer: Input Air, Output Air, Short Circuiting	71
3.7.1 Aspen Simulation of Seaweed Throughput Prediction and Energy Cost.....	71
3.7.2 Furnaces and Fans Effects on Energy Balance	74
4 CONCLUSIONS AND FUTURE WORK	77
4.1 Conclusions.....	77
4.2 Future Work	79
REFERENCES	80
APPENDICES	88

Appendix A. Supplemental Data from Aspen Simulations	88
Appendix B. Kelp Dryer Operations Guide.....	102
Appendix C. Calculations	117
Appendix D. Comparison Between Praveen Cabinet and Tuqa Dryer.....	121
BIOGRAPHY OF THE AUTHER	122

LIST OF TABLES

Table 3.1 Mass of water evaporation during drying process	58
Table 3.2 Mass balance calculation of the fan system.....	60
Table C.1 Mass of seaweed calculations during drying process	117
Table C.2 Calculation of the mass of water evaporated at each cycle.....	117
Table C.3 Calculation of the mass of water evaporated at each cycle after adding an imaginary cycle	117
Table C.4 Calculation of fan energy by using energy balance	118
Table C.5 Temperatures of different location of the dryer	118
Table C.6 Calculation of fan energy by using mass balance	118
Table C.7 Calculation of energy loss	119
Table C.8 Calculation of energy loss through the wall without insulation.....	119
Table C.9 Calculation of energy loss through the wall.....	119
Table C.10 Calculation of energy loss through the wall without insulation.....	120

LIST OF FIGURES

Figure 1.1: Sugar Kelp (<i>Saccharina Latissima</i>) grown in the Gulf of Maine. Image adapted from Gulf of Maine Research Institute website – Maine Growing Kelp.....	3
Figure 2.1: Overall kelp dryer model with drying chamber and utility room.....	15
Figure 2.2: The portable kelp dryer to serve the drying process	15
Figure 2.3: The drying chamber (from the loading entrance).....	16
Figure 2.4: Continuously rotating conveyor	17
Figure 2.5: Intake and exhaust vents of duct system on the exterior of container.....	17
Figure 2.6: The Inlet and exit air ducts suspended from the top of the drying chamber... ..	18
Figure 2.7: The control panel and the heaters in the control room	19
Figure 2.8: The Screen monitor interface (UI) and the navigation bar.....	20
Figure 2.9: System status screen in the control panel during running the dryer.....	20
Figure 2.10: The main operating panel and the electricity	21
Figure 2.11: The emergency switch.....	21

Figure 2.12: The control panel and the PLC.....	22
Figure 2.13: Transfer the kelp from the farm to the dryer	23
Figure 2.14: Wet sugar kelp laid out to be attached to a custom seaweed hanger.....	24
Figure 2.15: The method of weighing the wet seaweed before the drying.....	25
Figure 2.16: Wet kelp in the drying chamber to start the drying process	25
Figure 2.17: The dried seaweed with the hanger in container to weigh them.....	27
Figure 2.18: The dried seaweed collected in tote containers to send to the food science department	27
Figure 2.19: The regular clothes hangers with pegs to secure the kelp during drying.....	29
Figure 2.20: Model of stainless-steel hanger assembly	30
Figure 2.21: Process flow sheet for calculating energy balance calculations on differing ambient temperature and humidity conditions.....	39
Figure 2.22: The new simulation that represents of weather effects on the drying process as well as the interior recycle and unsaturated performance through the dryer	40
Figure 3.1: Constructed hanger assembled on conveyor track attachment.....	47

Figure 3.2: Control flowchart	53
Figure 3.3: The wet towels during testing of kelp dryer.....	55
Figure 3.4: Water evaporated mass of seaweed during drying process	58
Figure 3.5: Drying rate of seaweed drying process varies with the time.....	59
Figure 3.6: Graph represents temperature varies with time during June 8 seaweed experiment	61
Figure 3.7: Graph represents RH varies with time during June 8 seaweed experiment	61
Figure 3.8: The temperature of the intake and exhaust air duct that varies with time.....	63
Figure 3.9: The relative humidity of the intake and exhaust air duct that varies with time.....	63
Figure 3.10: Represents the temperature of four loggers that were set at different locations of the south and north wall of the dryer that varies with the time.....	65
Figure 3.11: Represents the Relative humidity of four loggers that were set at different locations of the south and north wall of the dryer that varies with the time	65
Figure 3.12: Represents the temperature of the four loggers that were set at different locations inside the chamber that varies with the time	67
Figure 3.13: Represents the relative humidity of the four loggers that were set at different locations inside the chamber that varies with the time.....	67

Figure 3.14: Shows simultaneous data from the different sources: the IR camera (South wall mid, End south wall mid), the control system of the dryer (Fresh vent T, Warm T), and the small loggers (logger 2, logger 3). These data were collected during cloudy weather	69
Figure 3.15: Shows simultaneous data from the different sources: the IR camera (South wall mid, End south wall mid), the control system of the dryer (Fresh vent T, Warm T), and the small loggers (logger 2, logger 3). These data were collected during sunny weather	69
Figure 3.16: The comparison between the cloudy and sunny weather	70
Figure 3.17: Responses of dryer performance (heated and outlet air temperatures, mass throughput, electricity, fuel, and total energy costs) versus ambient inlet air temperature at 50% RH	72
Figure 3.18: Trends of energy costs (Fan electricity, heater fuel and combined) with respect to ambient air RH at ambient air temperature of 10°C	73
Figure 3.19: Responses of dryer performance (heated and outlet air temperatures, mass throughput, electricity, fuel, and total energy costs) versus ambient inlet air temperature at 50% RH	76
Figure A.1: Responses of dryer performance (heated and outlet air temperatures, mass throughput, electricity, fuel, and total energy costs) versus ambient inlet air temperature at 0% RH	88

Figure A.2: Responses of dryer performance (heated and outlet air temperatures, mass throughput, electricity, fuel, and total energy costs) versus ambient inlet air temperature at 25% RH.....89

Figure A.3: Responses of dryer performance (heated and outlet air temperatures, mass throughput, electricity, fuel, and total energy costs) versus ambient inlet air temperature at 75% RH.....90

Figure A.4: Responses of dryer performance (heated and outlet air temperatures, mass throughput, electricity, fuel, and total energy costs) versus ambient inlet air temperature at 100% RH.....91

Figure A.5: Responses of dryer performance (heated and outlet air temperatures, mass throughput, electricity, fuel, and total energy costs) versus ambient inlet air temperature at 0% RH.....92

Figure A.6: Responses of dryer performance (heated and outlet air temperatures, mass throughput, electricity, fuel, and total energy costs) versus ambient inlet air temperature at 25% RH.....93

Figure A.7: Responses of dryer performance (heated and outlet air temperatures, mass throughput, electricity, fuel, and total energy costs) versus ambient inlet air temperature at 75% RH.....94

Figure A.8: Responses of dryer performance (heated and outlet air temperatures, mass throughput, electricity, fuel, and total energy costs) versus ambient inlet air temperature at 100% RH.....95

Figure A.9: Trends of energy costs (Fan electricity, heater fuel and combined) with respect to ambient air RH at ambient air temperature of 0°C.....96

Figure A.10: Trends of energy costs (Fan electricity, heater fuel and combined)

with respect to ambient air RH at ambient air temperature of 5°C.....	97
Figure A.11: Trends of energy costs (Fan electricity, heater fuel and combined)	
with respect to ambient air RH at ambient air temperature of 15°C.....	98
Figure A.12: Trends of energy costs (Fan electricity, heater fuel and combined)	
with respect to ambient air RH at ambient air temperature of 20°C.....	99
Figure A.13: Trends of energy costs (Fan electricity, heater fuel and combined)	
with respect to ambient air RH at ambient air temperature of 25°C.....	100
Figure A.14: Trends of energy costs (Fan electricity, heater fuel and combined)	
with respect to ambient air RH at ambient air temperature of 30°C.....	101

CHAPTER 1

INTRODUCTION

1.1 Motivation and Project Objectives

This research project is focused on designing and studying the performance of a transportable seaweed dryer in terms of temperature and humidity within the dryer, drying rate, and efficiency of the process. Historically, most seaweed in the US was collected from the wild. With its nutritional attributes, interest in seaweed as health food is growing in the US, especially when coming from clean Maine waters. Meanwhile, technology for farming seaweeds is developing and increasing numbers of people are interested in starting up seaweed farms compared to wild harvesting. Farming seaweed results in larger harvests over shorter harvest seasons, and preservation of the crop becomes a bottleneck in post-harvest processing.

Current drying methods include open air drying and greenhouse drying, both of which are weather dependent and provide little control over the drying conditions, which can diminish nutritional properties of the seaweed. Thus, this project seeks to help small scale kelp farmers looking for quality drying capability. Our dryer is designed to offer good control over the drying conditions, and since it is transportable, groups of small farms or Coops could potentially share one drying system.

A prototype drying system with energy optimized temperature, air inflow and recirculation has been designed and assembled at UMaine. The system is packaged inside a 40-foot shipping container, in which the seaweed is suspended from an overhead conveyor system that slowly rotates inside the chamber.

A utility room at one end of the container contains the control system, propane powered air heaters and ventilation fans, while the other end of the container with the standard doors gives access to the drying chamber. The system is unique in that it is transportable, it features a hanging system that prevents the sticky kelp from binding to solid surfaces, and the air flow has controlled recycle to achieve higher energy efficiency by increasing the air retention time. The controlled drying environment provides conditions that are not too hot and protected from UV rays, which helps to retain product and nutritional value and prevents degradation of the food quality.

The main objectives of this study were: Testing the performance of the dryer system and improving and addressing defects in the design. Developing an Aspen Plus process modeling software program to simulate the energy flows of the real drying process of the sugar kelp.

1.2 Seaweed

Seaweed (macroalgae or sea vegetable) is a general term that refers to several algae and marine plants that grow in oceans, seas, and rivers. There are more than 15,000 species of seaweed around the world [23]. Seaweeds serve many ecological functions and are crucial primary producers in oceanic aquatic food webs. Most species are classified into different types of seaweed, including red (Rhodophyta), green (Chlorophyta), and brown (Phaeophyta), based on their pigmentation [1,5,6,15,19,39,41]. Seaweed has a highly variable composition, which depends on the species, time of collection, conditions such as water, temperature, light intensity and nutrient concentration in water” [36] The smallest seaweeds are only a few millimeters or centimeters in size, while the largest routinely grow to a length of 30 to 50 meters. Seaweeds are important commodities as raw material for food, food additives or as a source of biomass [2].



Figure 1.1: Sugar Kelp (*Saccharina Latissima*) grown in the Gulf of Maine. Image adapted from Gulf of Maine Research Institute website – Maine Growing Kelp.

Seaweed is a rich source of fiber, vitamins, minerals, amino acids, lipids, and antioxidants, all of which contribute to a healthy diet [3,4]. Freshly harvested seaweeds are highly perishable due to their high moisture content, especially the brown algae which has a moisture content up to 94% wet basis [8] and will spoil quickly if not preserved. Therefore a common practice is to dry product to prolong storage life and to minimize the cost for transportation. In Asia, the greatest seaweed consumption is of brown algae (66.5%), followed by red algae (33%) and then green (5%) algae [7,19]. Many of the brown algae are referred to simply as “Kelp”. *Saccharina latissima* is one popular species of brown seaweed that is native to the Maine coast and also a commonly farmed species, as shown in figure 1.1. “There are three commercially important kelp species in Maine: sugar kelp (*Saccharina latissima*), winged kelp (*Alaria esculenta*), and horsetail kelp (*Laminaria digitata*)” [20]. Farmed sugar kelp is grown on submerged horizontal long lines located in leased sea farms, from September to May, while the harvest season usually starts in April and continues through June. In the wild, sugar kelp can live for 2 to 4 years [1].

1.3 History of Seaweed, Health Beneficial Effects and Industry Uses

Today there is growing demand to produce more food in a sustainable way because of an expected increase of the world population to over 9 billion people within the next 40 years. Seaweeds are considered a promising resource for the sustainable production of food and animal feed. Historically, edible seaweed has been consumed by coastal populations around the world. Seaweeds have been a part of Chinese life as a human food since as far back as 2500 years ago [13,14]. Nowadays, many Asian countries such as China, Japan and Korea are consuming seaweed as a part of their daily diet [10]. Indonesia and Malaysia, with tropical climates, also consume fresh seaweeds, especially as salad components [11].

As people migrated from their original countries like China or Japan to settle in new countries, they brought this tradition of eating seaweeds to their settled countries such as in Europe and the USA, where the use of seaweed was not as familiar to people. Today, seaweed use has been growing, and improving seaweed processing has enabled increasing demand for seaweed. The Seaweed industry has been developed through the past several years in Europe. In France, the first step was introducing seaweeds in restaurant menus, which added some success to the European Cuisine [12].

In the US, California, and Hawaii both have a daily human consumption of seaweed, spurred on by many Japanese restaurant and markets have been opened around these regions. The seaweed markets are also growing on the east coast of US and Canada, in Maine, New Brunswick, and Nova Scotia [12]. A new seaweed industry has been born in these areas, and the demand for seaweed is growing, especially in regions known for clean, fresh waters. Other coastal regions such as Ireland, Portugal, Chile, and Denmark are showing increasing seaweed consumption in their daily diet [69].

Seaweeds are known as a rich source of vitamins, minerals, antioxidants, omega-3 fatty acids and essential trace elements, and raw materials for the pharmaceutical and cosmetics industry [9]. “The seaweed industry provides a wide variety of products that have an estimated total annual value of US\$ 5.5–6 billion” [12]. The use of seaweed in Asian cuisine is very well known, but seaweeds are attracting increasing attention elsewhere as a valuable food source.

Nowadays there is a big movement towards studying seaweed and its importance in our lives. Many studies show that the edible seaweeds provide a good source of protein and large amounts of vitamins such as A, C, D, E, B₁₂, B₁, Folic-acid, minerals such as Ca, Mg, Fe, K, P, I and Zn, antioxidants, lipids, dietary fiber as well as fatty acids [15-18,21,22,24]. Seaweed products can be consumed as food in different ways: Dried as in sushi, snacks, soups, tea, mustard, pasta, breads, or can be used either frozen or as a raw product such as in salads and even powder. Recently seaweed extract has been used as an additive for food or beverages. Many consumers prefer to use cosmetic products that have natural ingredients because it is safe to use on skin without any side effects. Therefore, Seaweed is one of the natural resources that has been a part of the cosmetic industry. Seaweed is rich with bioactivity with compounds such as phenolic compounds, polysaccharides, pigments, polyunsaturated fatty acids (PUFAs), sterols, proteins, peptides, and amino acids can be used as active ingredients in cosmetic products. Seaweed has an antimicrobial property that can be used in cosmetic products to prevent the spoilage of the product by killing the microorganism and to prolong the shelf life of the product. Microorganisms, especially fungi, could spoil the product [33].

Significant activity has been noticed applying the use of seaweed in the manufacture of cosmeceutical products such as anti-wrinkle, skin-whitening, UV protective, anti-inflammatory, and antiallergic applications [32].

These activities could be beneficial for the manufacture of cosmeceutical products, making use of polyphenolic compounds such as phlorotannins and flavonoids. Seaweed is a rich source of phycocolloids such as alginate, agar, and carrageenan. These are high-value seaweed hydrocolloids, which are used as gelation and thickening agents in different applications such as: food, paints, toothpaste, stabilizing ice cream, pharmaceutical, and biotechnological applications [25,34,35]. High attention has been paid to seaweed as a functional source of valuable beneficial health effects for both prevention and treatment of many diseases. Seaweed can be a part of some therapeutic activities such as anti-obesity, anti-diabetic, antioxidant, anti-inflammatory, anticoagulants, antiviral, immunological and anticancer due to their fucoxanthin content, which is a marine carotenoid that can be found in seaweeds, especially the brown algae (Kelp) [26-29,34-36,42].

Seaweeds are an excellent nutrient source, containing high amounts of micronutrients like iodine, iron, zinc. Some studies show that the consumption of these micronutrients is very safe and important during pregnancy to prevent the micronutrient deficiency and work for development of the fetus brain [30]. Also, seaweed contains a range of bioactive compounds that perform an important role in modulating chronic diseases. Seaweeds have a significant role in nutraceutical industries due to the high content in proteins, vitamins, antioxidant and minerals and it is widely used in China, Japan, and Korea [31]. Beside all these benefits, seaweed can be used for animal feed. Some studies have shown that adding some seaweed to cattle feed can reduce methane emissions and can be useful additives to feed for farmed fish and fishery species [40].

Seaweed has been used in agricultural soil as fertilizer or compost that can improve the organic content of the soil, thus improving soil quality and reducing the need for industrial fertilizers [36]. Recently many companies have been focusing on developing and producing an edible food packaging from seaweed [37].

Nowadays seaweed has great potential as a renewable source of biomass for biofuel products that will contribute to reducing environmental pollution effects [12, 38]. Ethanol, biodiesel, biogas, renewable gasoline, diesel, and jet fuels are all form of fuels that can be produced from algae biomass [44]. Brown seaweed (sugar kelp) is an example of renewable energy source for producing biofuel [43].

Seaweed aquaculture plays a huge role in reducing the negative impacts of climate change through CO₂ sequestration, reduction of agricultural greenhouse gas emissions, and protection of shores from coastal erosion.

1.4 History of Drying of Seaweed

The technique of water removal from food products is considered one of the oldest preservation methods that mankind has known over the centuries. Reducing the water content in a food product to the lowest levels eliminates microbial deterioration and the rates of other deteriorative reactions are reduced significantly [45].

The dried food market has been growing over the past few years due to increased demand for processed food that is ready to eat, such as nuts, seeds, popcorn, chips, vegetables, fruits, meat, fish, and grains. Because vegetables and fruits are seasonally produced and they may not remain fresh through the year, drying is considered an effective solution to get better post-harvest processing for increasing the food's shelf-life. Drying also makes material handling easier by reducing the weight and minimizing packaging and transport cost, and it enables providing seasonal products throughout the year. There are many methods of drying, the oldest one that humans have been using through the ancient time is sun drying.

Open sun drying is a natural method and widely used for drying seaweed, especially in Asian countries that have very warm weather, and such as Indonesia or Malaysia. Open sun drying is a simple and low-cost technique [46] and provides a naturally dried seaweed by spreading or hanging the crops directly in the sun after harvesting. This method has several disadvantages because it is weather dependent, and takes a long time, which means the drying will not be sufficient if the drying process is carried out during a rainy, or a dusty day or it may be attacked by birds, insects, or rodents [47]. So, in some cases the result of this method can provide a poor-quality product and mold growth on the product may occur due to excessively slow drying. In addition, drying directly in the sun will cause UV damage for the crops which can result in bleaching of the desirable bioactive pigments. As a result of this, open sun drying has some limitations for drying seaweed in Maine.

Another application of solar drying, more advanced than conventional sun drying and widely use in tropical and subtropical countries such as Malaysia [52], is drying the product while set in a cabinet that is exposed to the sun and makes use of a solar collector made of glass or plastic. The advantage is that the product is not exposed directly to the sun, while the energy is still inexpensive and provides a high-quality product as compared with open air sun drying [49]. A solar drying system was designed and tested for drying of seaweed by Fudholi et al. [48]. An experiment was done for a large amount of red seaweed, about 40 kg, by using this type of solar drying. The system consisted of an auxiliary heater, blower, drying chamber, and double-pass solar collector. The solar collector array consists of four solar collectors. The bottom and sides of the collector have been insulated with fiberglass to minimize heat losses. The collector consists of the glass cover, and the insulated and black-painted aluminum absorber. The average solar radiation was 500 W/m^2 and the air flow rate of 0.05 kg/s .

A specific energy consumption was measured as 2.62 kWh/kg [48]. While the solar dryer can be an improvement to open sun drying, it still cannot be used during cloudy or rainy days, or at night. Many studies have been investigating how to get the best technique to dry seaweed with less time, cost, and energy with a high-quality product [55,57,70].

Currently oven drying and freeze drying are very widely used in drying of seaweed applications [50]. Freeze drying has been used in several applications for preserving food. Freeze drying involves the removal of moisture from a frozen product without thawing that product [50]. The water can be removed from the material by the process of sublimation. Because of the energy and capital cost of refrigeration, freeze drying is more expensive compared to many other drying methods. The freeze-drying method can produce an excellent quality product, but this technique is more expensive if compared with other techniques.

Microwave drying has been a very successful application in food processing, particularly for food drying to preserve food materials. Microwave-vacuum drying can reduce drying time and provides a product with a high quality, and it takes less space compared to oven drying. Microwave-drying could be a useful alternative to oven-drying. Osmotic dehydration has been used as an effective method to reduce the moisture content of seaweed [51]. Also, there are some drying methods that have been applied in the food drying sector such as heat pump drying, or superheated steam drying [57].

The drying field has been improved and developed by using new drying methods such as electromagnetic heating-infrared (IR) [53,54], which several studies have shown can improve the food quality and give shorter drying time compared with conventional heating. It also inhibits enzyme degradation [55]. Dielectric heating (radio frequency and microwave), and ohmic heating are other electromagnetic techniques.

Ohmic heating uses electrodes to convert electric energy into heat. The dielectric heating processes provide a high-quality product at the end of the process, reduce cooking time, and have efficient energy use [56,70]. Selecting the appropriate drying technique depends on several factors such as the cost, energy efficiency and the influence of the process on the food quality.

1.5 Effect of Drying Treatments on Nutrient Composition and Properties of Seaweed

Seaweeds have been a highly valued resource due to their rich nutritional composition including vitamins, minerals, antioxidants, and bioactive components. Freshly harvested seaweed has a high moisture content about (70-90) % wet basis [50,58], and it will spoil quickly if not preserved. Drying has been an effective technique to reduce water activity, prolong shelf life, prevent decomposition, minimize the size of product, and reduce the cost of transportation, however several studies have reported the method of drying can greatly impact the nutritional composition of the brown seaweed *Sargassum hemiphyllum* [50]. Many studies have shown that drying can have a negative impact on the bioactive, antioxidant, and volatile compounds (that provide aroma and flavor) found in seaweed, which are a heat sensitive [50]. Also, in addition to the chemical changes such as color and flavor, physical changes also occur during the drying process, such as shrinkage, texture, and porosity changes which are important characteristics of seaweed. Nowadays, consumers are looking for convenient health products that imitate the properties of the fresh product. It has been a big challenge for food researchers and industry to produce such high-quality dried products.

Many drying techniques have been applied to dry seaweed, the oldest one is open air sun drying, and other methods such as solar drying (SD, using solar heat in a mechanical drying system), convective drying (CD), Freeze drying (FD), and the new hot air drying (HD) techniques such as microwave, microwave-vacuum, microwave-air drying for obtaining faster and better drying and higher sensory quality in comparison with the conventional methods. Open sun drying causes loss of the nutrition and changes in color if the product is exposed directly to the sun for a long time due to ultraviolet radiation.

One study showed the effect of oven drying and freeze drying on the nutrition composition and physicochemical properties of two kind of seaweeds, and the results showed that oven drying for both seaweeds preserved some nutrients such as protein, crude, fiber, and fat content, but saw reduction in ash and mineral content [59].

Another study showed that oven drying with a high temperature for a long time may have a negative impact and on the bioactive compounds nutrients [66]. The effect of high temperature during the convective air-drying method at 70 °C compared to 40 °C on the shrinkage of the brown seaweed *Saccharina Latissima* was found to correlate with the glass transition temperature of the seaweed [62]. “The material state (glassy or rubbery) can highly influence its shrinkage while drying and hence, affects the textural properties and shelf-life” [62]. Some studies have reported that drying at high temperatures will cause a reduction in phytochemical substances such as phenolic compounds, pigments, together with modifications of the physicochemical and sensory properties (aroma, flavor) of the seaweed products [60-62]. Other studies have shown that freeze-drying has better results when compared to conventional technique in reducing the loss of volatile compounds, minimizing physical damage, enhancing reconstitution characteristics, and reducing the occurrence of oxidation and thermal reactions in seaweed due to drying [50].

A study by Hamid et al. [63] showed that freeze drying three different edible seaweeds (*Cladosiphon okamuranus*, *Saccharina japonica* and *Osmundea pinnatifida*) preserved a very high concentrations of certain metabolites when compared to the oven dried samples of the same seaweeds. Additionally, a study by Moreira et al. [64] showed that freeze-dried samples of *Ascophyllum nodosum* had higher antioxidant activity and contained more phenolic compounds than samples subjected to other drying procedures. Although the advantages of the freeze drying provide a high-quality product, this technique is considered an expensive method and cannot be used to dry seaweeds at large scale for commercial purposes [66,68]. Finally, a study by Stévant et al., Badmus et al. [65,66] on microwave- assisted drying is an alternative option which may offer rapid drying over short time periods and can maintain the green color and other valuable components of the original seaweed. “Understanding the behavior of the seaweed biomaterial is a key to developing processing strategies that will maximize the quality of the products to be used as food ingredients and as raw material for the provision of valuable compounds” [64].

1.6 Seaweed Drying Kinetics

A mathematical model was developed by Sappati [67] to simulate the drying process of sugar kelps that hang vertically in a hot air convective dryer, and to investigate the influence of air velocity, humidity, and temperature of the inlet air on the drying time as compared to the experimental data. The data obtained from that model were used to determine the inlet air condition for optimizing the energy consumption and the drying period for producing high-quality seaweed products for consumers. In Sappati’s study a hot air convective dryer was used for the drying experiments, which had a cross section area of 76.2 x 76.2 cm and bed length of 127 cm [67].

In this experiment a batch of 28 kelp blades of approximately 63.5 cm height, 15.2 cm width and 0.2 cm thickness were hung vertically in the dryer at 6 different conditions, consisting of 3 temperatures (30 °C, 50 °C, and 70 °C) and 2 levels of inlet relative humidity (RH: 25% and 50%) for estimating the drying time. The air velocity inside the dryer was maintained at 1 m/s. For the modeling analysis, the drying system was assumed to be an adiabatic system, meaning that there was an assumption of no heat transfer between the chamber and the surrounding area. For one condition (40 °C, 25% RH), the model predicted that the total drying time needed would be about 3 hrs., which was confirmed experimentally as it was very close to the drying time obtained from experimental data of about 3.13 hrs. [67] The mathematical model predicted similar drying times as compared to the experimental results, although it was most predictive at the drying conditions of 40 °C and relative humidity of 25%.

1.7 Simulation and Modeling of Seaweed Drying (Energy Balances)

Conservation of energy requires that for a system that is at steady state, energy entering a system must be equal to energy leaving the system. The seaweed dryer was operated for periods of time of several hours. Because the temperature control system in the dryer oscillated over a range of about 12°F, with a period of about 15 – 25 minutes, energy was cyclically accumulating or depleting in the dryer, but on average an energy balance could be developed over a period of several temperature oscillations. ASPEN Plus, a chemical engineering process simulation software, was used to model the energy costs and capacity of the drying process. Input variables of different ambient air temperature and humidity were assessed for their effects on cost and throughput. The model considers different modes of operation, such as the set point operating temperature for the incoming air and the rate of ventilation of the chamber.

CHAPTER 2

METHODOLOGY

2.1 Parameters for a Seaweed Dryer: Size, Internal Configuration, Unit Mobility, Energy Sources

A tall shipping container, 40'long x 8'wide x 9'tall was acquired to serve as the drying environment for the portable dryer. The container was divided into two sections: a larger, 33' foot long section in which the seaweed is dried, and a smaller, 7' long section that houses two furnaces, two blowers, an exhaust fan, and controls for the drier. The drying section includes duct work to distribute warm dry air into, and moist air out of, the drying chamber. The seaweed is suspended from an oval shaped overhead conveyor system, which is designed to slowly rotate around the length of the chamber at about 3 minutes/revolution. Hangers have been designed that connect to the conveyor and can each hold several kelp fronds to hang about 7 feet above the floor. A suspended, clear plastic curtain hangs down along the middle of the conveyor oval, which directs drying air to flow first through one side of the chamber and then through the next. The utility room in the container houses two parallel propane powered heaters with integral blowers, an exhaust fan, louvres on the air intake and recycle ducts, and a control system that operates the burners, fans, and louvre system to optimize drying properties and energy consumption. Figure 2.1 shows the overall kelp drying system. In December 2019, the dryer was moved from the Advanced Manufacturing Center to its current location outside the Process Development Center at Jennens Hall on the UMaine campus as shown in figure 2.2. Power to the system was installed in January 2020 and propane tanks were installed on the site in February.

After installing the Propane tanks, it was discovered that the gas meter was leaking, and so it was removed. The consequence was that for the subsequent experiments, we were not able to meter the amount of gas consumed.

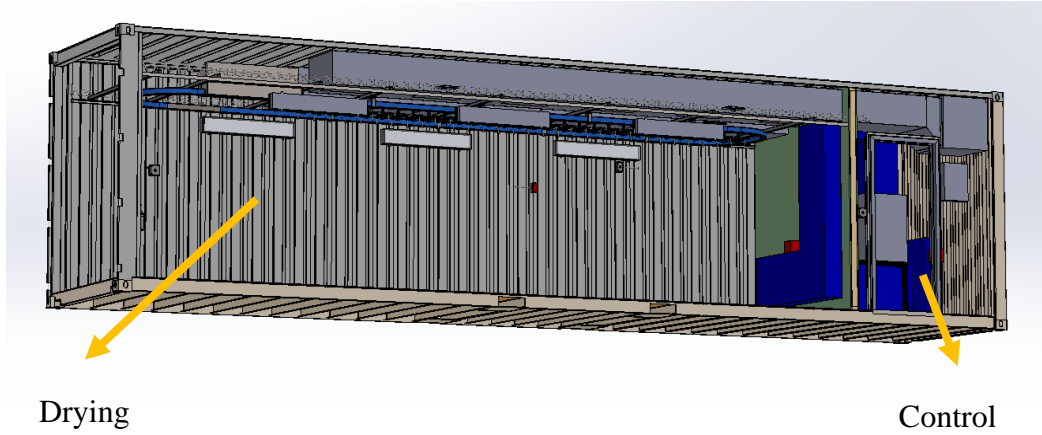


Figure 2.1: Overall kelp dryer model with drying chamber and utility room.



Figure 2.2: The portable kelp dryer to serve the drying process.

2.2 Dryer Design

2.2.1 The Drying Chamber

The drying system was built within a 40-foot-long shipping container. It is an automated drying system that is capable of drying kelp in a controlled environment that results in a more consistent and higher quality product. The seaweed dryer was developed to use warm (but not hot) air to decrease moisture content of the seaweed and avoids using high drying temperatures which degrade the food quality. This system with controlled temperature, air flow and exit humidity was developed and assembled in the advanced manufacturing center (AMC) at the University of Maine.

The dryer was divided into two sections: the large 33'foot long section, called the drying chamber, where the seaweed (or wet towels in some experiments) were hung by the hangers from the conveyor as shown in figure 2.3 at the beginning of the drying process.

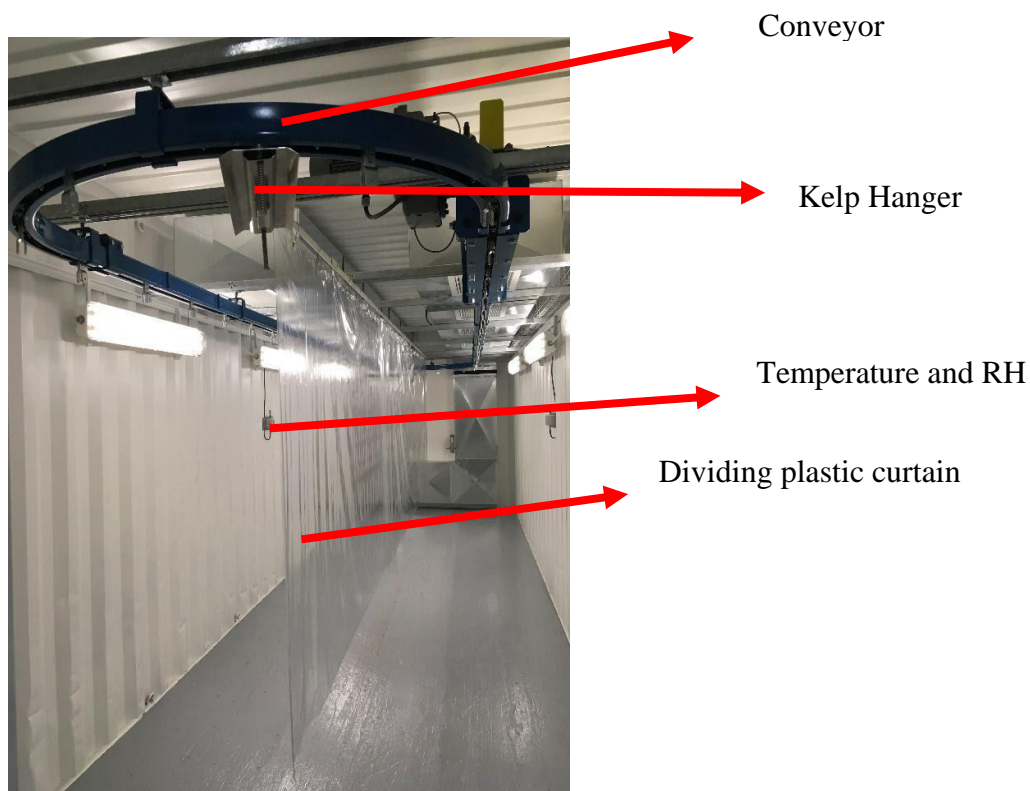


Figure 2.3: The drying chamber (from the loading entrance).

In the dryer chamber an oval track overhead conveyor was designed to hold the seaweed during the drying process by draping the seaweed from hangers attached with hooks to the conveyor. During the drying work, the conveyor was slowly rotated to give the seaweed uniform contact with the flow of warm drying air circulating through the chamber. Figure 2.4 shows the concept of how the dry air would flow past the seaweed during the conveyor rotation. The conveyor was controlled by a computer program set in the control panel located in the control room. A dividing plastic curtain was placed in the middle of the drying chamber to keep the air circulating through the the suspended seaweed during the drying process. The walls and the floor of the drying chamber were coated with a food quality protective coating to prevent any reaction with the seaweeds during the drying process.

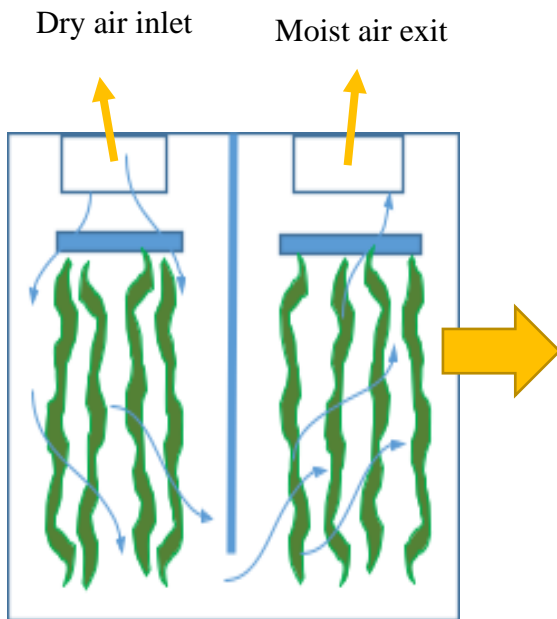


Figure 2.4: Continuously rotating conveyor.



Figure 2.5: Intake and exhaust vents of duct system on the exterior of container.

In the drying chamber there were two ducts as shown in figures 2.5 and 2.6. The inlet air duct delivered the warm drying air through four vents that were located in the duct so that the air could pass through the suspended seaweeds. The other duct is the outlet or exhaust duct that was responsible for removing the spent moist air and sending it out of the dryer during the drying process. In the seaweed dryer there were five sensors detecting temperature and relative humidity as shown in figure 2.3. One was mounted in the fresh air intake to the furnaces, and the other four were located in the drying chamber at different locations: two in the inlet and outlet ducts and two mounted on the walls of the inlet and exit sides of the chamber. These sensors measured the temperatures and the relative humidity at different locations of the drying chamber. Data from these sensors were fed into the control panel which enabled us to know the temperature and relative humidity at each location during the drying process.

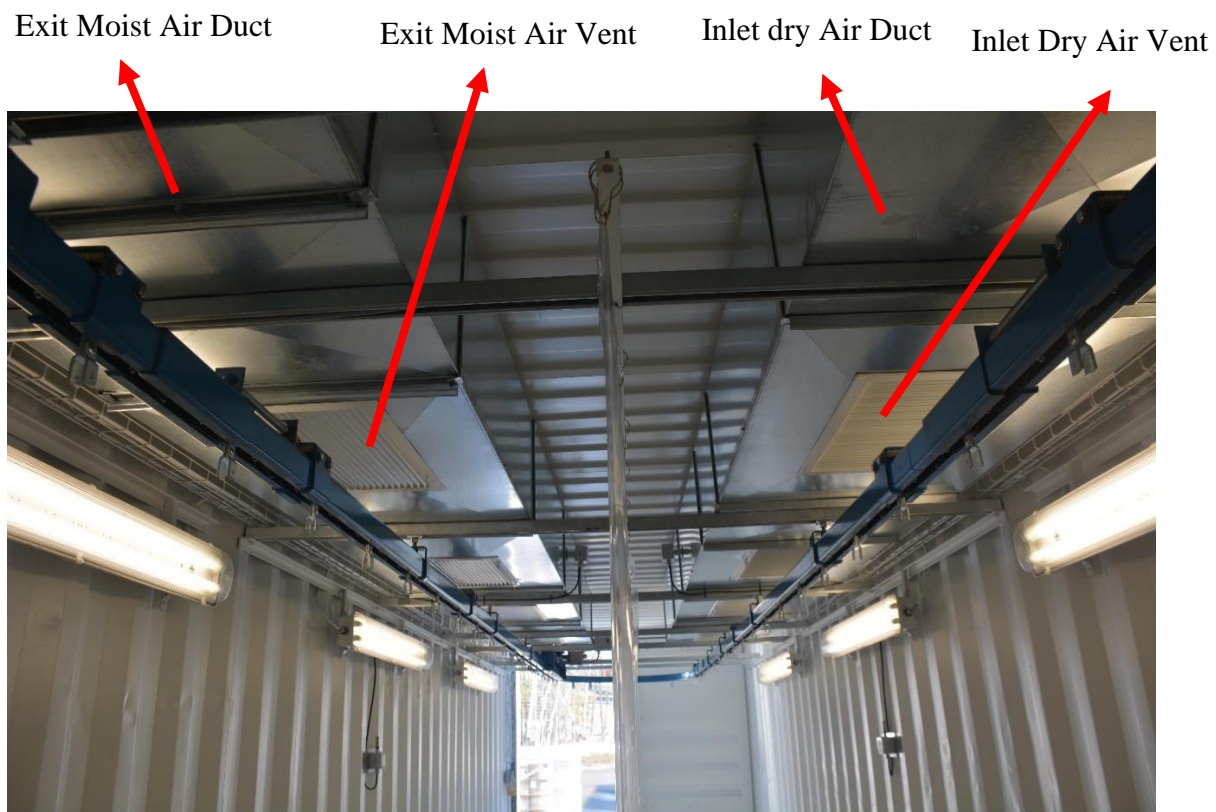


Figure 2.6: The Inlet and exit air ducts suspended from the top of the drying chamber.

2.2.2 The Control Room

The other section of the dryer was the control room that was designed to fit into the remaining 7' of the container. It is a small section of the container but was sufficient to house the two gas furnaces, their integrated blowers, the duct system controls and the exhaust fan for expelling the moist, used air. This room also hosted the control panel that controlled the temperature and relative humidity of the dryer during the experimental runs by setting the desired temperature and relative humidity. Figure 2.7 shows the furnaces and the control panel within the control room.



Figure 2.7: The control panel and the heaters in the control room.

The control panel has a screen called the Screen User Interface (UI) to monitor the temperature and relative humidity of the five sensors at different locations in the dryer as shown in figure 2.8. From this screen we can control and monitor the drying process, if the process was active the screen will show the status of the system, for example the system and the conveyor will be an example of the monitor screen in the control panel during the running of the dryer. On the right side of this screen is the Navigation Bar, which will enable you to move from menu to menu in the control panel. The current page will be displayed by a light on the function buttons, as shown in figure 2.8 and figure 2.9 below.

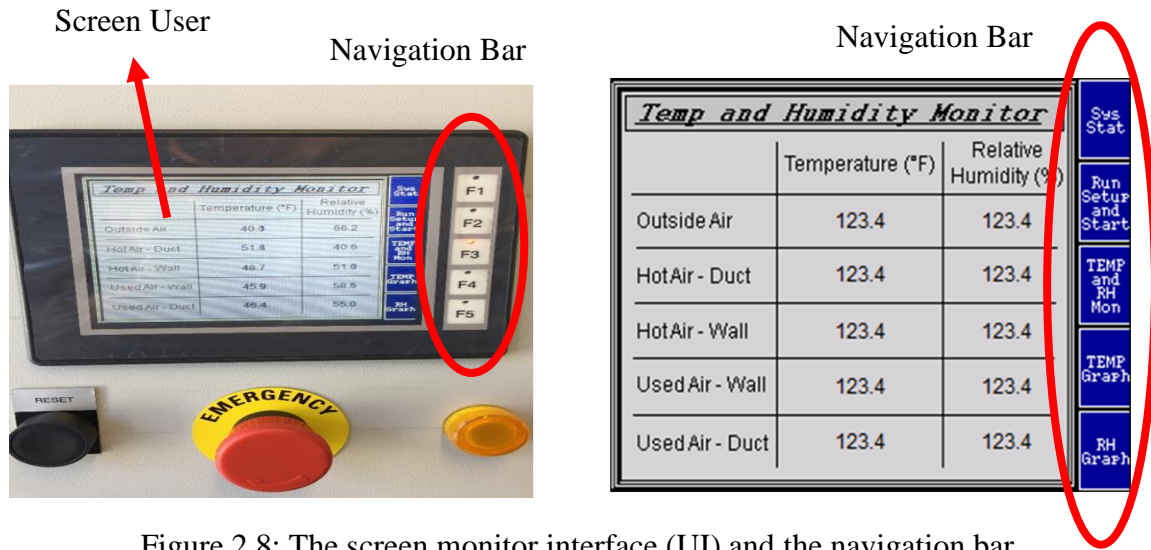


Figure 2.8: The screen monitor interface (UI) and the navigation bar.

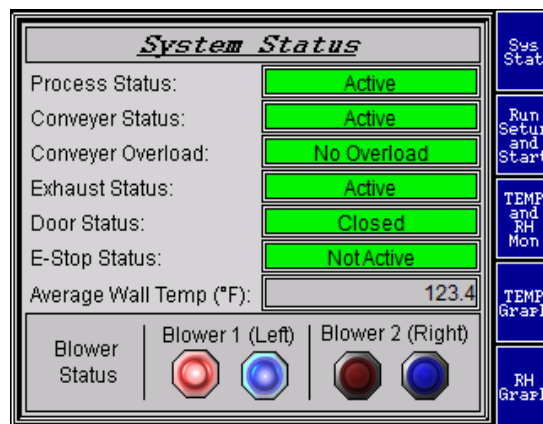


Figure 2.9: System status screen in the control panel during running the dryer.

The control room has a small breaker panel that controls the power to the operating systems. The panel has different breaker switches, such as the main switch to operate the control room, the drying chamber, furnaces, and the lights in the kelp dryer. Beside this panel there is also a small power meter to monitor the electric power that is consumed during the drying process, as shown in figure 2.10. The control room has an emergency switch for safety as shown in figure 2.11. The sensor for temperature and relative humidity of the fresh air is installed in the fresh air intake duct in the control room. This sensor was located in the utility room to measure the temperature and RH of the incoming fresh air.

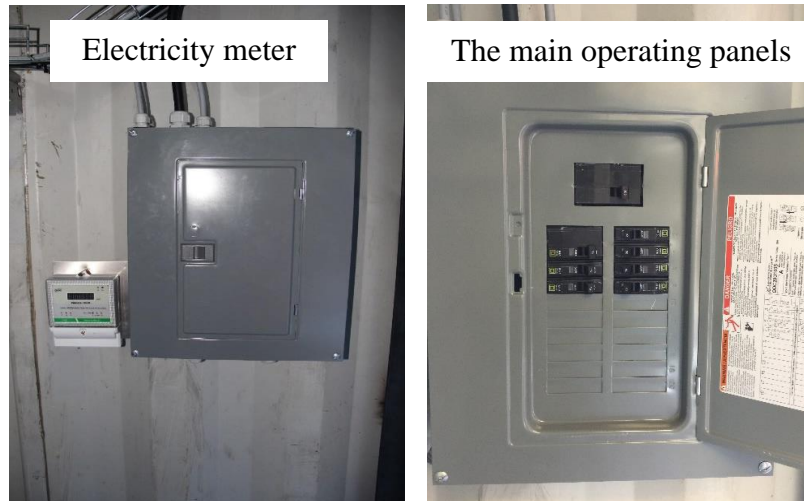


Figure 2.10: The main operating Panel and the electricity.



Figure 2.11: The emergency switch.

2.2.3 The PLC Logic and Data Logging

The PLC is a software program that is programmed inside the control panel to control the furnaces, the exhaust fan and the conveyor. In addition, a data logger is included to collect and download the data after the drying process or at the end of each cycle. The logged data obtained from the PLC showed the temperature and relative humidity behavior of the five sensors at the end of each cycle and the average temperature of the two walls at the end of each cycle. After completing each cycle of the drying process, we stopped the system to collect the data from the data logger using a USB cable from the bottom of the FC LOG port to a laptop computer. After finishing the data collection, the USB cord from the PLC port was detached from the laptop computer and the panel was closed. Figure 2.12 shows the PLC and data logger within the control panel.



Figure 2.12: The control panel and the PLC.

2.3 Seaweed Handling

Three drying experiments were done using sugar kelp. The first experiment of drying seaweed was run on May 20, 2020, with sugar kelp kindly supplied by Seth Barker at Maine Fresh Sea Farms. The fresh seaweed was transferred from the farm to the University of Maine using several coolers to keep the kelp cool and protect it from deterioration. The last experiment of the 2020 harvest season was done on June 8, 2020, using a new batch of fresh sugar kelp kindly provided to us by Sarah Redmond of Spring Tide Seaweed Farm. The seaweed was transferred by coolers to the dryer to start drying process. Figure 2.13 shows the containers used to transport the kelp from the farm to the dryer.



Figure 2.13: Transfer the kelp from the farm to the dryer.

After transporting the seaweed from the farm to the dryer location, we started our experiment by removing the seaweed from the containers and hanging them by the hangers. Figure 2.14 shows the process of hanging the seaweed from its stipes by the hangers. The mass of the wet seaweed was measured by putting a loaded seaweed hanger in a plastic tote container on an electronic balance to measure the mass of the wet seaweed before starting the drying process.

Figure 2.15 shows the way to measure the mass of the wet sugar kelp. After recording the mass, the hanger with its seaweed was moved into the drying chamber and hung up on the conveyor to start the drying process. Figure 2.16 explains the process of loading wet seaweed in the drying chamber to be ready for drying. Once all of the hangers were loaded and hung on the conveyor, the doors of the chamber were closed and the dryer turned on, activating the control system, the conveyor, furnaces and exhaust blower.



Figure 2.14: Wet sugar kelp laid out to be attached to a custom seaweed hanger.

The digital balance

The container with wet seaweed and hanger



Figure 2.15: The method of weighing the wet seaweed before the drying.



Figure 2.16: Wet kelp in the drying chamber to start the drying process.

In long running experiments, the drying process was interrupted periodically, about once per hour or so, to take mass measurements so that the rate of drying could be determined. These interruptions involved shutting of the furnaces, the fans and the conveyor, opening the doors to the drying chamber, removing and measuring the mass of ten selected hangers, replacing the hangers back onto the conveyor, and then closing the doors and re-starting the drying system.

These periodic measurements allowed us to see the progress in the dryer and make estimates of how much moisture had been removed during the previous drying period. After the final cycle of drying, we stopped the furnace and opened the chamber doors to measure the mass of all the dried seaweed as showed in figure 2.17.

This was done in the same manner as the intermediate massing events, except that for the final measurements, all of the hangers (not just the 10 selected hangers used for the intermediate measurements) were weighed on the balance. After all these steps the collected dry seaweed was collected in tote containers and were sent to Food Science department. Figure 2.18 shows the way of weighing dried seaweed after the drying process.



Figure 2.17: The dried seaweed with the hanger in container to weigh them.



Figure 2.18: The dried seaweed collected in tote containers to send to the Food Science Department.

2.4 Hanger Types

2.4.1 Regular Clothes Hangers

Because the kelp dryer is a food processing machine with a suspended conveyor, a hanger system was needed to hang the seaweed from the conveyor. Two kinds of hangers were used in our experiments. The first kind was a regular clothes hanger. For this kind of hanger, we used clothes pegs to secure the fronds of kelp during hanging to prevent them from falling off during drying process. Figure 2.19 shows the regular clothes hangers with pegs.

2.4.2 Custom Seaweed Hangers

The second kind of hangers (custom hanger design) were designed and assembled by the Advanced Manufacturing Center (AMC) within the University of Maine. The custom hanger was designed with an upper stainless-steel plate to shield the seaweed from any grease or any other materials that might fall on kelp while running the conveyor, as shown in figure 2.20.

Underneath this shield, the hangers were constructed with springs tensioning a bottom clamp bar that would close in the upwards position to clamp the seaweed between the top plate and the bottom bar. The bottom bar had its compression force adjusted by the spring and an undulating surface that could clamp onto seaweeds of varying thicknesses, which helped to prevent the seaweed from falling while in the drying process. The base plate has a capacity to hold 3 to 5 fronds of kelp depending on the width of the kelp in each hanger.

A handle was attached to the bottom of the clamp bar to provide a way to open the hanger to load the kelp. This clamping process is envisioned taking place either on or off the conveyor system, as the hooks attached to the upper plate allow simple removability of the hanger from the conveyor system as show in figure 2.20. Parts of hangers were selected to be replaceable and easily assembled while complying with food safety and minimizing corrosion.

The first testing of these custom hangers was done on May 20, 2020, with ten custom hangers. At that time most of the hangers that used on our experiments were regular clothes hangers with just ten custom hangers as preliminary testing for these ten custom hangers. There were 87 hooks set in the conveyor to fit all these hangers.



Figure 2.19: The regular clothes hangers with pegs to secure the kelp during drying.

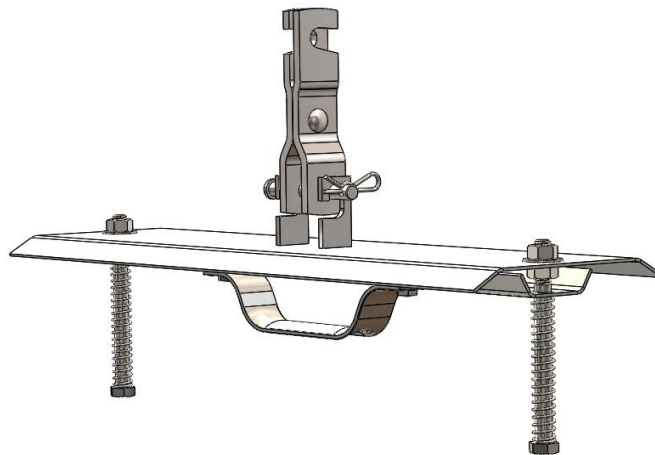


Figure 2.20: Model of stainless-steel hanger assembly.

2.5 Seaweeds Drying Process

The first experiment of drying sugar kelp was running on May 20 – 21, 2020 (Seaweed kindly supplied by Seth Barker at Maine Fresh Sea Farms) hung on 50 hangers from the conveyor. This first test of the drying system on seaweed also included the testing of a custom hanger design. Most of the hangers used were regular clothes hangers, but we also tested ten custom manufactured hangers that were designed to enable more rapid attachment of the seaweed and reduction in the number of small parts (clothes pegs) used with clothes hangers. This experiment had about 14 kg of sugar kelp hung up. We were near the end of seaweed season and most of the fronds hung up were relatively small, with many only 40 – 90 cm long. Thus, the dryer was operating at low capacity in this run. It ran for a period of 3.72 hours with a temperature set point range of 95 to 100°F (35 – 37.5 °C) and the wet seaweed was dried from 85 % (wet basis) to dryness, which was not quantified with subsequent oven drying, but was assumed to be close to 10 % (wet basis), suggesting that up to 13.3 kg of water was removed. The water removal was determined by weighing the initially wet seaweed and the final dry seaweed after drying.

This experiment included four cycles of operation averaging about 0.93 hours each, between which the dryer operation was interrupted and the mass of ten seaweed hangers (the same ten that were custom designed to hang seaweed) were measured to determine how much moisture content remained at the end of each cycle. The operation ran with 80 % air recycle with only one propane burner and fan working, which was sufficient to keep the dryer warm. The total power consumed during this run was 1.76 kWh. The weather was most cloudy on May 20 and the outside air temperature was 81 °F (27.2 °C) with RH about 46%. On May 21 the weather was partly cloudy and the outside temperature about 66 °F (18.9 °C) with RH 40% (<https://weatherspark.com>).

The last experiment of the 2020 harvest season was done on June 8 using a new batch of fresh sugar kelp (kindly provided to us by Sarah Redmond of Spring Tide Seaweed Farm). The dryer was run with the maximum number of hangers (87) and about 57.9 kg of wet seaweed. The seaweed used in this experiment had much larger fronds than the previous seaweed experiment, and most of the fronds were also in better condition than the seaweed used in the May experiment.

The dryer ran for a period about 6 hours with the temperature set to cycle between 95 and 100 °F. The wet seaweed was dried from 87 % (wet basis) to presumed 10% (wet basis), resulting in about 49 kg of water removed. The water removal was determined by weighing the initially wet seaweed and the seaweed after drying. This experiment included five cycles, in between each cycle the dryer was stopped to check the weight of the seaweed, again using the 10 custom hangers to represent all the seaweed as a whole. The operation ran with 80% air recycle and one propane burner used to maintain temperature. The total power demand for this experiment was about 1.7 kW. The weather forecast for June 8 was Mostly cloudy- Partly cloudy with outside temperature about 79 °F (26 °C) and RH 33%. For June 9 the weather forecast was partly cloudy with temperature 60 °F (15.6 °C) and RH about 58% (<http://www.solarelectricityhandbook.com/solar-irradiance.html>).

In spring and summer of 2021, we ran two more experiments, one by using wet towels and the other was using wet sugar kelp. The target of running these two experiments was to generate more data to understand the heat loss behaviors through the walls of the dryer. Since we had calculated from the previous experiments that there were some heat losses through the wall as well as some heat gain from the outside, especially during a sunny day. Eleven small battery powered temperature and relative humidity sensor-data loggers (Easy log – USB) were used in these two experiments by setting them on the outside of dryers' walls, ducts and inside the chamber (where the seaweed were hung).

Also, an IR camera (thermal Camera) was used to take temperature images of the dryer walls from outside the dryer to monitor the temperature of the dryer walls from outside during drying process.

2.6 Energy Balance Calculations

Two approaches were taken to developing an energy balance of the seaweed dryer. The first approach was to use temperature and humidity data collected from drying experiments, mass data on how much water had been evaporated, the heating and air flow capacities of the furnaces in the dryer, and heat transfer calculations (conductive, convective and radiation) to estimate heat loss (or gain from solar energy) through the walls of the dryer.

The second approach was to use ASPEN Plus, a process simulation program that applies thermodynamic calculations to determining mass and energy balances of material process systems. ASPEN Plus was used to simulate the ambient air temperature and humidity conditions, the conditions of the exiting air, and the furnace heating and air movement capacities to determine the cost of energy and the amount of heat that was lost from the dryer.

The aim of our study was to find agreement between these two modeling approaches, or, if no agreement were reached, identify where the energy balance calculations or data collection were insufficient to fully characterize the system.

2.6.1 Heating and Evaporation Calculations

Applied energy: Energy consumed for heating and drying seaweed. Equation (2.1) was used to calculate the heat of evaporation, which is later used to calculate the energy loss from the furnace by subtracting the heat of evaporation from the energy input of the propane burner.

$$q = m_1 C_p \Delta T + m_2 H_v \quad (2.1)$$

Where:

q: Energy of evaporation (kJ)

m_1 : mass of seaweed (kg)

C_p : specific heat capacity of seaweed (kJ/kg °C)

ΔT : the difference between T_1 (outside air temperature) and T_2 (inside temperature °C)

m_2 : mass of water evaporated (kg)

H_v : Heat of vaporization (kJ/kg)

2.6.2 Fan and Air Flow Calculation

2.6.2.1 Mass Balance Results

The mass balance determines how much water we have passing through the system during the drying process. The mass balance confirms our estimate of how much water we are evaporating from the dryer, that is, how much moisture is removed from the seaweed. During our drying runs we would periodically halt the drying process (approximately once per hour) and measure the mass of a selected group of seaweed hangers.

The percent moisture loss was applied to the entire seaweed contained in the drying chamber to estimate the total amount of water that was evaporated during this last drying cycle. On the other side of the mass balance equation, we looked at the air entering and exiting the dryer and how much humidity was being carried by the air streams.

For this calculation, we estimated the air flow based on the fan curve of the furnaces and the recycle ratio of the air circulation. Using a psychometric chart and the temperature and relative humidity data of the air entering and exiting the dryer, we calculated another estimate of the rate of moisture removal from the dryer.

Results showed that the air flow and seaweed mass measurements were relatively consistent for later drying cycles, when the seaweed was partly dried, but that the two methods of calculating water removal deviated significantly for the earliest cycle when the moisture content of the kelp was still very high.

2.6.2.2 Energy Balance Results

Convective loss: Energy consumed for heating air. Equation (2.2) was used to calculate the change in air enthalpy, by subtracting the enthalpy of air coming in from the enthalpy of air coming out. Enthalpy was determined by considering both the temperature and humidity of the air.

Equation (2.3) is used later to find the energy loss from the air exchange by fan driven convection. The net mass flow rate of air exchange was determined from the fan curve of the furnace blower and the degree of recycle.

$$\Delta H = H_2 - H_1 \quad (2.2)$$

Where:

ΔH : The change of air enthalpy (kJ/kg)

H_1 : Enthalpy of air coming in (kJ/kg)

H_2 : Enthalpy of air exhaust (kJ/kg)

$$E_{Loss} = m \Delta H \quad (2.3)$$

Where:

E_{loss} : Total enthalpy loss from air exchange (kJ)

m : mass of air (kg)

2.6.3 Heat Loss Through the Walls of Dryer Calculations

Conductive loss: Energy lost through the walls of the dryer Equation (2.4) was used to calculate the heat loss through the walls of the dryer by conduction. From our observations of the warm walls and our calculations, it was obvious on cool days that a lot of heat was being lost through the walls.

We applied normal heat transfer coefficients for convective surface heat transfer on vertical and horizontal surfaces and estimated the likely loss of heat through the uninsulated steel walls. The area of the walls was adjusted to account for the corrugations in the steel walls, which increased the conduction area.

$$Q = U A (T_2 - T_1) \quad (2.4)$$

Where:

Q: Heat loss of conduction through the walls of dryer (Watt)

U: Overall heat transfer coefficient (W/m² °C)

A: surface area of the dryer (m²)

T₁: Ambient air temperature (outside temp.) °C

T₂: Interior air temperature, measured near the walls (inside the dryer) °C

It became apparent through the operation of the dryer that considerable heat losses were caused by conduction through the dryer walls, and that if insulation were to be added, even at a modest level of R1 insulation, the energy saving would be substantial.

2.6.4 Solar Energy Calculations

Solar Energy Gain: Energy from sun radiation landing on the dryer. It was observed that on a warm sunny day during a May run, the control system that was drying a relatively small and mostly complete drying load was not detecting a temperature drop after the propane burner was shut off. This appeared to be because there was enough solar heat being captured to maintain the drying chamber at its desired set point.

Thus, in some cases, solar gain could offer sufficient energy to conduct the dryer without burning fuel. Equation (2.5) was used to calculate the net contribution of solar radiation on the dryer.

Data on solar radiation were available from the websites:

(<http://www.solarelectricityhandbook.com/solarirradiance.html>) and (<https://weatherspark.com>), which reports average horizontal insolation rates considering specific dates, times of the day and cloud cover. The radiation level for the particular time of day, date and cloud cover was integrated over time and multiplied by the area of the roof or the south facing wall of the dryer to determine incoming radiant energy.

The re – radiation of the captured energy was then split between radiation into the dryer vs. radiation back to the outdoors, depending on the relative temperatures inside and outside of the dryer. Calculation for the vertical capture of radiation considered the date and angle of the sun that day,

$$q = \sigma \varepsilon A_h (T_h^4 - T_c^4) \quad (2.5)$$

Where:

q: net radiation rate.

ϵ : emissivity coefficient of oxidized steel.

σ : Stefan – Boltzmann Constant (5.6703E-08) (W/m² K⁴)

A_h : area of the dryer (m²)

T_h : Temperature of the wall radiating heat from the sun (K)

T_c : Temperature of cold surrounding (K)

2.6.5 Energy Modeling of The Dryer Using Aspen Plus

2.6.5.1 Aspen Simulation of Seaweed Throughput Prediction and Energy Cost

Several approaches have been developed to model the thermodynamics and drying dynamics of the kelp drying system. ASPEN Plus, a chemical engineering process simulation software, was used to model the energy costs and capacity of the drying process. Input variables of different ambient air temperature and humidity were assessed for their effects on cost and throughput. The model considers different modes of operation, such as the set point operating temperature for the incoming air and the rate of ventilation of the chamber.

Figure 2.21 represents the ideal system that we modeled in Aspen Plus. The system starts with dry air coming in, which is then split into two streams at a desired flow ratio to create a desired % relative humidity. After the split, one stream stays dry, the other is completely humidified. A mixer will then re-mix the two air streams to attain the desired relative humidity for the incoming air.

By setting the temperature and varying the split ratio, we can simulate any level of temperature and relative humidity entering the dryer. The incoming air is then heated up by the furnace to the drying temperature set point for the drying conditions. The heated air then goes to the dryer where the seaweeds are suspended from the overhead conveyor. The calculations of the energy needed to evaporate the water was done inside the dryer. The exit air that coming out of the dryer that represents the VAPOR stream in our model was assumed to be saturated.

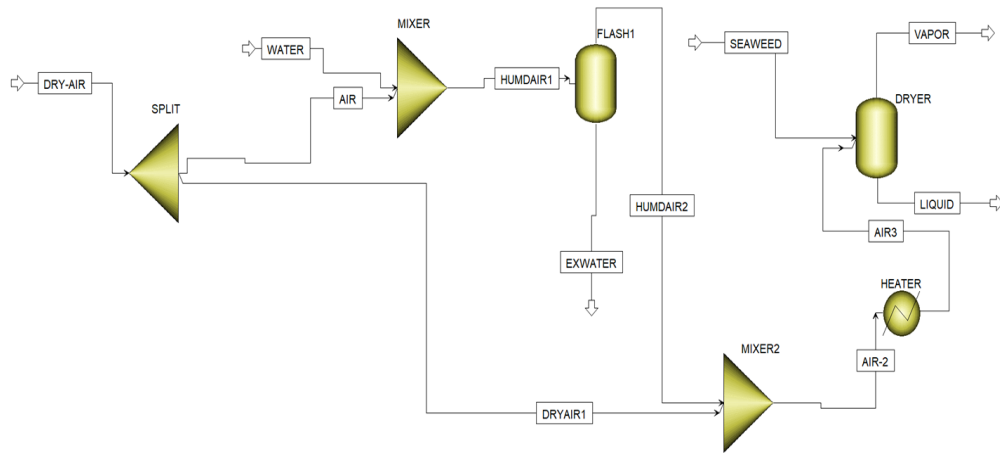


Figure 2.21: Process flow sheet for calculating energy balance calculations on differing ambient temperature and humidity conditions.

2.6.5.2 Furnaces and Fans Effects on Energy Balance

Additional work was done to improve this model, which is shown in Figure 2.22. This model included: non-saturated air exiting the dryer, air recycle, conductive heat loss and solar warming. In this round of simulations, we modelled three different possible operating scenarios for the system: in the first case we ran the model with two burners and two fans (2,2), the second case was running the model with one burner and with two fans (1,2) and the last case the model was running with just one fan and one burner (1,1), which was the most common mode of operation. We again ran the model with different conditions for the ambient air temperature and humidity to show how these different operating scenarios affected our drying process.

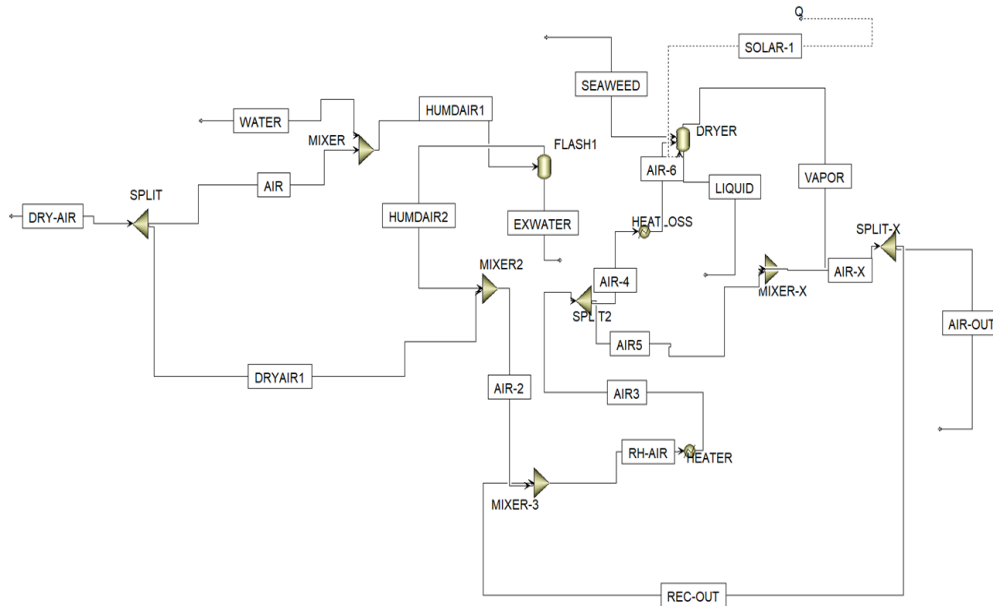


Figure 2.22: The new simulation that represents of weather effects on the drying process as well as the interior recycle and unsaturated performance through the dryer.

2.6.5.3 Weather Effects (Temperature and RH of Ambient Air and Solar Energy)

Most of the energy analysis done during the fall 2020 and into the winter 2021 was focused on improving an Aspen Plus process modeling software program simulating the energy flows of the real drying process of the sugar kelp. The initial ASPEN studies had been run with an assumption of saturated exiting air, relatively fast (2 hour) drying time, full heat capacity from the heaters (2 furnaces in parallel) and no air recycle. In contrast, our updated model was developed to be considerably more realistic. It incorporated unsaturated exiting air, slower drying time (>4 hours), considerably less than full furnace capacity (one of two furnaces operating and cycling on and off roughly half the time), and 80% air recycle. We retained the ability to simulate exterior air temperatures and humidity.

We also added a solar heating component to study the effect of solar energy on the drying process as part of our new simulation for the realistic dryer that was affected by solar and gained some heat through the drying process. The most important improvement to the model was that we coded into the software several design specifications that would modify internal material and energy flows until conditions matched those that had been recorded on the seaweed drying runs. For example, the heated air stream destined for the dryer was split in two, with some air entering the dryer and some following a bypass stream that circumvented the dryer and recombined with the spent air exiting the dryer. The dryer is modeled as a flash unit, which results in fully saturated air leaving the dryer.

By combining this saturated stream with the drying air that circumvented the dryer, the simulation could fix the ratio of the two air streams to result in the actual temperature and humidity measured by the sensors in the dryer.

The design specification adjusted the split ratio between these two streams to achieve the necessary relative humidity, while a second design specification varied the heat losses from the dryer to achieve the final recorded temperature of the air exiting the dryer. In this manner we were able to determine how much heat must have been lost to conduction through the dryer walls. In the new simulations we set the same temperature and relative humidity of the real outside air that we collected from the data logged by the dryer's control system. We are still in the process of matching more of the simulated process streams to equal those of the collected data to thus develop a clear map of how the energy flows through the dryer system.

Figure 2.22 shows the new Aspen model that simulated the effects of weather (temperature and RH of outside air) on the dryer while also matching the ducting configuration and sensor data of the actual runs (80% recycle, ascending exit Temperature and descending RH < 100%). Figure 2.22 shows the most recent version in which we have added a source of solar energy as a simulation of the actual dryer to study the effect of solar energy on the drying process.

CHAPTER 3

RESULTS AND DISCUSSIONS

3.1 Design and Assembly of The Dryer

Developing the design of the dryer involved input from seaweed growers, faculty, students and staff from Food Science, Chemical and Biomedical Engineering, Seagrant and the Advanced Manufacturing Center at UMaine.

Additional expertise was contributed by contractors hired to assemble the different systems of the dryer (heating and ventilation systems, conveyor system, control systems, and instrumentation). Design modifications and improvements to the dryer were made in response to preliminary runs and analysis of the dryer data.

3.1.1 Temperature

One of the most important design parameters was temperature of the drying process. The dryer was operated at a temperature of around 100 °F to avoid cooking the seaweed during the drying process.

A study done by Sappati [67] found that drying at temperature at about 100 °F at low relative humidity was the optimal solution to achieve drying in a reasonable amount of time while preserving the bioactive compounds of sugar kelp during drying process.

3.1.2 Mobile Unit

The plan for the drier was to have it be a mobile unit that would still be large enough to provide suitable throughput. A mobile unit was desired since it was thought that a small farm operation would only need to use the drier for a few days per harvest season, which would be insufficient to justify purchasing a dedicated drying system.

In contrast, a mobile unit could be shared by several farmers, or made available to various users on a rental basis. Thus, mobility was considered to be desirable. The first plan to design the kelp dryer was to have the system contained in a mobile tractor trailer.

However, it became apparent that there were some disadvantages to this initial idea. Tractor trailers are quite high off the ground, and stakeholders thought that this might complicate the loading and unloading of the kelp.

In addition, having a truck trailer would require road inspections, insurance and a license. An alternate plan was to make use of a large (40 x 9 x 8 ft) shipping container. The container would be easy to load and unload from ground level and it was simpler to manage a container in terms of paperwork and regulations.

It was also decided that to maintain the easy mobility of the system, the heating and ventilation equipment and control systems would be integrated within the container itself. This reduced the volume available for the drying chamber, but it was thought that the consolidation of the system in one container would simplify transport and set up of the system.

3.1.3 Avoiding Stickiness of Seaweed

3.1.3.1 Hanger System

Studies done by Sappati [67] and the UMaine AMC found that when sugar kelp starts to dry, it passes through a stage when sugars seep to the surface of the kelp fronds and the seaweed becomes extremely sticky. At this time, any surfaces the seaweed touches hold fast to the seaweed and as it continues to dry it becomes strongly bonded to the surface, making it very difficult to remove from the dryer and then to clean the surfaces. The seaweed fronds will also stick to each other, which slows down the drying because of reduced drying surface area and it also made the fronds difficult to separate. Due to the problem of stickiness, the design team chose to simulate the method used by seaweed farmers for open air drying, which is to hang the seaweed from an overhead support rather than letting it rest on a horizontal surface, which is the conventional approach for most food products. This prompted the development of the hanger system to address the stickiness issue.

3.1.3.2 Conveyor

Part of the design of the kelp dryer was to have an overhead conveyor from which the seaweed would be suspended. Because of concerns that the airflow in the container would not be uniform everywhere, circulating the kelp inside the dryer would give even drying to all of the seaweed. The asymmetry of the air conditions in the dryer were confirmed during the running the dryer, as the incoming air on one side was warmer and less humid than the air exiting on the opposite side of the drying chamber. The conveyor assured that the seaweed fronds would all be exposed to the same average drying conditions despite the different air flows and zones of the dryer during the drying process.

3.1.3.3 Hanger Design

Hanging the seaweed from the conveyor would require some sort of hanger system. It was expedient and inexpensive to use simple metal clothes hangers suspended from the conveyor, oriented perpendicular to the conveyor track to accommodate multiple fronds per hanger. When using clothes hangers, we used conventional clothes pins to secure the frond in place, which worked effectively but this approach was time consuming while loading and unloading the hangers.

Although the hangers worked to demonstrate the operation of the dryer, there were several reasons to develop a custom designed hanger for suspending the seaweeds. Using clothes hangers and pins was time consuming, and also these hangers were not made of food handling grade materials. Since the hangers are suspended beneath the conveyor, there was concern that grease or dirt from the conveyor system might fall on the seaweed below.

The result was a design of a custom hanger, built of stainless steel and able to load and unload seaweed more easily than using a clothes hanger. The design is shown in figure 3.1. The hanger consists of an overhead shielding plate that protects the hanger and its load from any falling debris and a single spring tensioned clamp that can hold several fronds in place with one fastening. These hangers worked quite well and facilitated the loading and unloading of kelp. Completion of the drying unit should include a full set of dedicated hangers (to date we have used only 41 out of a possible 87 hanger hooks).

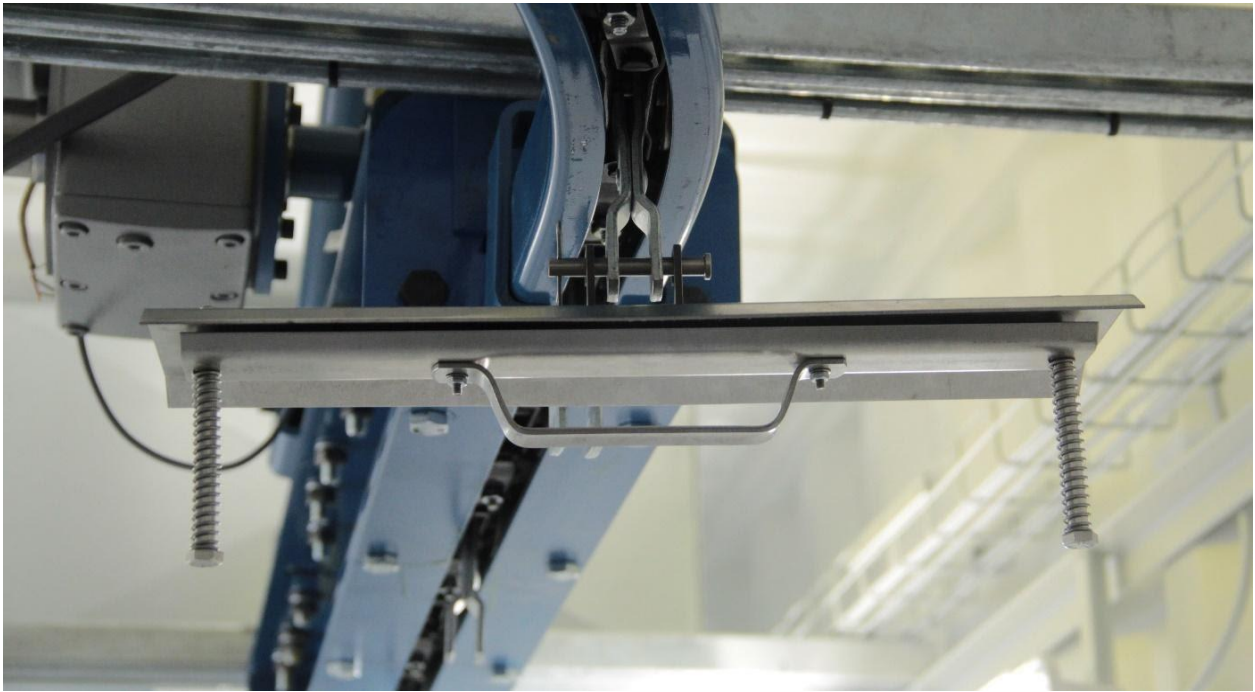


Figure 3.1: Constructed hanger assembled on conveyor track attachment.

We chose not to make a complete complement of the custom hangers because we expected that with some additional experience, especially in a commercial setting, yet better improvements could be made to the hangers. For example, it could be that longer hangers, if hung alternatively between the existing hangers, could support some additional seaweed loading. We feared that making all of the hangers longer would result in the fronds touching while the conveyor turned its sharp corner at each end of the conveyor oval, but it could be that every second hanger could have room to be extended by a few centimeters, enabling perhaps an extra 43 fronds of kelp per load.

3.1.4 Loading and Unloading

During the running of the dryer, we found that we still might need to come up with a better idea for the loading and unloading of the seaweed. Through talking with the seaweed growers, we came up with the hanger approach and design, which works well but will require some practiced skill of the operator to handle the seaweed quickly. We considered a number of other ideas, as well. One of the ideas that might have worked was to use a distributed vacuum system that would suspend the seaweeds from an array of vacuum portals, instead of a mechanical hanging system.

The idea was to have multiple tubes that would each find and suspend the seaweed frond and just hold it up on the conveyor. This could potentially increase the loading and unloading of the system. We did find that a suction tube with a soft suction cup worked well to pick up individual seaweed fronds, but the mechanical aspects of scaling this up to hundreds of fronds per batch was too complicated. So, suspending the seaweed is an area where we believe that the design could still be improved. Other options also came to mind. For example, if we wanted to use the dryer for different types of seaweed that are not so sticky, such as the red seaweeds, then we may be able to use conventional drying trays suspended from the conveyor, in a sort of stacked basket system.

3.1.5 Solar Energy

We considered a few options for collecting solar heat to help reduce fuel consumption of the dryer. Using solar collectors to pre-heat the incoming fresh air would reduce the energy costs of drying the kelp. We decided against using solar collectors that would be separate structures from the dryer, as this would increase the complexity of setting up the dryer, decreasing the mobility of the system.

Solar collectors mounted on the dryer itself seemed to be a better option, the simplest configuration being to use the container itself as the radiation absorption surface and enclosing the roof and one or more walls that would be oriented southward with a clear plastic shell, allowing the sun to heat the air between the surface of the container and the transparent wall. Fans could then move the warm air to the inlet of the furnace system. While this system would likely have been effective at capturing solar heat, we were concerned about handling and transporting the whole system. Encasing the steel container in a thin, fragile, clear shell outside the box would likely lead to breakage of the shell or even having it blow away in windstorms or while being transported on the highway. For this prototype model dryer, we decided to simply make use of solar energy by setting the container in the sun and benefitting from the solar gain captured by the walls and roof of the container.

3.1.6 Insulation

We also considered insulating the steel container, since the steel walls offer basically zero insulation. Insulating the inside of the dryer walls would reduce the volume available for drying and likely complicate meeting washing and hygiene requirements, while insulating the exterior would add bulk to the container and possibly suffer damage when being transported. We also realized that insulation is helpful when it is cold outside, but not very helpful if it is a sunny day since we are counting on capturing some solar heat through the walls of the container. A potential solution to the issues of protecting the insulation when transporting the container, and also making use of solar heat when available, would be to develop a large retractable blanket system. This system could be removed from the exterior, rolled up and stowed inside the drying chamber during transport.

Such a blanket system would be deployed when operating the dryer at night or on cloudy days but retracted on clear sunny days. Our analysis of the heat transfer through the walls suggests that even a minimal improvement of the wall insulation up to $R= 1$ would significantly reduce conductive heat losses.

3.1.7 Heat Pump vs. Furnace

Dryers are typically designed to use either a source of heat, such as a furnace, or a heat pump, to provide the warm drying air. Building the seaweed dryer using a heat pump would be more energy efficient but at a cost of higher capital cost than a furnace. Due to the short drying season for kelps, the energy savings of using a heat pump would probably not be large enough to pay for the higher capital cost of a heat pump. For this reason, we decided to design the dryer with furnace system powered by propane. Natural gas would be less expensive, but many locations on the coast are not yet served by natural gas. For locations where there is natural gas available, the propane furnaces could be modified to burn this less expensive fuel.

The kelp dryer is equipped with two furnaces that can be run simultaneously or cycled sequentially. Our initial calculation that we might be able to load up to 500 kg of kelp per drying batch called for this heating capacity, but according to our experimental trials, the most that we have been able to hang in the drier is a bit more than 50 kg of wet seaweed. This limit is largely depending on the size and length of the kelp fronds, and as discussed above, improved hangers may allow for some additional capacity. As a result of this smaller than expected kelp load, we have about one tenth of the amount of seaweed of our design case and we do not need the two furnaces. Perhaps if different crops are dried that could be loaded more densely than the kelp the capacity of the two furnaces could be put to use.

3.1.8 Air Flow Velocity

A previous study done by Sappati [67] found that the air moving through a bed of hanging kelp with speed of one meter per second did not create any problems with stickiness. The fear was that if the air flowed too fast, then the seaweed would start flapping around like a flag and it would touch a neighboring frond and they would stick together. Accordingly, we chose to maintain a target air flow speed of at most one meter per second in the larger dryer system.

We estimated the flow velocity by dividing the dryer volume by the volumetric flow rate of the furnace fan, giving us a residence time, and then predicting the likely pathway that air would follow through the dryer. This calculation resulted in an estimated velocity of only about 0.1 m/s, which was well below the maximum of 1 m/s. While running the dryer we did not have any problems with the seaweed blowing around and sticking to itself or blowing off the hangers or anything such outcomes caused by high air velocity.

3.1.9 Recycling Air

The experiments done by Sappati [67] using a drying cabinet with directed air flow found that the air became saturated very quickly. In fact, the air was picking up so much humidity that the heat pump used to maintain the conditions in the environmental chamber had trouble keeping the humidity of the air at the desired set point.

It was not until the seaweed was mostly dry that the drying conditions could be maintained. As a result of this experience, we were not sure that recycling exhaust air would be needed during the first stages of the large dryer operation.

It was thought that at the beginning of a run when all the seaweed was still quite wet, we would not be recycling, but that later on in the drying process, once the seaweed had mostly dried, that we would start recycling the exhaust air in order to increase the humidity of the circulating air before it was exhausted to the outdoors.

What we found in practice was, unlike in the smaller scale drying cabinet, that our seaweed dryer did not increase the relative humidity very much, even when drying freshly wet kelp, so we ended up recycling air all the time.

3.1.10 Dryer Control System

The kelp dryer has a control system that uses input data of temperature, relative humidity, and air pressure inside the drying chamber. See figure 3.2 for a diagram of the control logic. The system maintains a desired inside average temperature (usually 100°F in our work) within a certain tolerance range (5°F) and attempts to optimize exhaust RH by increasing or decreasing the recycle rate.

The recycle turns on and off depending on what the relative humidity is, but as mentioned above, in most cases the recycle operated at its maximum value of 80%, and used only one furnace at a time, cycling on and off with the temperature fluctuations, to heat the dryer.

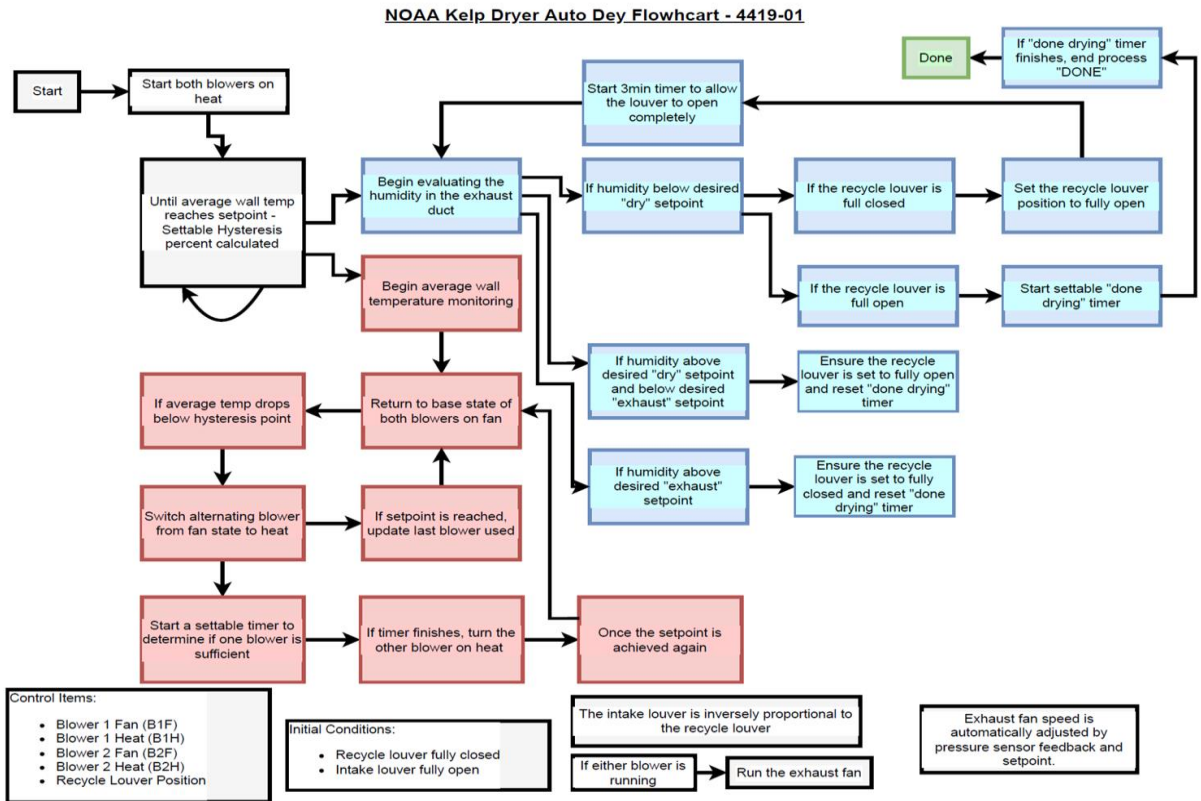


Figure 3.2: Control flowchart

3.1.11 Volume of The Cabinet and The Dryer

The size of the shipping container (kelp dryer) is 40' x 8' x 9'. The container is divided into two sections: a larger chamber, a 33' foot long section in which the seaweed is dried, and a smaller, 7' long section that houses the two furnaces, the exhaust fan, recycle duct work and the control systems. The chamber was built with a capacity of 87 hangers for hanging the seaweed. Each hanger could hold between 3 – 6 kelp fronds, depending on their size, with 4 being the median number. The hangers are about 2 m above the floor. In some cases, very long fronds more than 2 m long were hung suspended between two hangers. If we compare this system with the cabinet that Sapatti [67] used to dry seaweed, the cabinet size was built with of the cross-sectional area of 30 x 30 inch and bed length of 50 inches with a capacity of one batch of 28 kelp blades of medium length.

The cabinet dryer used for preliminary testing had an order of magnitude greater seaweed density than the drying chamber in the shipping container: 7.3 kg/m^3 for the cabinet, 0.86 kg/m^3 for the container. This provides an explanation as to why the exhaust duct in the cabinet dryer had more humid exit air, while the shipping container exhaust duct has much lower humidity air.

3.2 Initial Test Run Results

Preliminary runs of the drier had been run using wet towels hanging from regular clothes hangers. The first run was done on March 9, 2020, with 25 wet towels (238.4g dry weight) hanging from the conveyor. The outside air temperature was $33 \text{ }^\circ\text{F}$ ($0.6 \text{ }^\circ\text{C}$) with relative humidity about 69% and the weather was cloudy to mostly cloudy [1]. The dryer ran for a period of an hour and half, the towels were dried from a moisture content of about 73% (Wet basis) to 10% (wet basis), totaling about 23.3 kg of water removed.

The water removal was determined by weighing the initially dry towels, the wet towels, and the towels after running the dryer. The operation ran with either minimal (20%) or no recycle of air. The electric power consumed for the $1 \frac{1}{2}$ hours was about 2.6 kWh ($\sim 1.8 \text{ kW}$), which included power for the controls, the conveyor, and the fans with minimal recycle. The base load for lights, control system and conveyor (no fans running) were about 0.3kW, hence, the fans contribute most of the electricity load.

Two burners were operating through this experiment. Figure 3.3 shows the test of the kelp dryer with wet towels. A second run was initiated to operate the system with the recycle. This was done by lowering the temperature set point which, when reached, would initiate the recycle control algorithm

A third run was done with an increased number of wet towels (48), with attention paid to the temperature control (furnaces on/off) and the humidity control (degree of recycle). Unfortunately, during this experiment the control system suffered a hardware failure, and the experiment was not completed. The failure of the control system was traced to a single module of the PLC, which was replaced by the manufacturer. On March 30, 2020, a new PLC module was installed. Some modifications to the control system included dampening out signal noise, which appeared to induce the shutdown of the furnaces, and logging the position of the recycle control louvers. The dryer was run for testing its operation, with no towels in the drying chamber. Unfortunately work on the dryer was then halted temporarily due to the COVID-19 shut down of most research activity on campus. In May we were given permission to resume work on campus with new COVID-19 protocols in place. A new experiment was run with 50 wet towels hanging from regular clothes hangers on May 12, 2020.



Figure 3.3: The wet towels during testing of kelp dryer.

The temperature of the outside air was 51 °F (10.6 °C) with relative humidity about 69.8% and the weather was partly cloudy [1]. The dryer ran for a period of 3.82 hours and the towels were dried from a moisture content of about 64% (Wet basis) to 32% (wet basis), totaling about 27.5 kg of water removed. The temperature set point range for the drying was between 80 and 110 °F (26.7 – 43.3 °C). The water removal was determined by weighing the initially dry towels, the wet towels, and the towels after running the dryer. The operation ran with an air recycle rate of 75%, which helped to raise the humidity of the exhausting air and thus reducing the amount of lost drying capacity. The electric power consumed was about 0.41 kWh, which included power for the controls, the conveyor, and the fans. Only one burner and fan were used through this run which helped to reduce the electricity demand. The drying system is equipped with five temperature and humidity sensors which logged data every 0.5 seconds. Examination of the drying runs shows that as air passes through the drying chamber it decreases in temperature and gains humidity, as expected. It became apparent that partial recycling of the air is important for achieving high exit humidity and lower energy cost. In early runs, the data showed that air was short circuiting through the dryer and circumventing the hanging material being dried. This flaw was partly resolved by adding some metal sheeting at the top of the conveyor and partially blocking two ventilation ports. We also noted that the temperature measurement of the internal air was being affected by the level of recycle and furnace activity. It can also be seen that through the duration of the drying work, the exiting air shows a steady trend of rising temperature and decreasing RH.

Analysis of the energy dynamics for the system shows that more data are needed to consistently close the energy balance, particularly with respect to metering the propane used, the rate of air flow into and out of the system, as well as weather conditions, insolation rate and orientation to the sun. Estimated values for these variables suggest that insulating the walls of the container, except on bright sunny days, will likely be cost effective.

3.3 Modifications to Control Logic Simulation and Modeling

During one of our initial runs of the dryer the control system suffered a hardware failure. A faulty module in the PLC was replaced and reprogrammed with some modifications to the control system that included dampening out signal noise, which appeared to have induce unwanted shutdown of the furnaces and logging the position of the recycle control louvers.

3.4 Mass of Water Evaporated Calculation

Table 3.1 presented the data of the water mass that was evaporated from the seaweed during the drying process of the seaweed experiment that ran on June 17, 2021. The data that were recorded from the 9 hangers, at each cycle the dryer was stopped to check the moisture content during the drying process. During this experiment we created an imaginary cycle (0.1), this cycle represented the amount of moisture that was evaporated during the hanging of the seaweed. Hanging the seaweed from the hangers took about 2 hours to complete the loading of seaweeds. It was noticed that at the end of the time required to hang all of the seaweed, some of the hanging seaweed was notably drier than they had been before being hung up.

During this experiment there were four cycles, on the last cycle (the fourth cycle) the control system suffered a failure, the last cycle ran just for three minutes from the closing of the door of the dryer. At the end of the fourth cycle the door of the dryer was opened, and the last check of water mass was calculated. Because of the failure the drying process did not complete, and the seaweed drying was completed by exposing it to the sun for five hours. Fig 3.4 shows the mass of water evaporated from the seaweeds during the drying process. While the fig 3.5 shows how the drying rate varies with the time during the experiment that was running on June 17,2021.

No. of cycle	Cycle time (min)	Moisture content	Whole mass (g)	remaining water (g)	Water evaporated (g)
0	0	0.88	41309	36495	0
0.1	120	0.82	26927	22113	14381
1	62	0.73	17927	13113	9000
2	59	0.66	14108	9294	3602
3	60	0.57	11225	6411	2883
4	3	0.46	8834	4020	2391
5 (sun drying)	300	0	4814	0	4020

Table 3.1: Mass of water evaporated during drying process

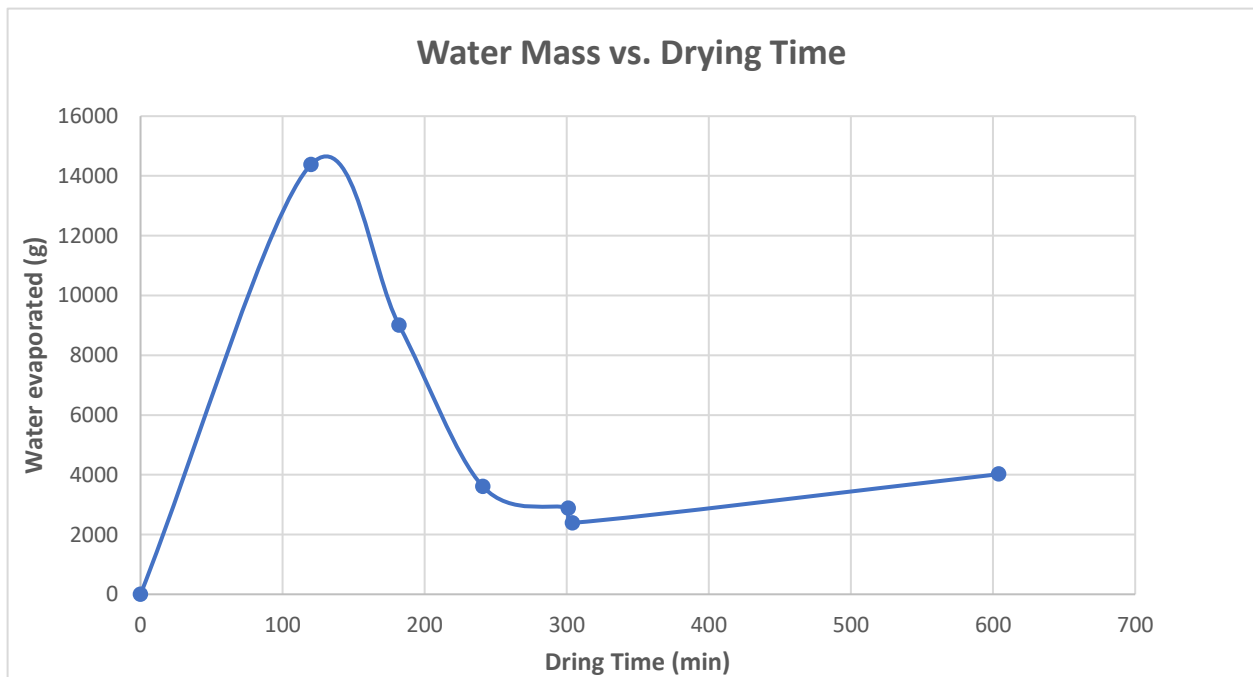


Figure 3.4: Water evaporated mass of seaweed during drying process.

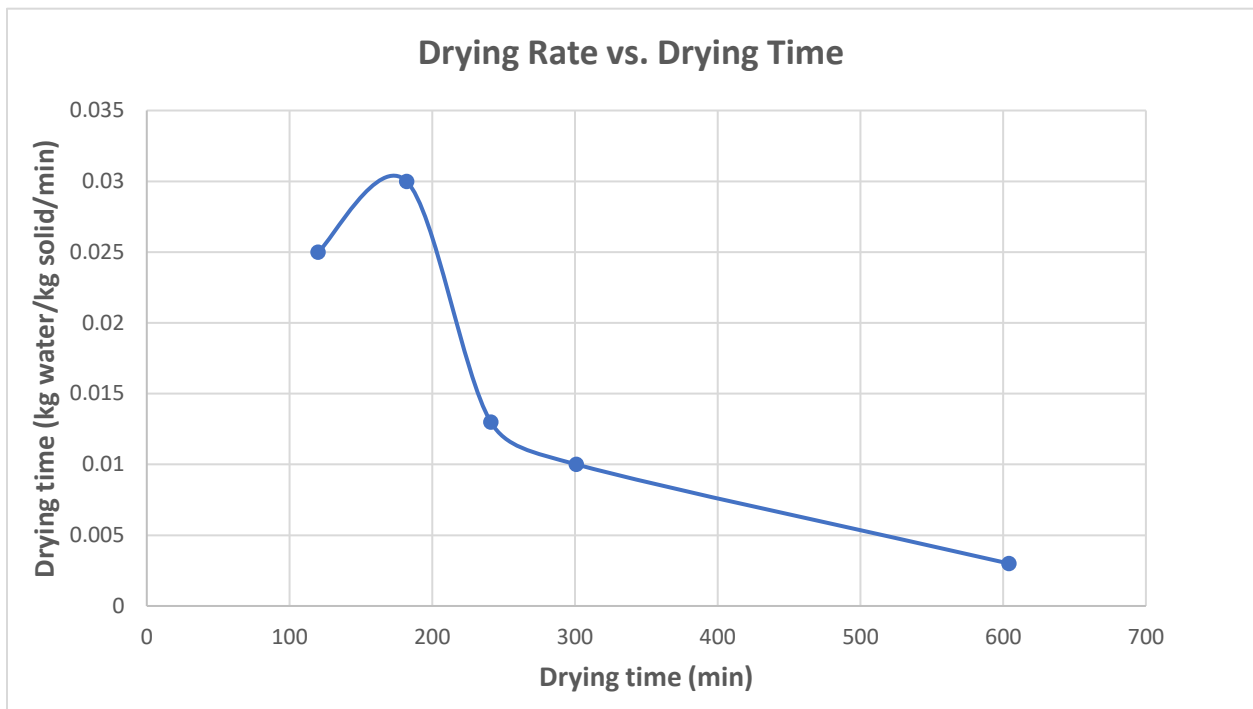


Figure 3.5: Drying rate of seaweed drying process varies with the time.

Also, another calculation was done on mass balance through the fan system. Table 3.2 shows the method that was used to calculate the mass balance of the fan system by considering the temperature and relative humidity of both the fresh air temperature (ambient air) and the inside temperature of the dryer to know how much water was in the air going in and out. For cycle 1, we believe that the deviation came from natural drying after weighing the seaweed and before running the dryer (ambient drying occurring), for which the cycle 0.1 in table 3.1 was developed. Towards the end of the experiment, the later cycles presented in table 3.2 matched the mass balance much better because the seaweed was partly dried and was not drying as quickly.

Cycle No.	Fan operating Time (hr)	g water/ kg (d.a) in	g water/ kg (d.a) out	g water/ kg (d.a) change	Water evaporated (end) g	g/hr water changed	kg/hr dry air	flow rate L/s	flow rate CFM	20% full flow	Fraction
1	1	6.922	16.69	9.8	23599	23599	2416	586	1242	485	0.39
2	1	6.492	13.79	7.3	3602	3602	494	120	254	485	1.91
3	1	6.492	11.03	4.5	2883	2883	635	154	327	485	1.49
4	1	6.313	9.83	3.5	2391	2391	680	165	349	485	1.39

Table 3.2: Mass balance calculation of the fan system.

3.5 Seaweed Drying Runs

Figure 3.6 (below) shows how the temperatures of different locations in the dryer cycled through time with the control system seeking to keep the system within the range of 95 – 100°F. This was done by monitoring the average temperature of the air near two walls of the dryer. One thermometer was mounted on the wall of the fresh air side of the drying chamber, while the other was mounted on the used air side of the dryer. The average of these two measurements was used to trigger the cycling of the furnace to keep the temperature within range. Other measurements of temperature shown in figure 3.6 were the air temperature of the heated air leaving the furnace, the air exiting the dryer, and fresh air coming in from outside. This latter measurement was made with a sensor located directly underneath the furnace intake and appears to have been affected by the condition of the recycled air. It can be seen that the temperature of the fresh intake air is affected by the furnace heating cycle. Figure 3.7 shows the relative humidity measurements in these same five locations of the dryer.

Comparing figures 3.6 and 3.7, it can be seen the RH level goes down as the temperature goes up, and vice versa. It can also be seen that through the duration of the drying work, the RH shows a downward trend as time goes by, which makes sense since the seaweed is losing moisture over time.

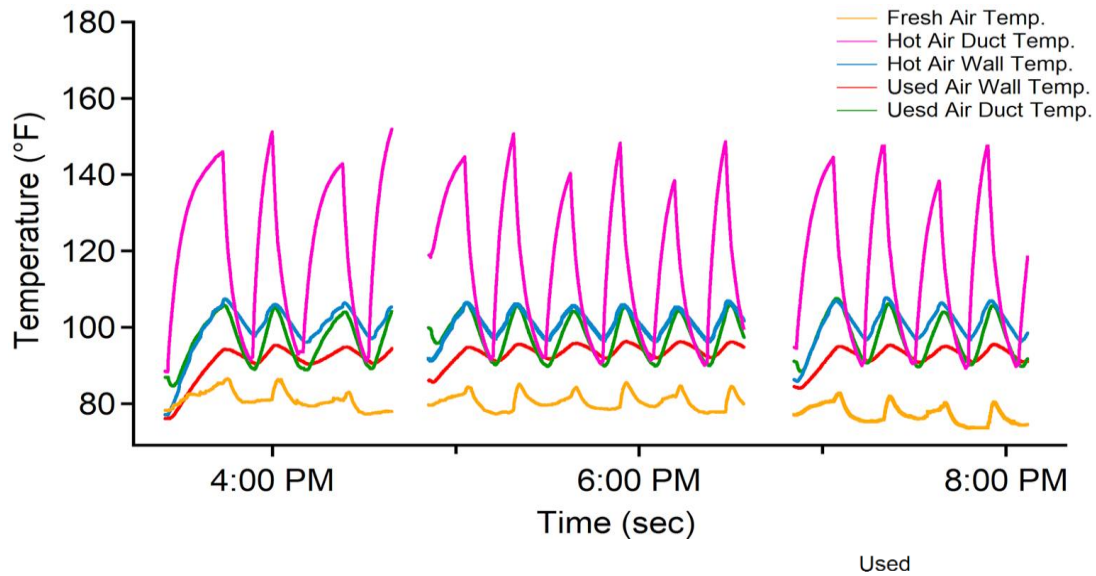


Figure 3.6: Graph represents temperature varies with time during June 8 seaweed experiment.

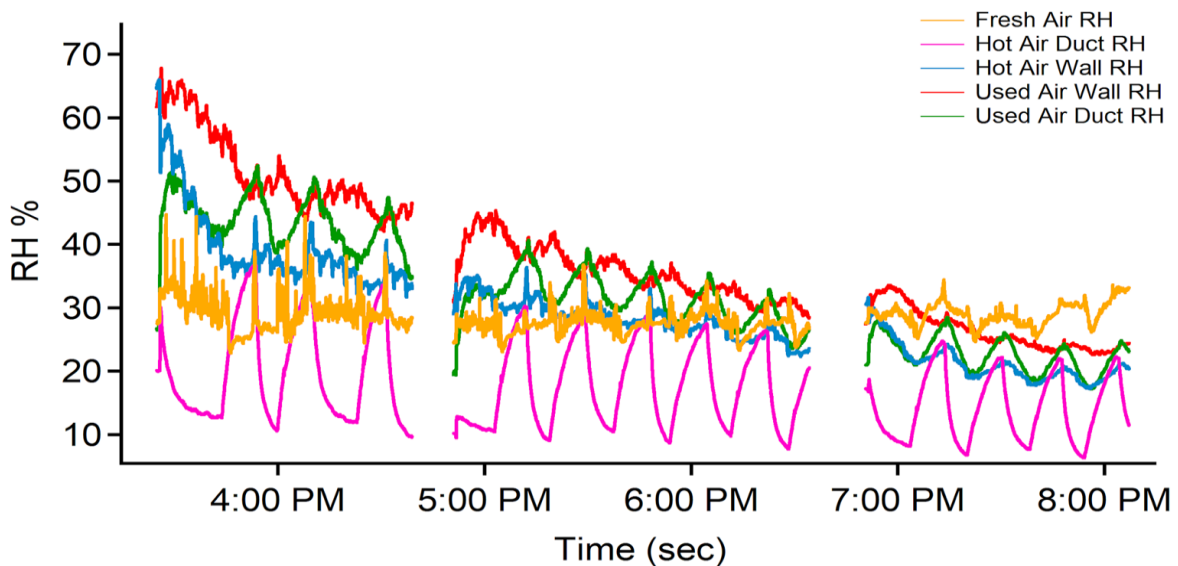


Figure 3.7: Graph represents RH varies with time during June 8 seaweed experiment.

3.6 Seaweed Drying Data

3.6.1 EasyLog USB Data

Fig. 3.8 below shows the data that were obtained from the small loggers (EasyLog USB) that were set outside of the dryer to test the temperature and relative humidity of the air passing through the inlet and outlet ducts. Logger 1 represents the temperature of the ambient air in the inlet duct that records air conditions during the time of drying. The data of logger 1 shows how the temperature of intake air is relatively constant and was not affected by the recycle system, as what the case for the data logged by the dryer control the computer. In contrast, the data of logger 11 shows how the temperature of the exhaust air duct was cycling in time with the heating cycles during the drying of the seaweed. Fig. 3.9 shows how the relative humidity of the inlet and outlet air varies with the time. Logger 1 shows how the relative humidity of inlet air varies with time and is relatively constant, while logger 11 shows how the relative humidity of exhaust air, also representative of the recycled air, cycling with time. Additional data that were obtained from USB loggers that were set outside the dryer at different locations on the exterior wall of the dryer, especially on the north and south facing walls of the drying chamber. The data obtained were recording the temperature and relative humidity of the air in contact with the exterior walls. Fig 3.10 below shows how the loggers 2 and 3 reflect the oscillations of temperature that coincide with the heating cycles inside the dryer, suggesting that the temperature inside the dryer is affecting the air temperature immediately outside the dryer. Logger 2 was set in the middle of the south wall and showed the highest temperature. This was because it was located on the sunny side of the dryer and also because the interior heating ducts were supplying freshly heated air along this portion of the wall. In contrast, logger 3, while it was also located on the sunny side of the dryer, was not positioned near the location of an interior heating duct, and thus the wall, and its adjacent exterior air, were somewhat cooler.

This cooler region at the east end of the south wall is also seen in the IR images of the wall of the dryer, showing that the region served by the heating ducts is demonstrably warmer than the end of the drying chamber where there are no heating ducts. This suggests that the air circulation inside the dryer is not resulting in uniform mixing of the interior air.

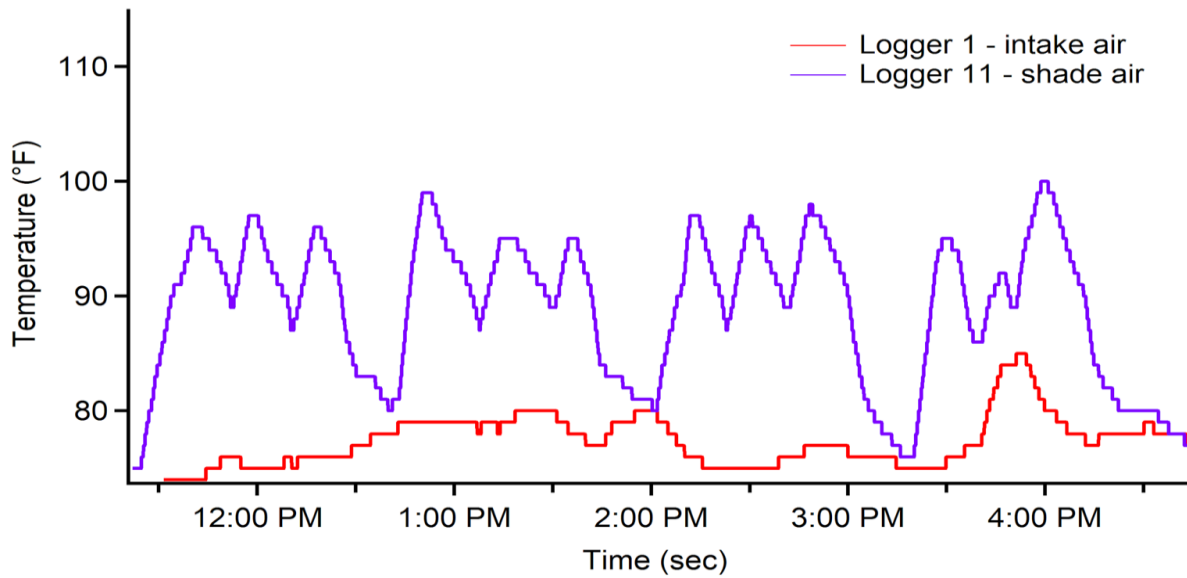


Figure 3.8: The temperature of the intake and exhaust air duct that varies with time.

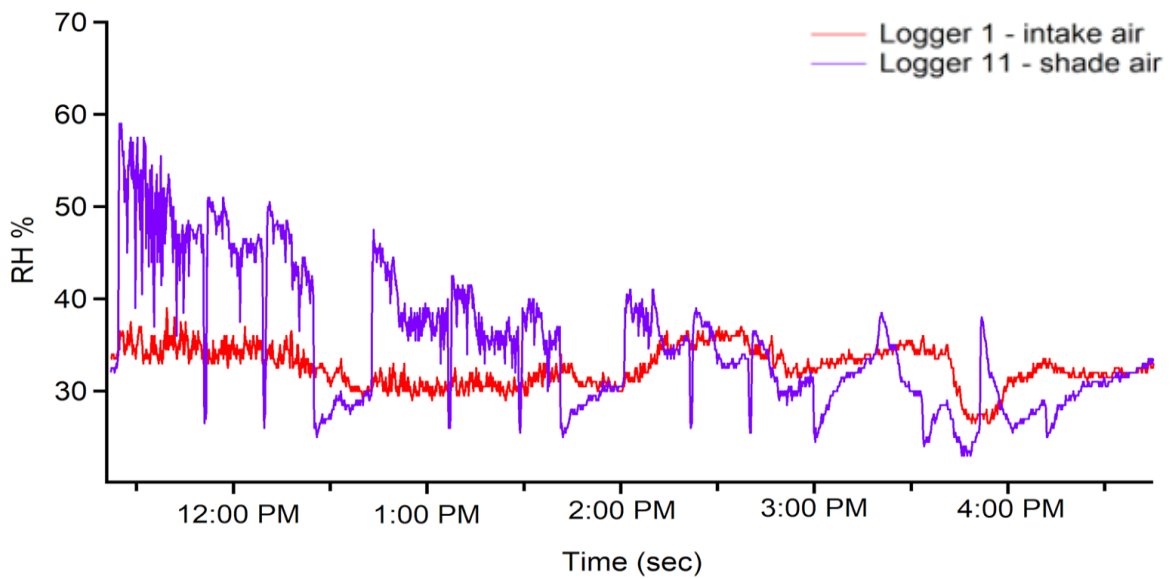


Figure 3.9: The relative humidity of the intake and exhaust air duct that varies with time.

Data loggers 2 and 3 also showed the dramatic effects of sunshine on the temperature of the air near the exterior dryer walls. In this experiment, the sun was shining brightly up until about 1:00 o'clock, while the skies had become mostly cloudy by 2:00 o'clock. The data that were recording by loggers 4 and 5, located on the northern wall of the dryer, showed lower temperatures as showed in fig 3.10.

As expected, the temperature difference between the north and south walls were more pronounced while the sun was shining, and less so while it was cloudy. The two loggers on the north wall were also on the side of the dryer where used air was being removed from the dryer, as opposed to the south side which was receiving freshly heated air.

Thus, the north wall was exposed to the cooler spent air inside the dryer, which resulted in less heat transfer to the north wall. It can also be seen that the height at which the sensors are mounted on the exterior wall affects the temperature. On the north wall, Logger 4 was located low on the wall, while logger 5 was mounted higher up.

Not surprisingly the higher mounted sensor detected warmer temperature, which confirms the hypothesis that the air in the interior of the drying chamber is not very well mixed, and there appears to be a temperature gradient from bottom to top inside the dryer. Fig. 3.11 shows how the relative humidity of these loggers varied with the time of drying process.

It can be seen that in general, the air alongside the exterior dryer walls reflects lower relative humidity when the wall is warmer, and higher humidity when the wall offers less heat to the ambient air.

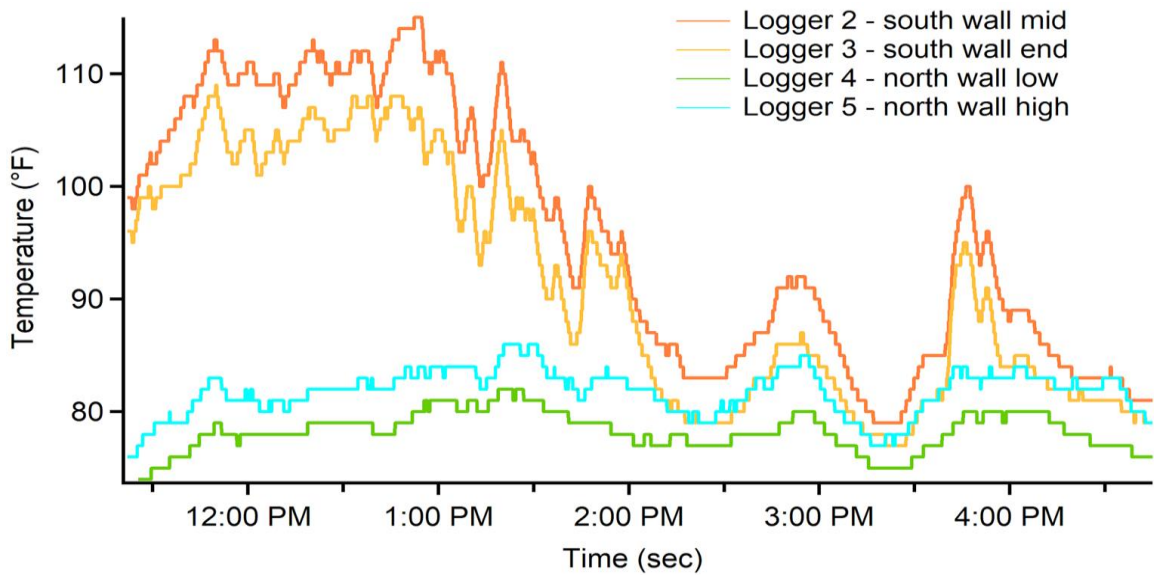


Figure 3.10: Represents the temperature of four loggers that were set at different locations of the south and north wall of the dryer that varies with the time.

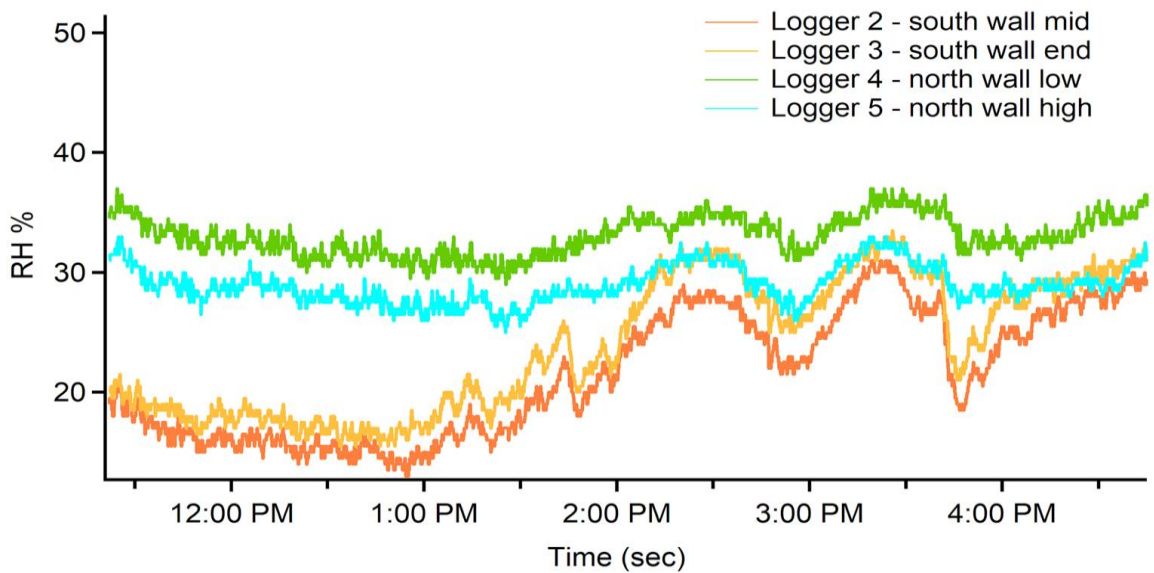


Figure 3.11: Represents the Relative humidity of four loggers that were set at different locations of the south and north wall of the dryer that varies with the time.

Fig. 3.12 shows results obtained from USB loggers that were set at different locations inside the drying chamber where the seaweed was hanging. The data obtained from these sensors showed how the temperature inside the chamber varied with the time of the drying process. Logger 8 was set on the floor of the chamber that showed a very low temperature compared with the other loggers. This confirms the presence of a vertical stratification of temperature inside the chamber. Loggers 6 and 7, both located high up in the dryer, reflect a temperature difference of a few degrees F between them, caused by the absence (logger 6) or presence (logger 7) of direct heating air supply. Logger six was located about 6 feet from the nearest heating duct, while logger 7 was within a few feet of two heating duct outlets. Fig. 3.13 shows how the relative humidity of these loggers varied with the time of drying. As expected, RH and temperature are inversely related as the heating cycles operate. One exception is the times when the chamber doors were opened to collect seaweed mass data. A few times during the experiments the drying system was paused, and the doors of the dryer were opened so that we could measure the mass of the drying seaweed. In these cases, (occurring at around 12:30, 1:45 and 3:15) the temperature would go down, since the heating system was turned off and cooler exterior air was allowed into the drying chamber, and the humidity would also go down, since opening the doors allowed fresh, less humid air to enter the drying chamber. Logger 9, which was located on the conveyor of the dryer, shows an interesting pattern that appears to coincide with the rotation of the conveyor. Each rotation of the conveyor took about 3 minutes, and during each cycle, the seaweed would be exposed at one time to the freshly heated air entering on the south side of the dryer, and at other times it was exposed to the cooler, more humid air on the exiting side of the dryer. These short cycles are reflected in the humidity data shown in figure 3.13, where the short cycle oscillations reflect these rotations from one side of the dryer to the next. The amplitude of these variations wane as the drying process progresses since the moisture content of the seaweed is decreasing as the drying process continues.

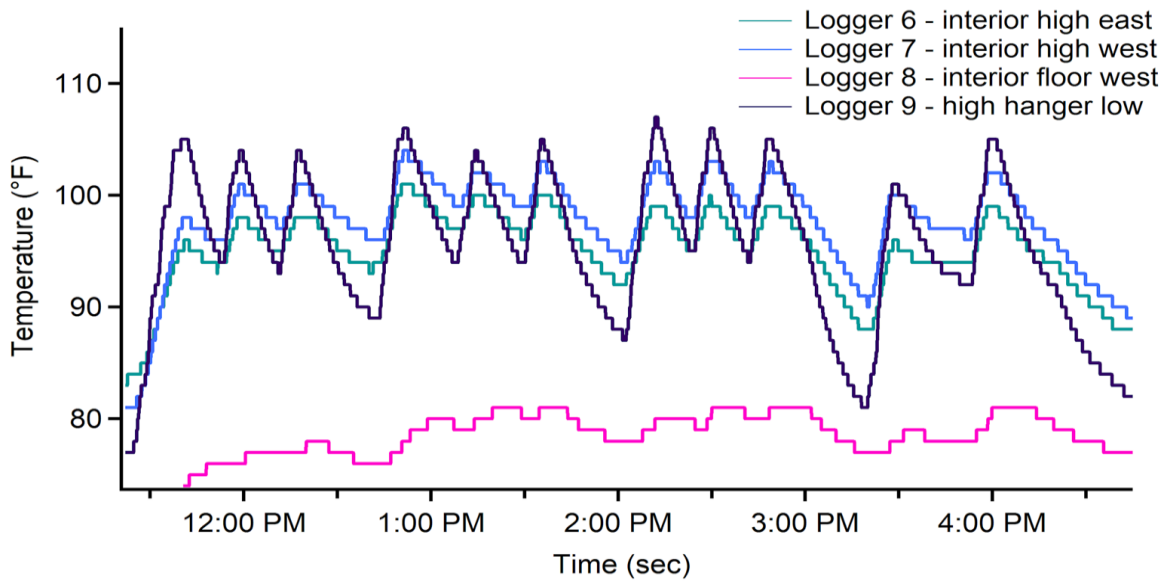


Figure 3.12: Represents the temperature of the four loggers that were set at different locations inside the chamber that varies with the time.

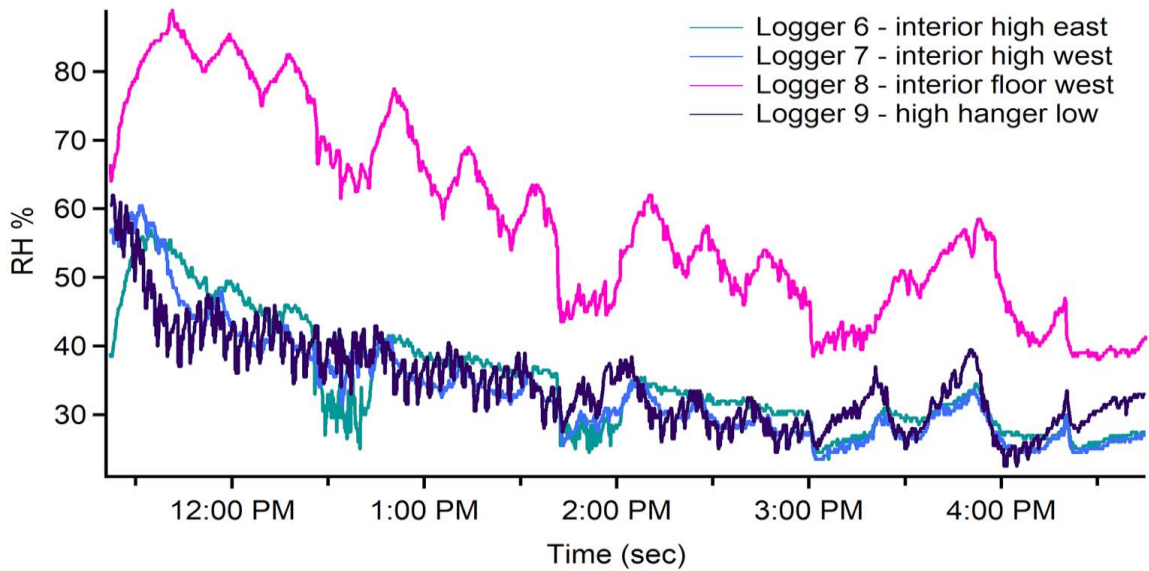


Figure 3.13: Represents the relative humidity of the four loggers that were set at different locations inside the chamber that varies with the time.

3.6.2 Infrared (IR) Camera Data

Data from both the small loggers and the IR camera showed temperature gradients between the interior and exterior of the dryer that were affected by the heating cycles of the furnace and the amount of insolation from outside.

Fig. 3.14 shows a comparison between the control system data of the computer, the data of the small loggers and the data of the IR images during the cloudy time of the day. The “Fresh vent T” is the air temperature of heated air entering the drying chamber while the “warm wall T” represents the air temperature in the up-stream side of drying the chamber. This was one of two sensors used to control the inside temperature at around 100°F. “South wall mid” and “South wall end” are IR measurements and show that the walls of the dryer are not as warm as the dryer interior, therefore the dryer is losing heat through the wall.

The “Logger 2” and “Logger 3” data are measuring the air temperature next to the outside of the drying wall. These temperatures are lower, respectively, than their IR counterparts, confirming that there is a temperature gradient descending from the interior air, through the solid wall, and then on to the exterior air.

These data were collected while the sky was cloudy. Similar data while the sun was shining as shown in fig. 3.15 showed that the wall and outside air were warmer than shown in fig 3.14, and thus the temperature gradient flattened out towards the wall, suggesting less heat loss while the wall was irradiated.

The interior temperature was generally the same regardless of insolation, since the temperature control system was controlling the temperature to ~ 100°F. Figure 3.16 shows temperature gradients between the interior and exterior of the dryer during the cloudy and sunny weather.

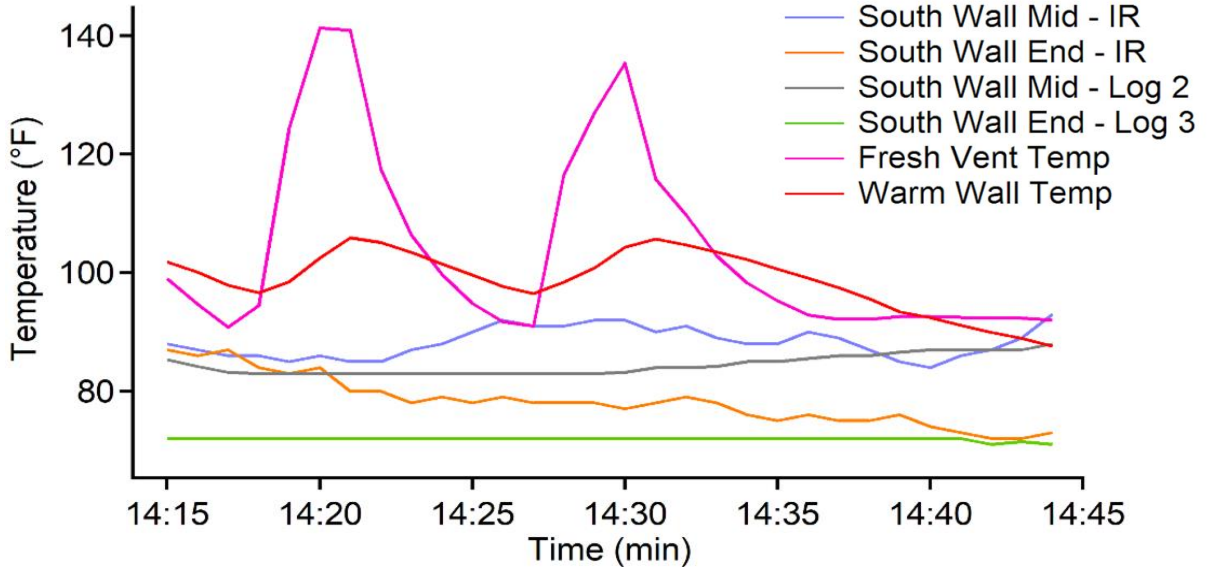


Figure 3.14: Shows simultaneous data from the different sources: the IR camera (South wall mid, End south wall mid), the control system of the dryer (Fresh vent T, Warm T), and the small loggers (logger 2, logger 3). These data were collected during cloudy weather.

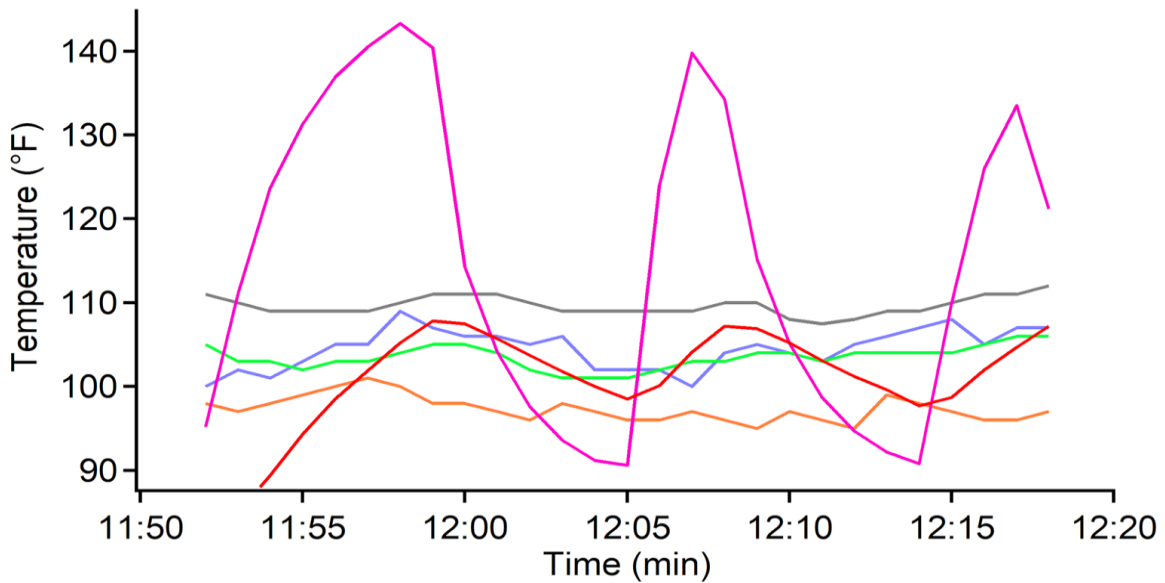


Figure 3.15: Shows simultaneous data from the different sources: the IR camera (South wall mid, End south wall mid), the control system of the dryer (Fresh vent T, Warm T), and the small loggers (logger 2, logger 3). These data were collected during sunny weather.

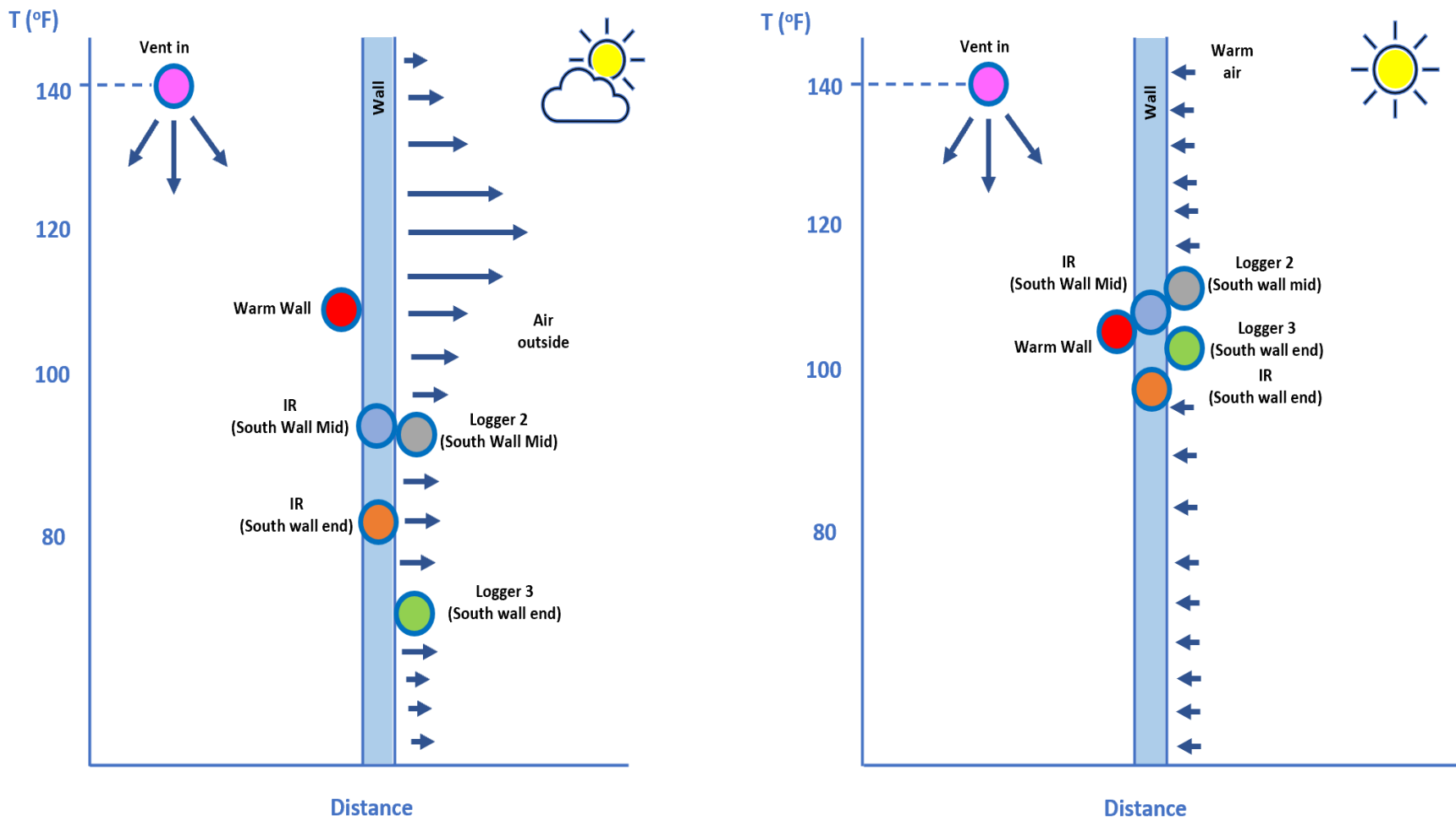


Figure 3.16: The comparison between the cloudy and sunny weather.

3.7 Aspen Simulation of The Dryer: Input Air, Output Air, Short Circuiting

3.7.1 Aspen Simulation of Seaweed Throughput Prediction and Energy Cost

Results from the ASPEN thermodynamic model showed the response of process temperature variables (air temperature exiting the heater and the temperature of exhaust air) to the ambient air temperature and humidity. The model also determined the amount of seaweed throughput could be sustained at different ambient air conditions and the energy costs of the fan and heater systems. Results showed that energy costs decreased with increasing ambient air temperature and decreased air flow, but in some cases high air flow was necessary to maintain a heated air temperature of no more than 50°C. Fig. 3.17 illustrates these trends for ambient air entering the drying system at 50% RH.

Other simulations looked at different RH values ranging from 0 to 100% RH in the ambient air. Trends with higher inlet RH showed decreased seaweed throughput. Fig. 3.18 showed results from simulations plotting the effects of energy costs in response to RH. The figure showed that ambient RH increases fuel costs to some degree but mostly impacts the amount of power needed for the fans, since the higher ambient RH requires the use of more air per kg of seaweed.

The results from the thermodynamic model represented upper limits to the performance of the system since the model assumes fully saturated air in the exhaust air. Note that in these simulations shown in figures 3.17 and 3.18, the choice of four potential air flow rates is for illustrative purposes and do not representative of out built drying system. The furnaces installed in our dryer did not have the capability of running different fan speeds and had only on/off controls for the fans.

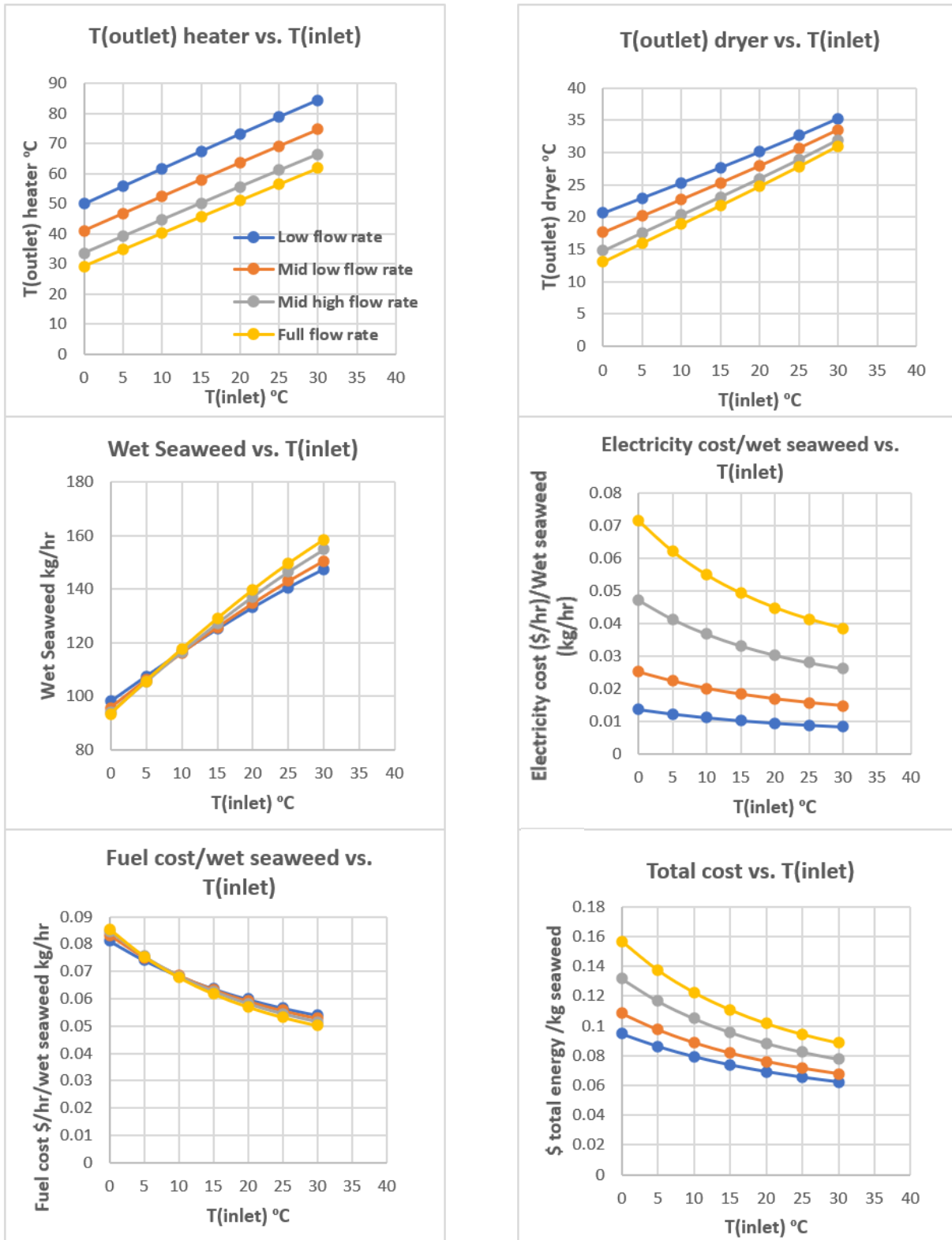


Figure 3.17: Responses of dryer performance (heated and outlet air temperatures, mass throughput, electricity, fuel, and total energy costs) versus ambient inlet air temperature at 50% RH.

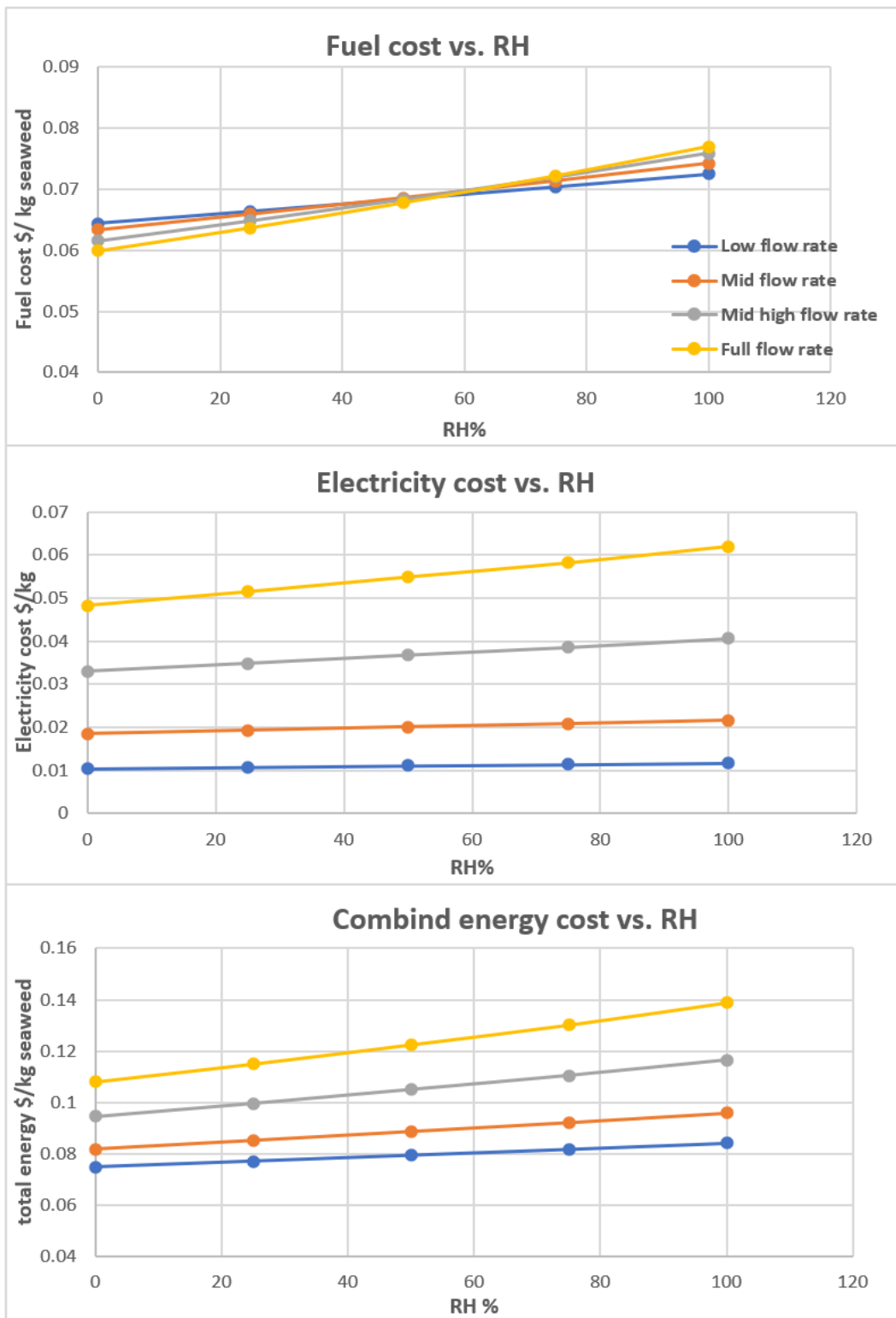


Figure 3.18: Trends of energy costs (Fan electricity, heater fuel and combined) with respect to ambient air RH at ambient air temperature of 10°C.

3.7.2 Furnaces and Fans Effects on Energy Balance

Seaweed throughput was largely accomplished using either one or two furnaces, with the two-furnace condition drying nearly twice as much seaweed as the single furnace, shown in fig. 3.19 (A). Each furnace had one fan that operated at a steady rate. Both furnaces could be operated at the same time, each with their fans running, here referred to as two furnaces, two fans (2,2) configuration, or one furnace could be operated, giving a one furnace, one fan (1,1) configuration. It was also possible to run a one furnace, two fans mode (1,2), which involved operating one furnace with its fan, and also running just the fan in the second furnace. In practice, the (1,2) configuration was only applied when the heating system was cycling from one furnace to the other: while one furnace was shutting off and cooling down with its fan running, the other was running its fan and waiting to be started again. Increasing air throughput by running two fans with only one furnace (1,2) increased drying capacity above the (1,1) configuration a small amount, primarily at higher ambient temperature. The two systems with the same number of fans and furnaces, (2,2) and (1,1), operated at approximately the same temperatures for both the air exiting the heater as shown in fig. 3.19 (B) and the air exiting the dryer in fig. 3.19 (C).

Conversely, the (1,2) system showed lower temperatures for both the heated air and the exit air figures 3.19 (B) and (C). These results are consistent with the fact that the simulation model assumed saturated air at the exit. The (2,2) system gave slightly higher temperatures than the (1,1) system because the higher air flow rate through the same ductwork resulted in more back pressure for the two fan systems, and thus less than double the air flow, resulting in slightly higher temperatures.

Fuel cost decreases as ambient air temperature increases, and fuel costs on a per kg seaweed are very similar for the (1,1) and (2,2) systems as in fig. 3.19 (D), while the (1,2) system enjoyed lower fuel cost, but higher fan cost on a per kg seaweed basis fig. 3.19 (E). Combining the fuel and power costs for the fans shows that the most economical system on a per kg seaweed basis is the (1,1) system and the most expensive is the (1,2) system, fig. 3.19 (F). This outcome is a result of dramatically higher power costs to run two fans. These results need to be verified experimentally, since the calculations depend heavily on the pressure drop in the system, which is not yet known, but it was observed that the power meter reading for the entire dryer system registered significantly more power demand while running two fans instead of one.

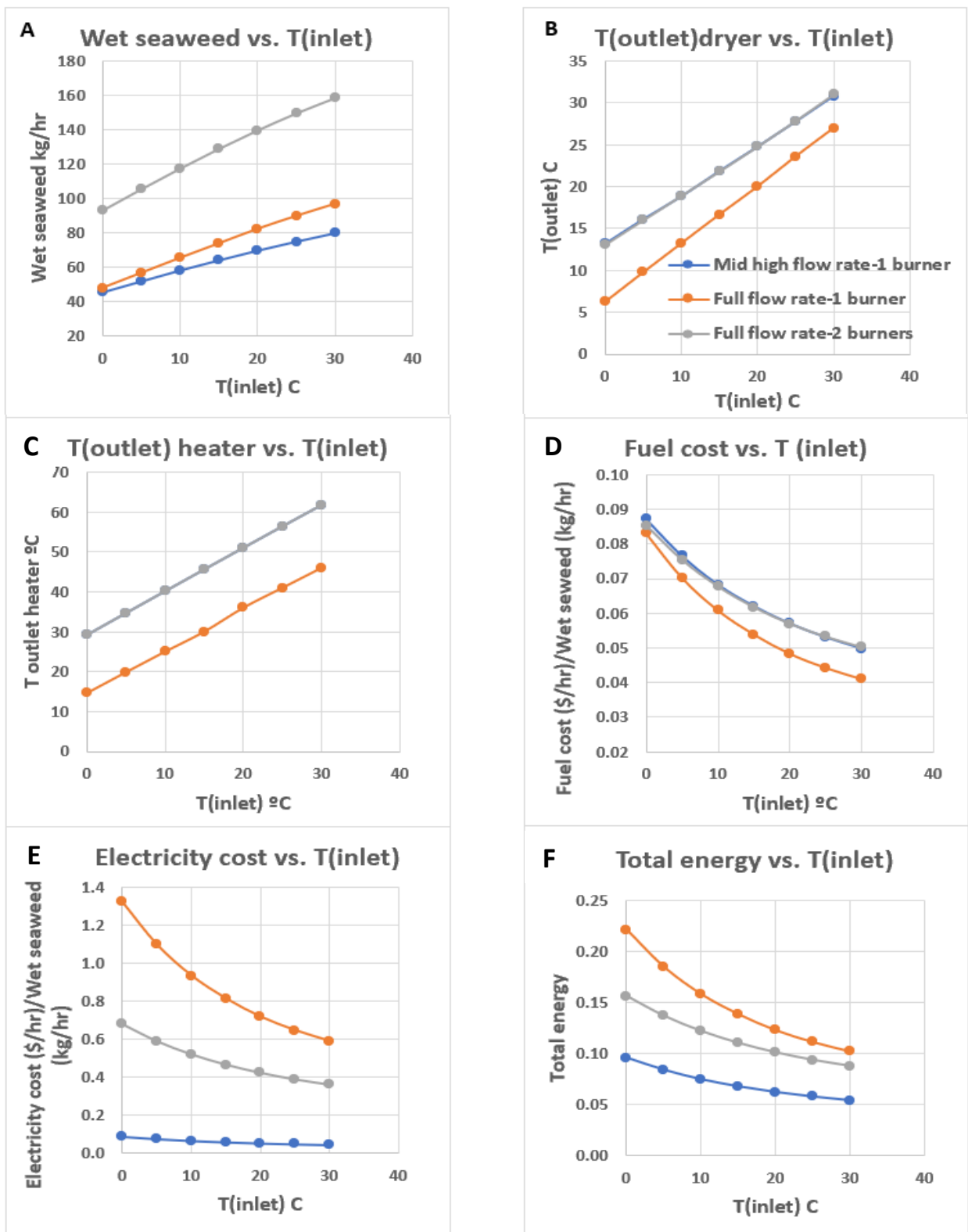


Figure 3.19: Responses of dryer performance (heated and outlet air temperatures, mass throughput, electricity, fuel, and total energy costs) versus ambient inlet temperature at 50% RH.

CHAPTER 4

CONCLUSIONS AND FUTURE WORK

4.1. Conclusions

The main objectives of this study were: Designing and testing the performance of the dryer system, improving, and addressing defects in the design; developing mass and energy balances to understand the operation and efficiency of the system, including the use of an Aspen Plus process modeling program to simulate the energy flows of the real drying process of the sugar kelp. The results that were obtained from drying runs show that:

- The air temperature and humidity are inversely related.
- Recycling is important to reduce the energy cost and raise exit humidity.
- The temperature measurement of the intake air logged by the control computer was being affected by the level of recycle and furnace activity.
- As air passes through the drying chamber, it decreases in temperature and gains humidity, with the exiting air showing a steady trend of rising temperature and decreasing RH as the process progresses. Partial recycling of the air achieves higher exit humidity, which reduces energy losses.
- It became apparent through the operation of the dryer that considerable heat losses were caused by conduction through the dryer walls, and if insulation were to be added, even at a modest level of R1 insulation, significant energy savings could be realized.
- It was observed that solar gain could be a significant source of energy, however this benefit would be diminished if the dryer were to be insulated. Thus, there appears to be a need for

optimizing the use of insulation. Potential solutions could be removable insulation, such as perhaps a large insulating blanket that could be rolled back on sunny days.

- Data from both the small loggers and the IR camera showed temperature gradients between the interior and exterior that were affected by the heating cycles of the furnace and also the amount of insolation from outside.
- The air flow configuration of the drying chamber is very important for making best use of the heated air and reducing short circuiting of air through the drying chamber.

Results that we obtained from the thermodynamic model (Aspen Plus Diagram) showed that:

- The outcomes of the process temperature variables (temperature of air exiting the heater and the temperature of the exhaust air) were affected by the ambient air temperature and humidity.
- The model also determined the amount of seaweed through put could be sustained at different ambient air temperature and humidity conditions.
- Energy costs decreased with increasing ambient air temperature and decreased air flow but in some cases high air flow was necessary to maintain a heated air temperature of no more than 50 °C.
- Runs with higher inlet RH show decreased seaweed throughput.
- Ambient RH increases fuel cost to some degree but mostly impacts the amount of power needed for the fans, since the higher ambient RH requires the use of more air per kg of seaweed.

4.2. Future Work

While the dryer worked well, and several experiments were run through two seasons of seaweed harvesting, there remain some needs to be addressed in the future:

- Better instrumentation would provide more confidence in mass and energy balance assessments (metering the propane, temperatures of different surfaces of the dryer, measuring the air flow into and out of the system).
- Modify and improve control logic and user interface to facilitate operations.
- Optimizing use of insulation. Develop removable insulation, perhaps a large removable insulating blanket that could be stored in the drying chamber when not in use or while in transport.
- Improve the design of new hangers to speed up the hanging process and reduce labor.
- Run more seaweeds experiments at different times of the harvest season to collect more variety of ambient conditions data.
- Improve and calibrate fluid flow and transport models of the drier.
- Improve a model for solar effects on energy balance.

REFERENCES

- [1] C. L. Hurd, P. J. Harrison, K. Bischof and C. S. Lobban. *Seaweed Ecology and Physiology*. C. L. Hurd, P. J. Harrison, K. Bischof and C. S. Lobban 2014.
- [2] M. Djaeni and D. A. Sari, “Low Temperature Seaweed Drying Using Dehumidified Air,” *Procedia Environmental Sciences*, vol. 23, no. Ictcred 2014, pp. 2–10, 2015.
- [3] S. Gupta, S. Cox, and N. Abu-Ghannam, “Effect of different drying temperatures on the moisture and phytochemical constituents of edible Irish brown seaweed,” *LWT - Food Science and Technology*, vol. 44, no. 5, pp. 1266–1272, 2011.
- [4] Y. Athukorala, K. N. Kim, and Y. J. Jeon, “Antiproliferative and antioxidant properties of an enzymatic hydrolysate from brown alga, *Ecklonia cava*,” *Food and Chemical Toxicology*, vol. 44, no. 7, pp. 1065–1074, 2006.
- [5] G. Bonanno and M. Orlando-Bonaca, “Chemical elements in Mediterranean macroalgae. A review,” *Ecotoxicology and Environmental Safety*, vol. 148, no. October 2017, pp. 44–71, 2018.
- [6] M. B. Kasimala, L. Mebrahtu, P. P. Magoha, and D. G. Asgedom, “A Review on Biochemical Composition and Nutritional Aspects of Seaweeds,” *Caribbean Journal of Science and Technology*, vol. 3, no. January 2015, pp. 789–797, 2015.
- [7] J. M. Lorenzo et al., “Proximate Composition and Nutritional Value of Three Macroalgae: *Ascophyllum nodosum*, *Fucus vesiculosus* and *Bifurcaria bifurcata*,” *Marine Drugs*, vol. 15, no. 11, pp. 1–11, 2017.
- [8] S. L. Holdt and S. Kraan, “Bioactive compounds in seaweed: functional food applications and legislation,” *Journal of Applied Phycology*, vol. 23, no. 3, pp. 543–597, 2011.
- [9] V. J. Chapman and D. J. Chapman. *Seaweeds and their Uses*. Chapman and Hall Ltd., 1980.

- [10] R. Peñalver, J. M. Lorenzo, G. Ros, R. Amarowicz, M. Pateiro, and G. Nieto, "Seaweeds as a Functional Ingredient for a Healthy Diet," *Marine Drugs*, vol. 18, no. 6, 2020.
- [11] Food and Agriculture Organization of the United Nations (FAO), "FAO Globefish Research Programme," vol. 124, p. 120, 2018.
- [12] Dennis J. McHugh and Australian Defence Force Academy. A guide to the seaweed industry. FAO 2003.
- [13] C. K. Tseng, "The past, present and future of phycology in China," *Hydrobiologia*, vol. 512, pp. 11–20, 2004.
- [14] M. P. Pati, S. Das Sharma, L. Nayak, and C. R. Panda, "Uses of seaweed and its application to human welfare: A review," *International Journal of Pharmacy and Pharmaceutical Sciences*, vol. 8, no. 10, pp. 12–20, 2016.
- [15] C. Dawczynski, R. Schubert, and G. Jahreis, "Amino acids, fatty acids, and dietary fibre in edible seaweed products," *Food Chemistry*, vol. 103, no. 3, pp. 891–899, 2007.
- [16] A. Jimenez-Escrig and F. J. Sanchez-Muniz, "Dietary Fibre from Edible Seaweeds: Chemical Structure, Physicochemical Properties and Effects on Cholesterol Metabolism," *Nutrition Research*, vol. 20, No. 4, pp. 585-598, 2000.
- [17] K. J. McDermid and B. Stuercke, "Nutritional composition of edible Hawaiian seaweeds," *Journal of Applied Phycology*, vol. 15, no. 6, pp. 513–524, 2003.
- [18] V. K. Dhargalkar and N Pereira, "Seaweed: Promising Plant of The Millennium," *Science and Culture*, vol. 5, pp. 60-66, 2005.
- [19] X. G. Keyimu and M. Abuduli, "Seaweed Composition and Potential Uses," *International Journal of ChemTech Research*, vol. 12, no. 01, pp. 105–111, 2019.

- [20] S. Redmond, S. Belknap, and R. C. Uchenna, "Aquaculture in shared waters fact sheet - Kelp Aquaculture," Maine Sea Grant Publications, vol. 127, 2016.
- [21] M. H. Norziah and C. Y. Ching, "Nutritional composition of edible seaweed *Gracilaria changgi*," *Food Chemistry*, vol. 68, no. 1, pp. 69–76, 2000.
- [22] P. Matanjun, S. Mohamed, N. M. Mustapha, and K. Muhammad, "Nutrient content of tropical edible seaweeds, *Eucheuma cottonii*, *Caulerpa lentillifera* and *Sargassum polycystum*," *Journal of Applied Phycology*, vol. 21, no. 1, pp. 75–80, 2009.
- [23] D. Vuong, M. Kaplan, H. J. Lacey, A. Crombie, E. Lacey, and A. M. Piggott, "A study of the chemical diversity of macroalgae from South Eastern Australia," *Fitoterapia*, vol. 126, no. October 2017, pp. 53–64, 2018.
- [24] J. Ortiz et al., "Dietary fiber, amino acid, fatty acid and tocopherol contents of the edible seaweeds *Ulva lactuca* and *Durvillaea antarctica*," *Food Chemistry*, vol. 99, no. 1, pp. 98–104, 2006.
- [25] P. Kaladharan, N. Kaliaperumal, and J. R. Ramalingam, "Seaweeds-products, processing and utilization," *Marine Fisheries Information Service*, vol. 157, pp.1-9, 1998.
- [26] S. M. Kim et al., "A potential commercial source of fucoxanthin extracted from the microalga *Phaeodactylum tricornutum*," *Applied Biochemistry and Biotechnology*, vol. 166, no. 7, pp. 1843–1855, 2012.
- [27] N. M. Sachindra, M. K. W. A. Airanthi, M. Hosokawa, and K. Miyashita, "Radical scavenging and singlet oxygen quenching activity of extracts from Indian seaweeds," *Journal of Food Science and Technology*, vol. 47, no. 1, pp. 94–99, 2010.
- [28] K. Kanazawa et al., "Commercial-scale Preparation of Biofunctional Fucoxanthin from Waste Parts of Brown Sea Algae *Laminaria japonica*," *Food Science and Technology Research*, vol. 14, no. 6, pp. 573–582, 2008.

- [29] H. T. V. Lin, W. J. Lu, G. J. Tsai, C. Te Chou, H. I. Hsiao, and P. A. Hwang, “Enhanced anti-inflammatory activity of brown seaweed *Laminaria japonica* by fermentation using *Bacillus subtilis*,” *Process Biochemistry*, vol. 51, no. 12, pp. 1945–1953, 2016.
- [30] A. Ramu Ganesan et al., “A comparison of nutritional value of underexploited edible seaweeds with recommended dietary allowances,” *Journal of King Saud University - Science*, vol. 32, no. 1, pp. 1206–1211, 2020.
- [31] H. A. R. Suleria, S. Osborne, P. Masci, and G. Gobe, “Marine-based nutraceuticals: An innovative trend in the food and supplement industries,” *Marine Drugs*, vol. 13, no. 10, pp. 6336–6351, 2015.
- [32] I. Priyan Shanura Fernando, K. N. Kim, D. Kim, and Y. J. Jeon, “Algal polysaccharides: potential bioactive substances for cosmeceutical applications,” *Critical Reviews in Biotechnology*, vol. 39, no. 1, pp. 99–113, 2019.
- [33] V. Jesumani, H. Du, M. Aslam, P. Pei, and N. Huang, “Potential use of seaweed bioactive compounds in skincare—a review,” *Marine Drugs*, vol. 17, no. 12, pp. 1–19, 2019.
- [34] S. Kim, editor. *Advances in Food and Nutrition Research, Volume 73, Marine Carbohydrates: Fundamentals and Applications, Part B*. Elsevier Inc., 2014.
- [35] O. Benjama and P. Masniyom, “Biochemical composition and physicochemical properties of two red seaweeds (*Gracilaria fisheri* and *G. tenuistipitata*) from the Pattani Bay in Southern Thailand,” *Songklanakarin Journal of Science and Technology*, vol. 34, no. 2, pp. 223–230, 2012.
- [36] T. Morais et al., “Seaweed potential in the animal feed: A review,” *Journal of Marine Science and Engineering*, vol. 8, no. 8, pp. 1–24, 2020.
- [37] <https://foodtank.com/news/2018/09/have-your-food-and-eat-the-wrapper-too/>
- [38] A. Vergara-Fernández, G. Vargas, N. Alarcón, and A. Velasco, “Evaluation of marine algae as a source of biogas in a two-stage anaerobic reactor system,” *Biomass and Bioenergy*, vol. 32, no. 4, pp. 338–344, 2008.

- [39] N. C. Afonso, M. D. Catarino, A. M. S. Silva, and S. M. Cardoso, "Brown macroalgae as valuable food ingredients," *Antioxidants*, vol. 8, no. 9, 2019.
- [40] I. Muzzalupo, editor. *Food Industry*. Intechopen, 2013.
- [41] J. Fleurence and I. Levine, editors. *Seaweed in Health and Disease Prevention*. Elsevier Inc., 2016.
- [42] S. Mohamed, S. N. Hashim, and H. A. Rahman, "Seaweeds: A sustainable functional food for complementary and alternative therapy," *Trends in Food Science and Technology*, vol. 23, no. 2, pp. 83–96, 2012.
- [43] J. M. Adams, J. A. Gallagher, and I. S. Donnison, "Fermentation study on *saccharina latissima* for bioethanol production considering variable pre-treatments," *Journal of Applied Phycology*, vol. 21, no. 5, pp. 569–574, 2009.
- [44] A. Fudholi, K. Sopian, M. Y. Othman, and M. H. Ruslan, "Energy and exergy analyses of solar drying system of red seaweed," *Energy and Buildings*, vol. 68, no. PARTA, pp. 121–129, 2014.
- [45] G. B. Pradana, K. B. Prabowo, R. P. Hastuti, M. Djaeni, and A. Prasetyaningrum, "Seaweed drying process using tray dryer with dehumidified air system to increase efficiency of energy and quality product," *IOP Conference Series: Earth and Environmental Science*, vol. 292, no. 1, 2019.
- [46] A. J. N. Khalifa, A. M. Al-Dabagh, and W. M. Al-Mehemdi, "An Experimental Study of Vegetable Solar Drying Systems with and without Auxiliary Heat," *ISRN Renewable Energy*, vol. 2012, pp. 1–8, 2012.
- [47] H. M. Fargali, A. E. S. A. Nafeh, F. H. Fahmy, and M. A. Hassan, "Medicinal herb drying using a photovoltaic array and a solar thermal system," *Solar Energy*, vol. 82, no. 12, pp. 1154–1160, 2008.

- [48] A. Fudholi, K. Sopian, M. Y. Othman, and M. H. Ruslan, "Energy and exergy analyses of solar drying system of red seaweed," *Energy and Buildings*, vol. 68, no. PARTA, pp. 121–129, 2014.
- [49] S. Suherman, M. Djaeni, A. C. Kumoro, R. A. Prabowo, S. Rahayu, and S. Khasanah, "Comparison Drying Behavior of Seaweed in Solar, Sun and Oven Tray Dryers," *MATEC Web of Conferences*, vol. 156, pp. 0–3, 2018.
- [50] K. Wong and P. C. Cheung, "Influence of drying treatment on three *Sargassum* species: 1. Proximate composition, amino acid profile and some physico-chemical properties," *Journal of Applied Phycology*, vol. 13, no. 1, pp. 43–50, 2001.
- [51] A. Collignan and A. L. Raoult-Wack, "Dewatering and salting of Cod by immersion in concentrated sugar/salt solutions," *Lebens Wiss-Technol.*, vol.27, 259–264, 1994
- [52] A. Fudholi, K. Sopian, M. H. Ruslan, M. A. Alghoul, and M. Y. Sulaiman, "Review of solar dryers for agricultural and marine products," *Renewable and Sustainable Energy Reviews*, vol. 14, no. 1, pp. 1–30, 2010.
- [53] S. Suna, "Effects of hot air, microwave and vacuum drying on drying characteristics and in vitro bioaccessibility of medlar fruit leather (pestil)," *Food Science and Biotechnology*, vol. 28, no. 5, pp. 1465–1474, 2019.
- [54] S. A. Aboud, A. B. Altemimi, A. R. S. Al-Hilphy, L. Yi-Chen, and F. Cacciola, "A comprehensive review on infrared heating applications in food processing," *Molecules*, vol. 24, no. 22, 2019.
- [55] G. Yadav, N. Gupta, M. Sood, N. Anjum, and A. Chib, "Infrared heating and its application in food processing," *The Pharma Innovation Journal*, vol. 9, no. 2, pp. 142–151, 2020.
- [56] S. G. Pereira et al., "Influence of ohmic heating in the composition of extracts from *Gracilaria vermiculophylla*," *Algal Research*, vol. 58, 2021.
- [57] Z. Jia, B. Liu, C. Li, T. Fang, and J. Chen, "Newly designed superheated steam dryer bearing heat recovery unit: Analysis of energy efficiency and kinetics of Kelp drying," *Drying Technology*, vol. 36, no. 13, pp. 1619–1630, 2018.

- [58] E. Albers et al., “Influence of preservation methods on biochemical composition and downstream processing of cultivated *Saccharina latissima* biomass,” *Algal Research*, vol. 55, no. March, p. 102261, 2021.
- [59] M. S. F. Nurshahida, M. A. N. Aini, W. I. W. M. Faizal, I. A. Hamimi, and Z. Nazikussabah, “Effect of drying methods on nutrient composition and physicochemical properties of Malaysian seaweeds,” *AIP Conference Proceedings*, vol. 2030, no. 020113, November, pp. 1–6, 2018.
- [60] R. Moreira, F. Chenlo, J. Sineiro, S. Arufe, and S. Sexto, “Drying temperature effect on powder physical properties and aqueous extract characteristics of *Fucus vesiculosus*,” *Journal of Applied Phycology*, vol. 28, no. 4, pp. 2485–2494, 2016.
- [61] C. Tello-Ireland, R. Lemus-Mondaca, A. Vega-Gálvez, J. López, and K. Di Scala, “Influence of hot-air temperature on drying kinetics, functional properties, colour, phycobiliproteins, antioxidant capacity, texture and agar yield of alga *Gracilaria chilensis*,” *LWT - Food Science and Technology*, vol. 44, no. 10, pp. 2112–2118, 2011.
- [62] P. K. Sappati, B. Nayak, and G. P. van Walsum, “Effect of glass transition on the shrinkage of sugar kelp (*Saccharina latissima*) during hot air convective drying,” *Journal of Food Engineering*, vol. 210, pp. 50–61, 2017.
- [63] S. S. Hamid, M. Wakayama, T. Soga, and M. Tomita, “Drying and extraction effects on three edible brown seaweeds for metabolomics,” *Journal of Applied Phycology*, vol. 30, no. 6, pp. 3335–3350, 2018.
- [64] M. Gisbert, M. Barcala, C. M. Rosell, J. Sineiro, and R. Moreira, “Aqueous extracts characteristics obtained by ultrasound-assisted extraction from *Ascophyllum nodosum* seaweeds: effect of operation conditions,” *Journal of Applied Phycology*, vol. 33, no. 5, pp. 3297–3308, 2021.
- [65] P. Stévant et al., “Effects of drying on the nutrient content and physico-chemical and sensory characteristics of the edible kelp *Saccharina latissima*,” *Journal of Applied Phycology*, vol. 30, no. 4, pp. 2587–2599, 2018.

[66] U. O. Badmus, M. A. Taggart, and K. G. Boyd, “The effect of different drying methods on certain nutritionally important chemical constituents in edible brown seaweeds,” *Journal of Applied Phycology*, vol. 31, no. 6, pp. 3883–3897, 2019.

[67] P. K. Sappati, author. *Processing Modeling of Hot Air Convective Drying of Sugar Kelp*. PhD Thesis, University of Maine, 2020.

[68] D. P. Nagahawatta et al., “Drying seaweeds using hybrid hot water Goodle dryer (HHGD): Comparison with freeze-dryer in chemical composition and antioxidant activity,” *Fisheries and Aquatic Sciences*, vol. 24, no. 1, pp. 19–31, 2021.

[69] B. Tiwari and D. Troy, editors. *Seaweed Sustainability Food and Non-Food Applications*. Elsevier Inc., 2015

[70] R. Indiarto and B. Rezaharsamto, “A review on ohmic heating and its use in food,” *International Journal of Scientific and Technology Research*, vol. 9, no. 2, pp. 485–490, 2020.

APPENDICES

Appendix A: Supplemental Data from Aspen Simulations

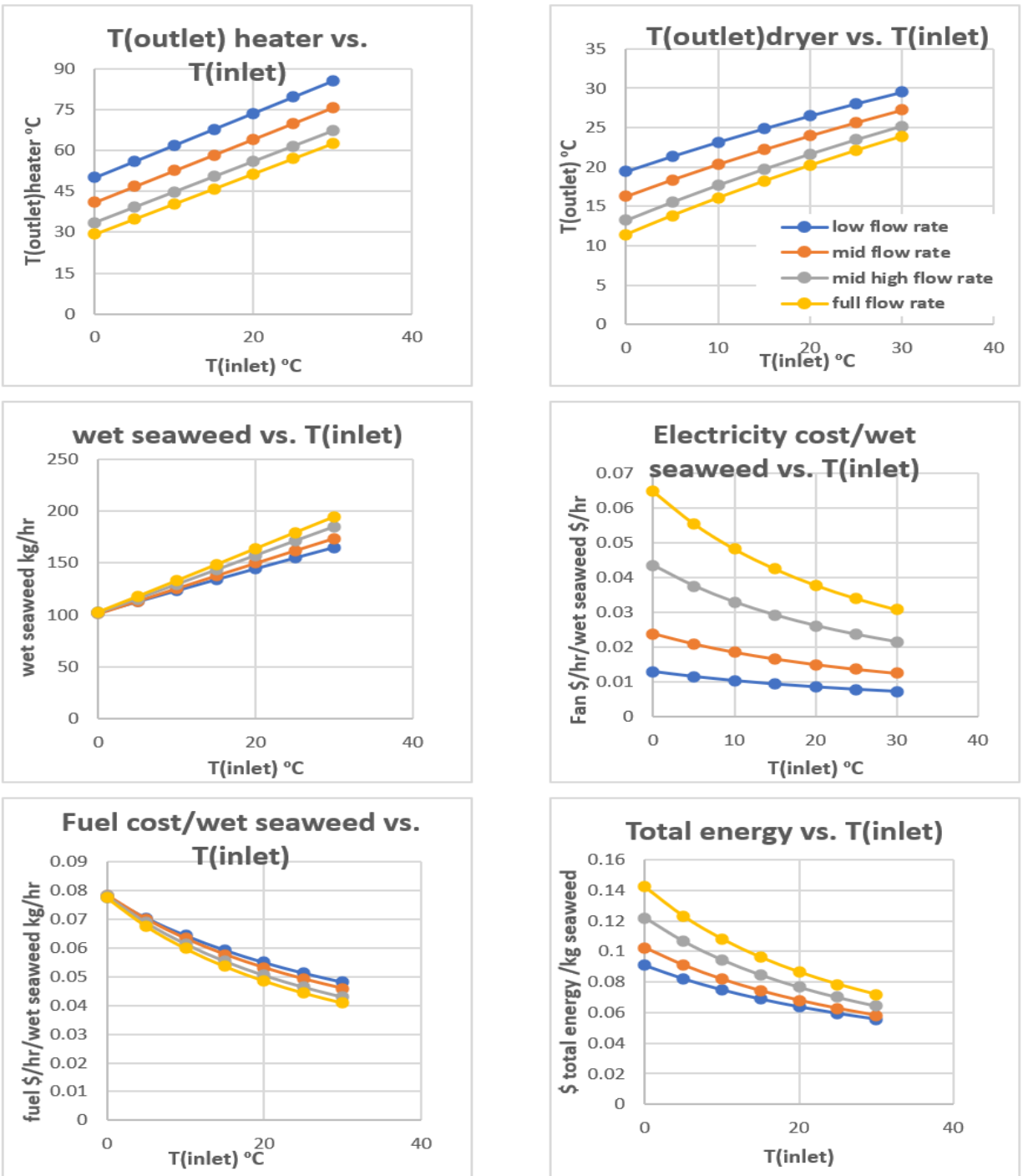


Figure A.1: Responses of dryer performance (heated and outlet air temperatures, mass throughput, electricity, fuel, and total energy costs) versus ambient inlet air temperature at 0% RH.

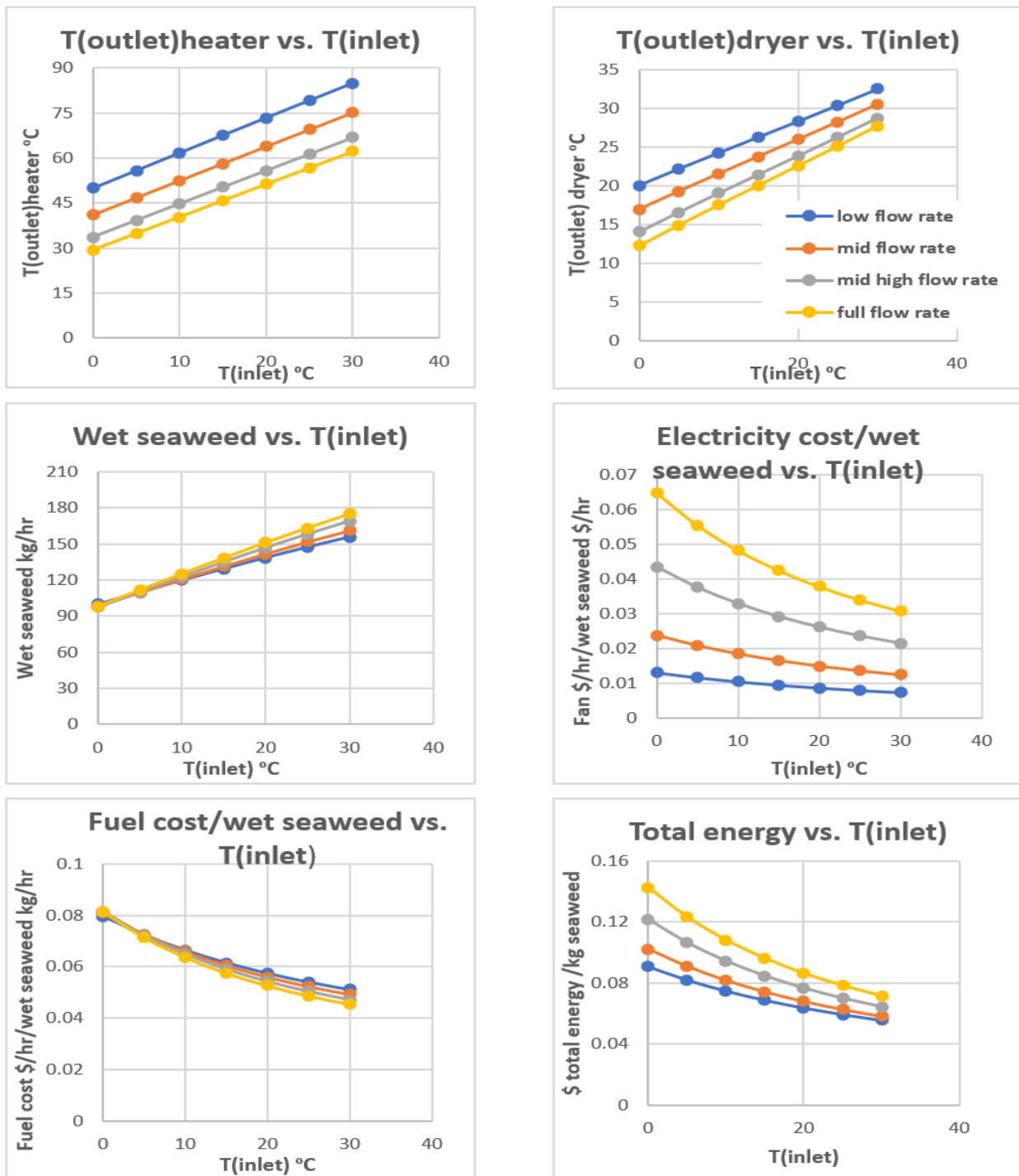


Figure A.2: Responses of dryer performance (heated and outlet air temperatures, mass throughput, electricity, fuel, and total energy costs) versus ambient inlet air temperature at 25% RH.

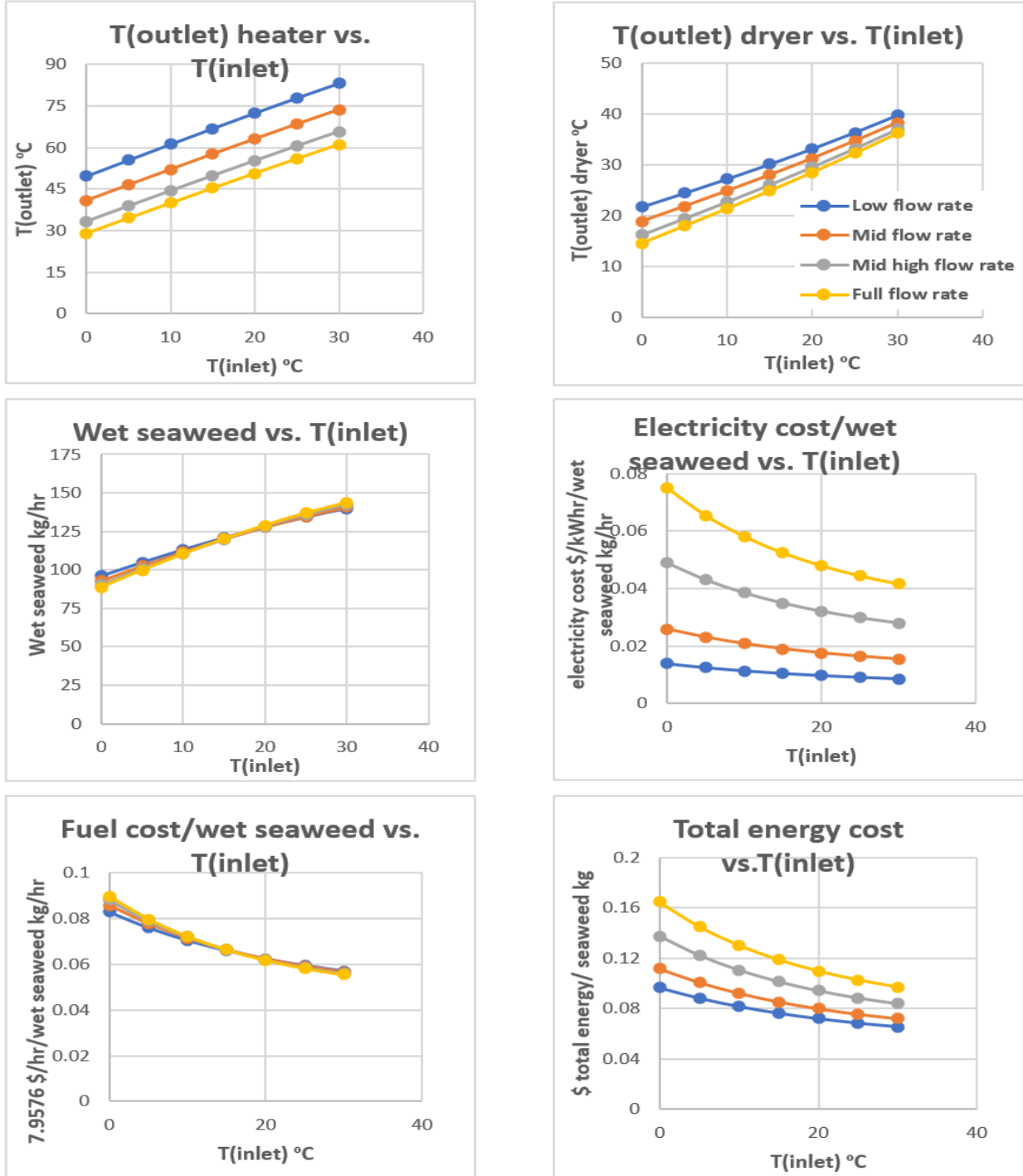


Figure A.3: Responses of dryer performance (heated and outlet air temperatures, mass throughput, electricity, fuel, and total energy costs) versus ambient inlet air temperature at 75% RH.

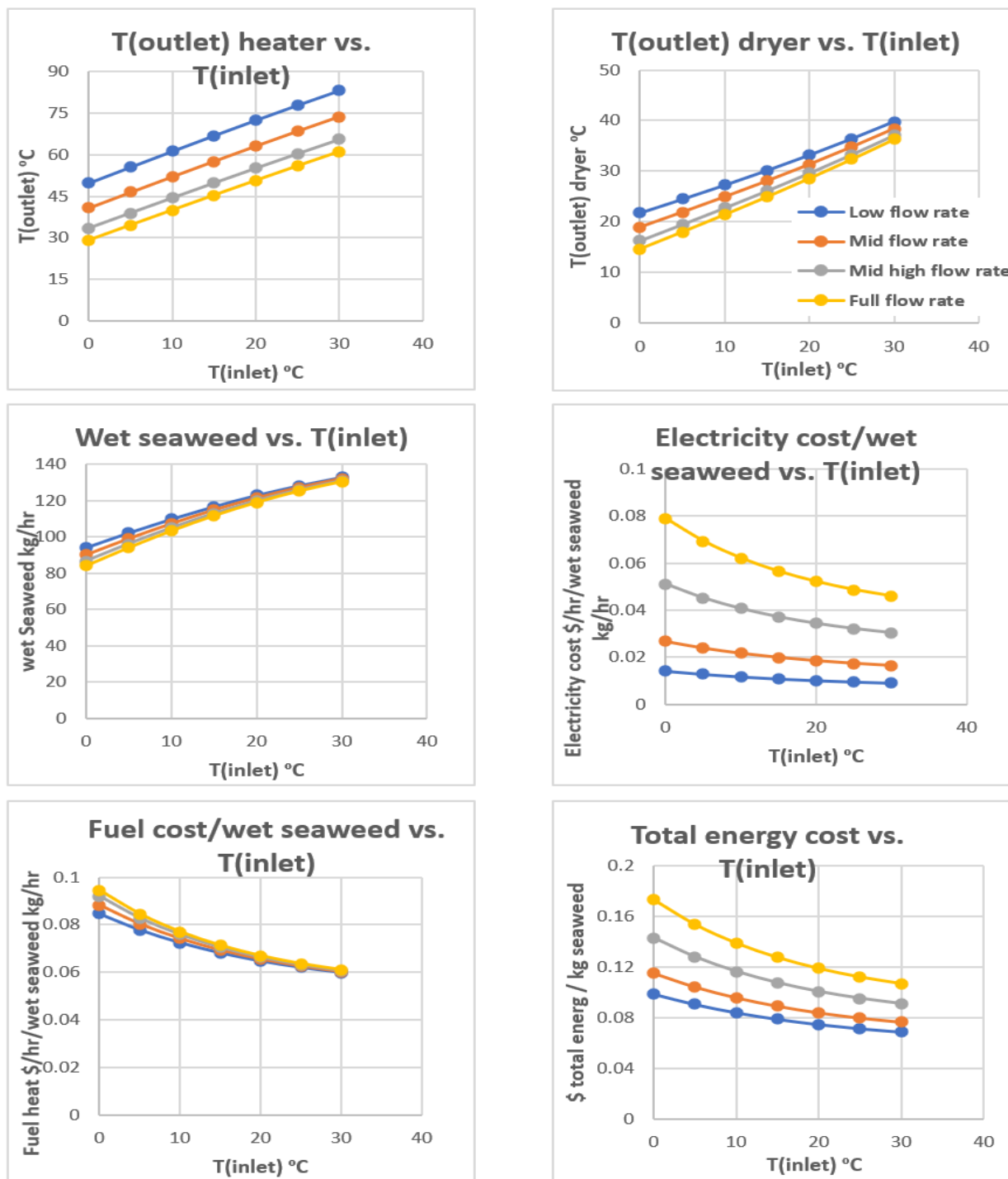


Figure A.4: Responses of dryer performance (heated and outlet air temperatures, mass throughput, electricity, fuel, and total energy costs) versus ambient inlet air temperature at 100% RH.

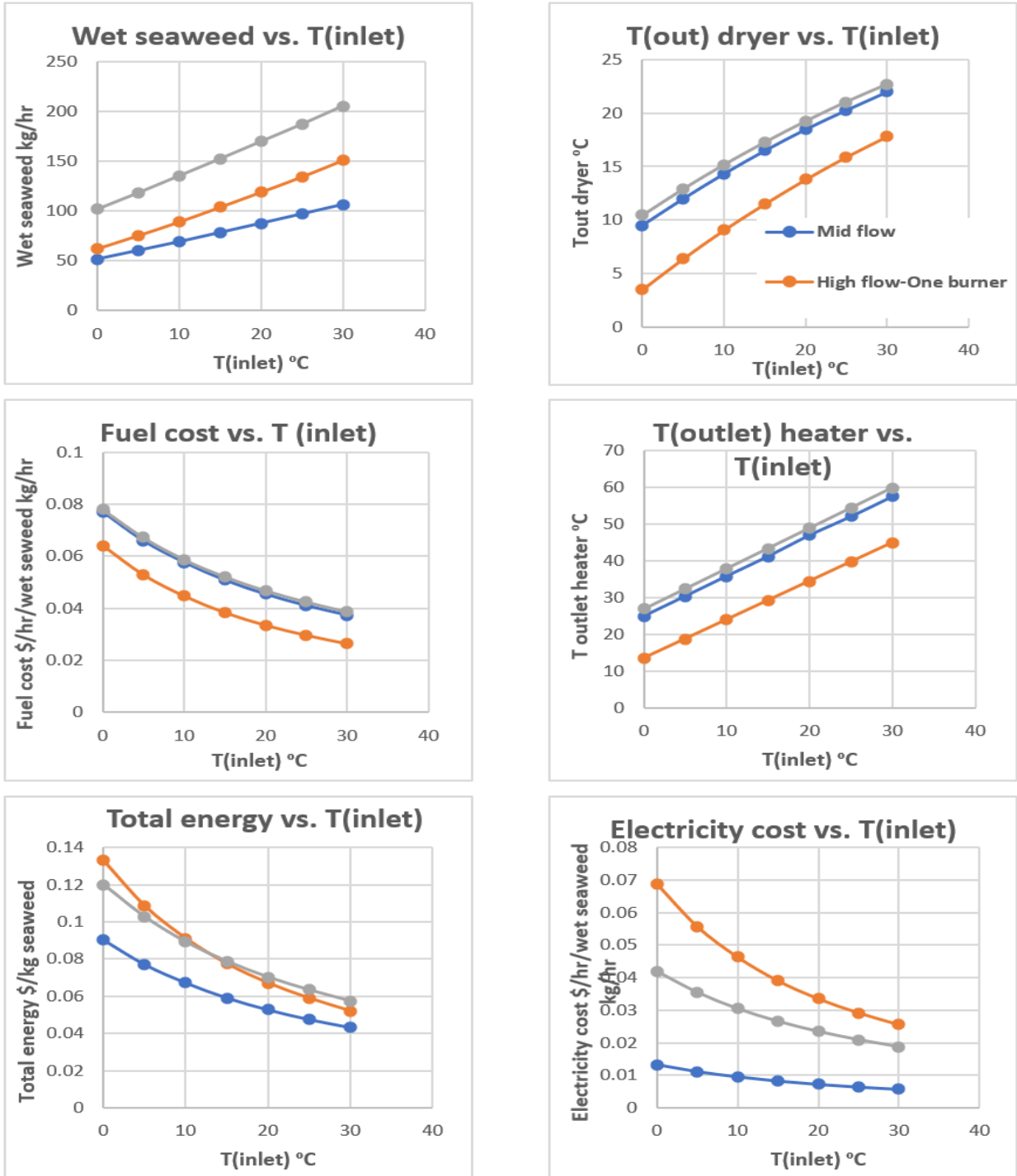


Figure A.5: Responses of dryer performance (heated and outlet air temperatures, mass throughput, electricity, fuel, and total energy costs) versus ambient inlet air temperature at 0% RH.

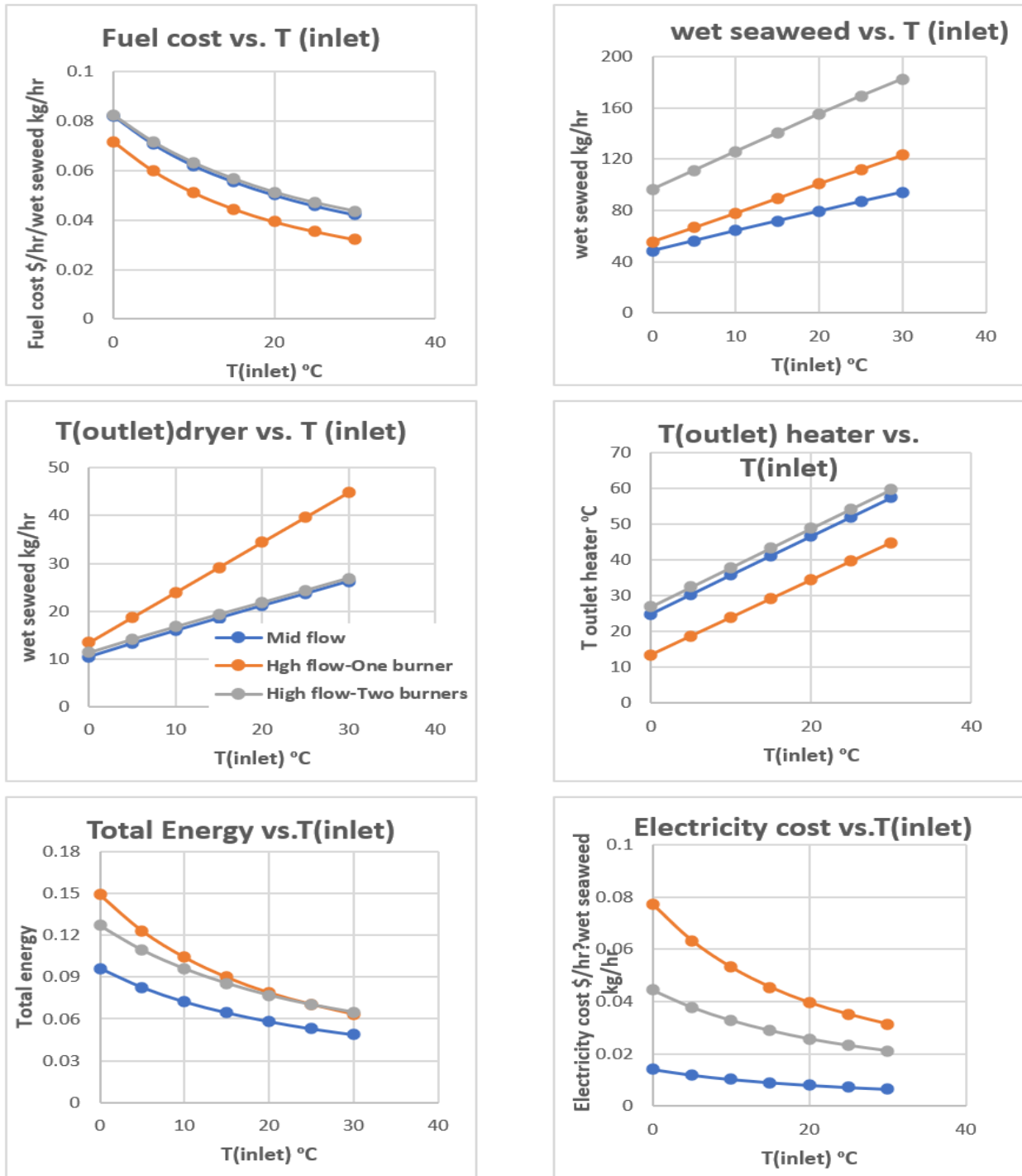


Figure A.6: Responses of dryer performance (heated and outlet air temperatures, mass throughput, electricity, fuel, and total energy costs) versus ambient inlet air temperature at 25% RH.

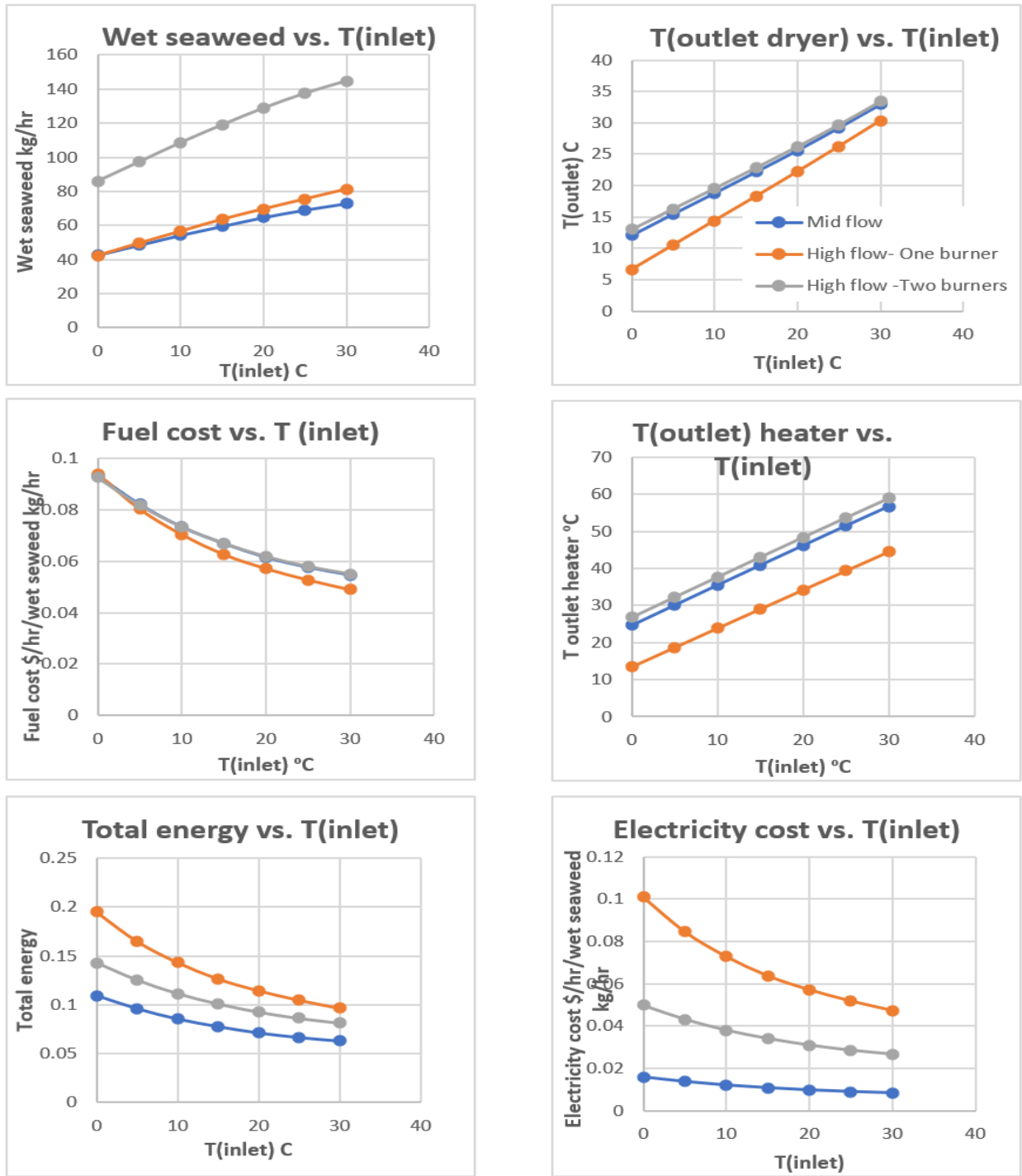


Figure A.7: Responses of dryer performance (heated and outlet air temperatures, mass throughput, electricity, fuel, and total energy costs) versus ambient inlet air temperature at 75% RH.

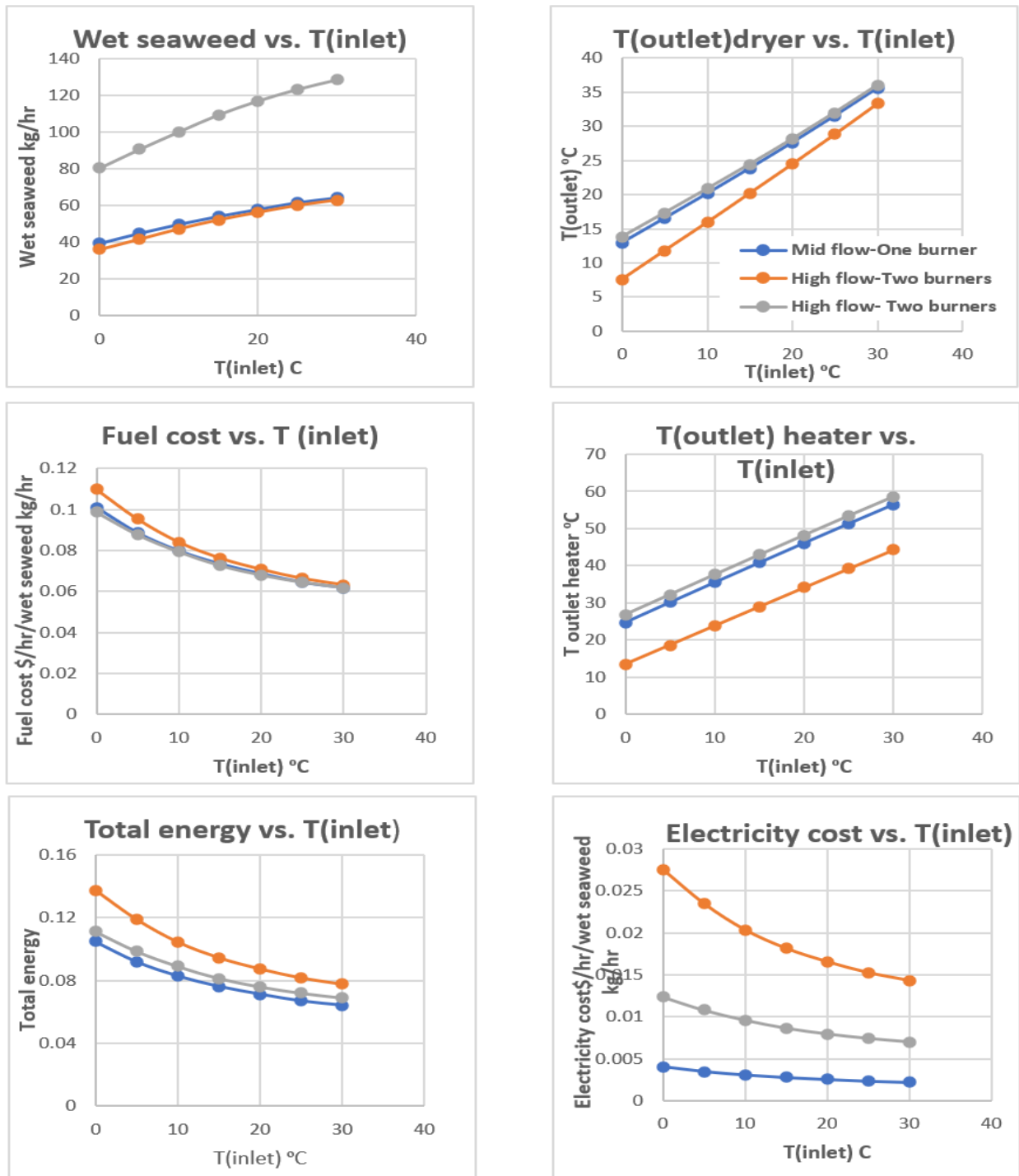


Figure A.8: Responses of dryer performance (heated and outlet air temperatures, mass throughput, electricity, fuel, and total energy costs) versus ambient inlet air temperature at 100% RH.

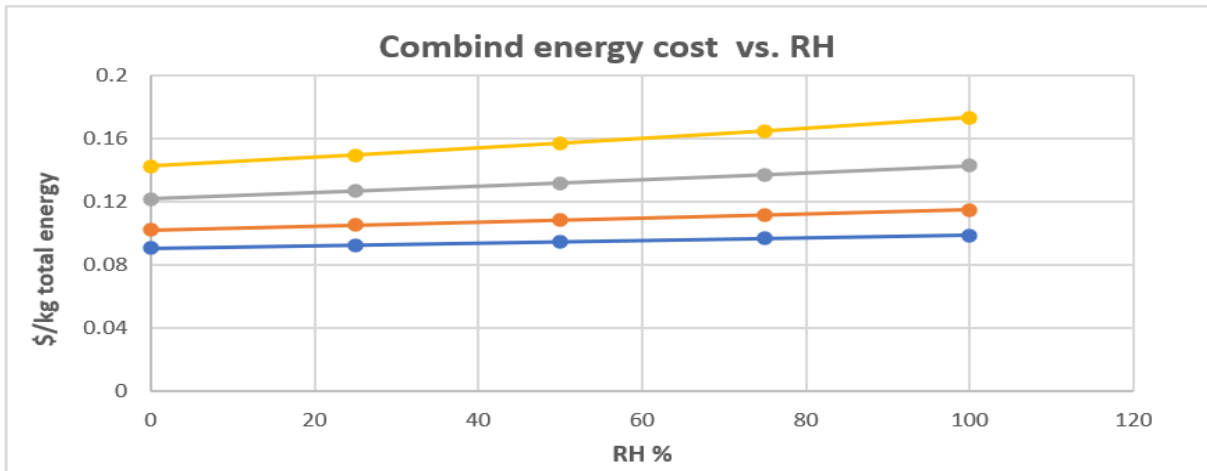
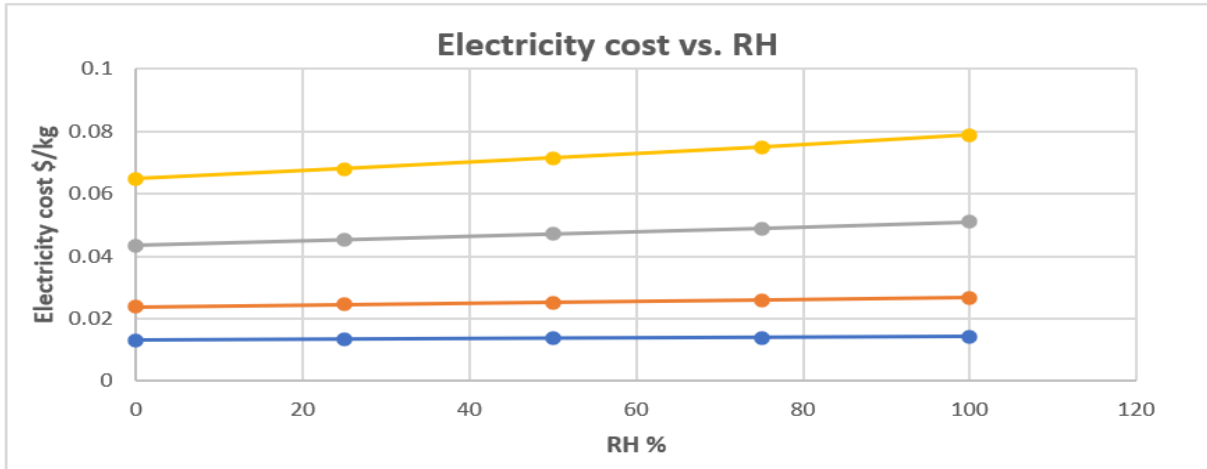
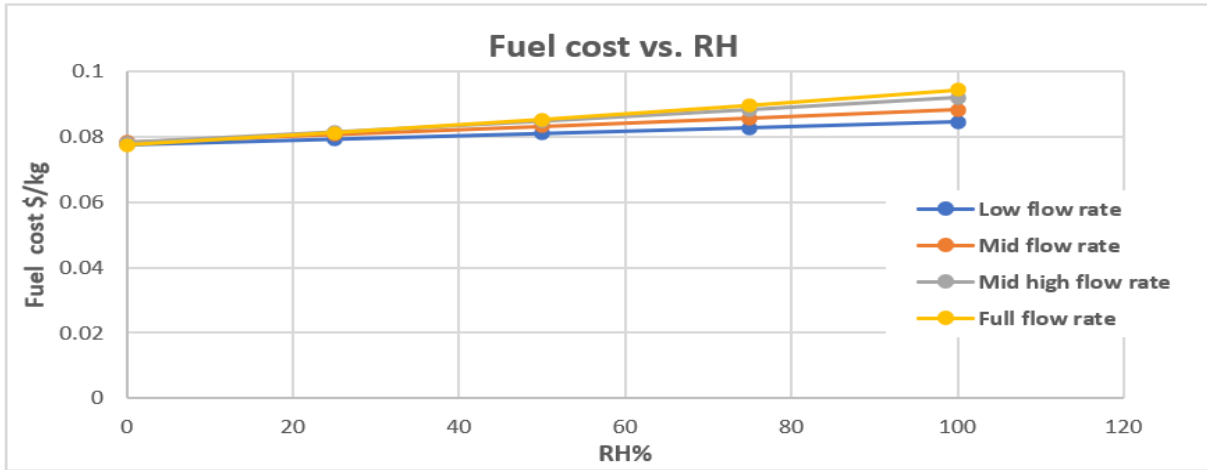


Figure A.9: Trends of energy costs (Fan electricity, heater fuel and combined) with respect to ambient air RH at ambient air temperature of 0°C.

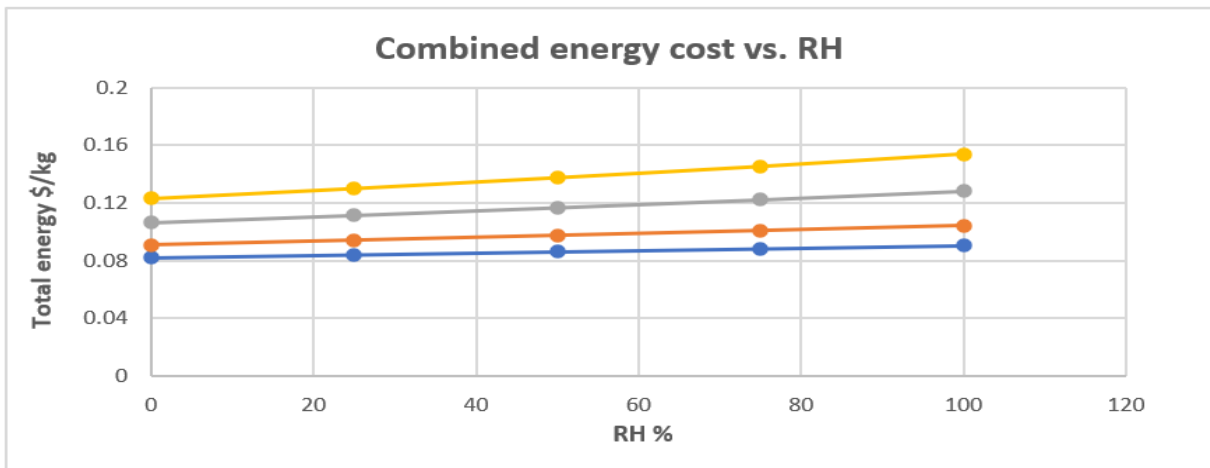
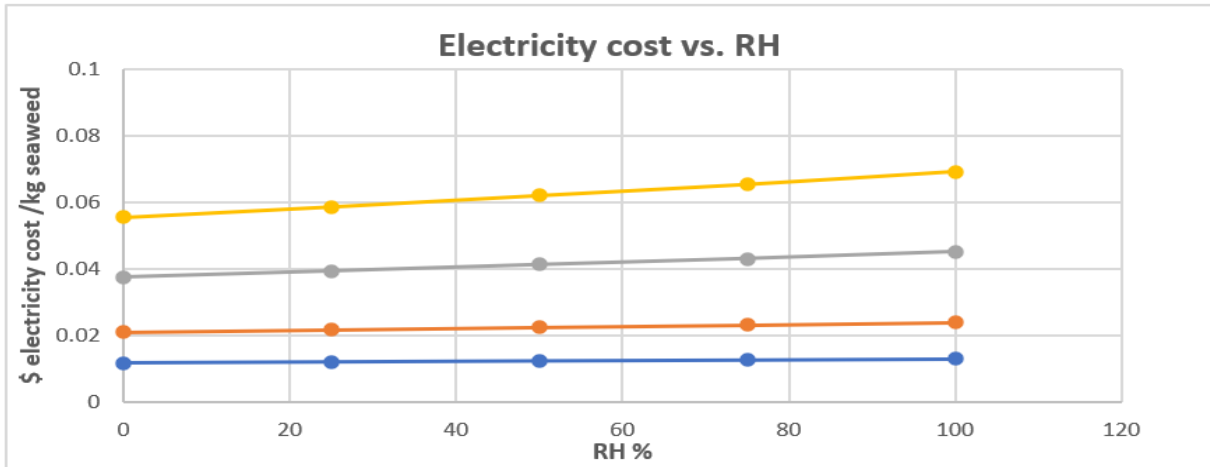
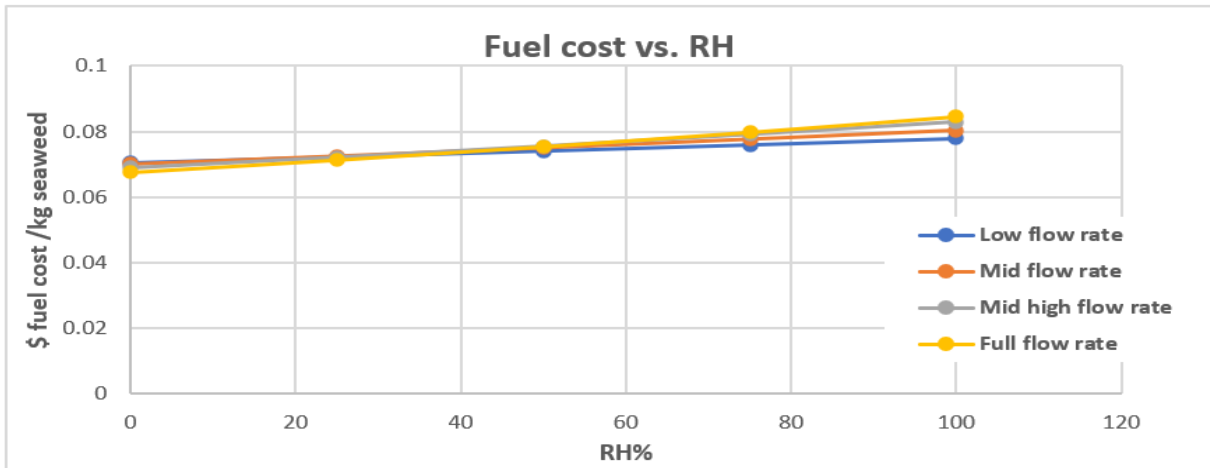


Figure A.10: Trends of energy costs (Fan electricity, heater fuel and combined) with respect to ambient air RH at ambient air temperature of 5°C.

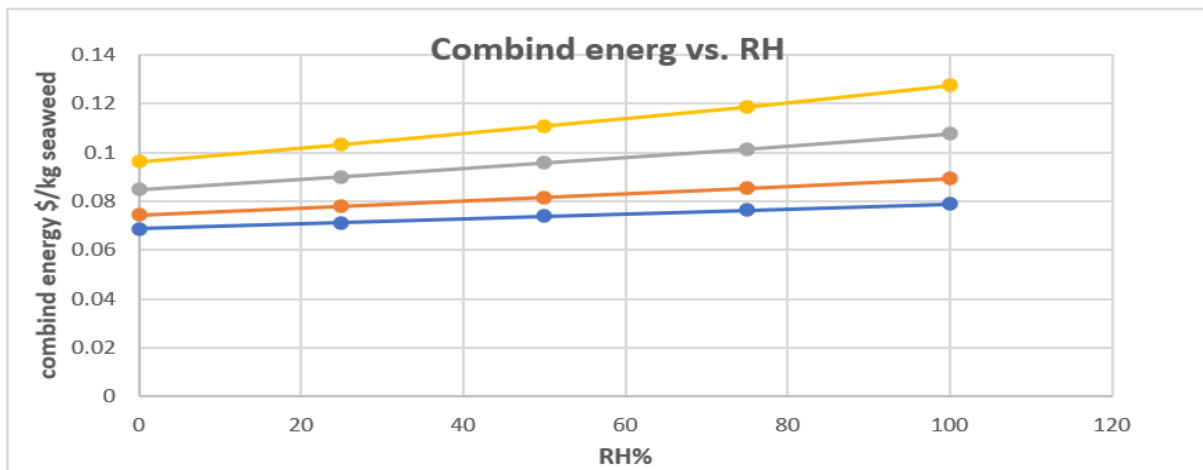
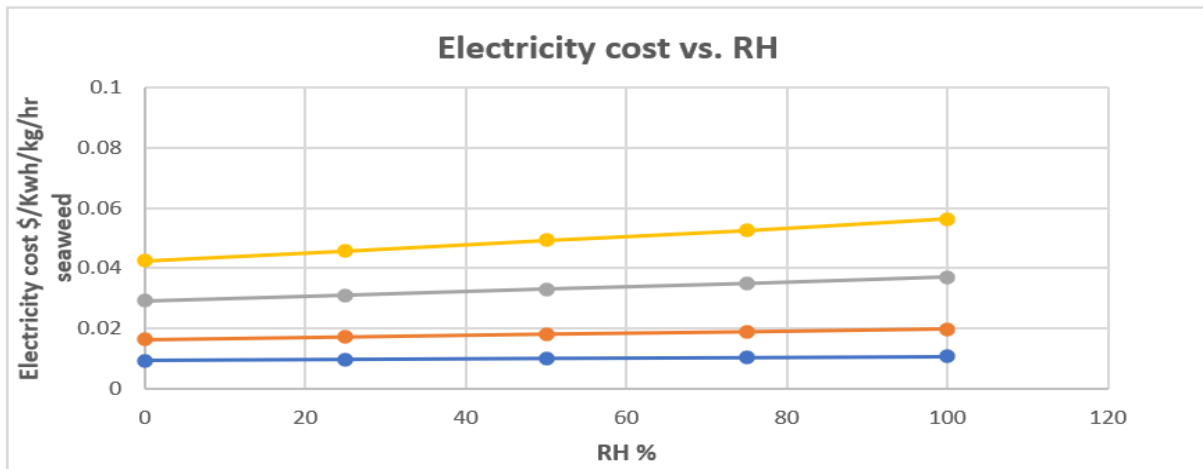
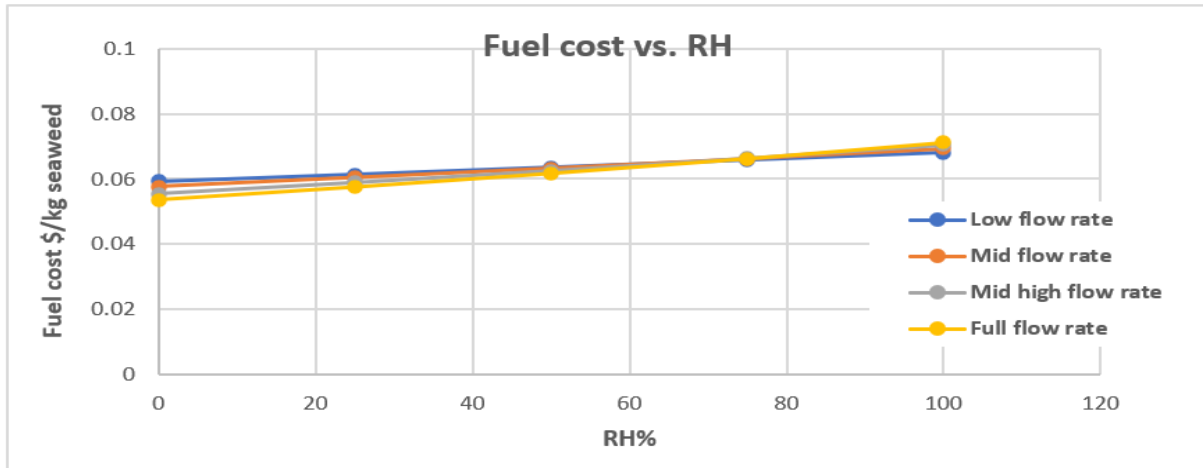


Figure A.11: Trends of energy costs (Fan electricity, heater fuel and combined) with respect to ambient air RH at ambient air temperature of 15°C.

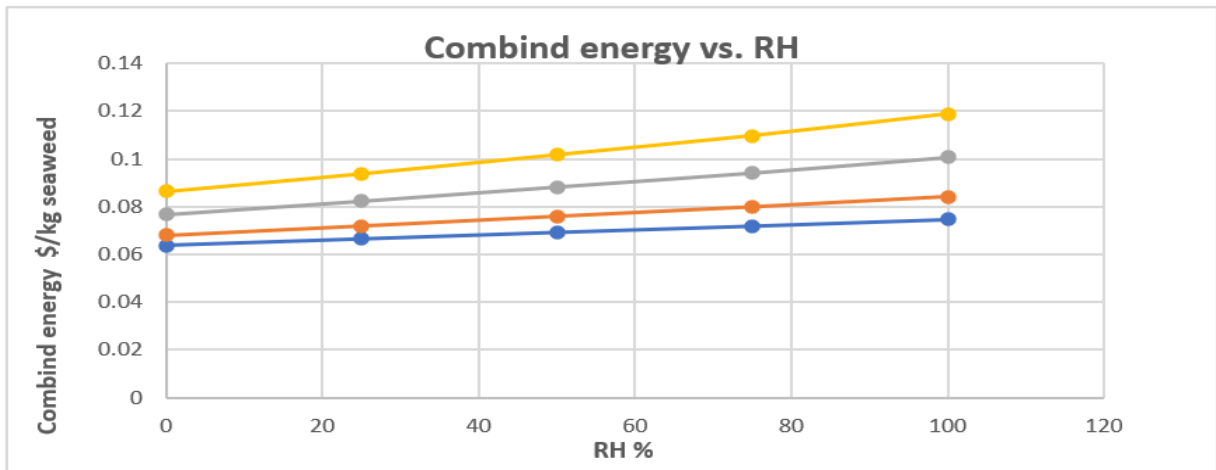
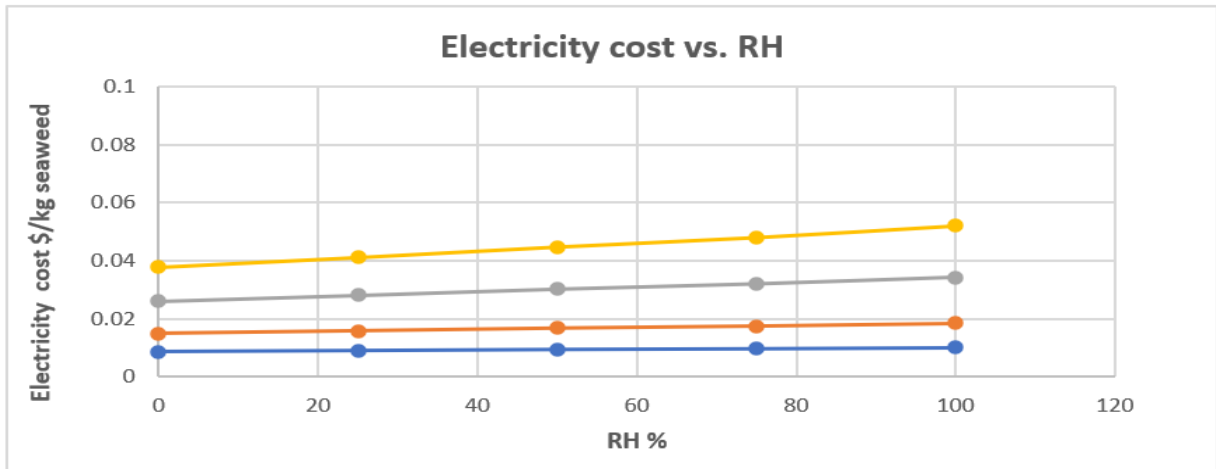
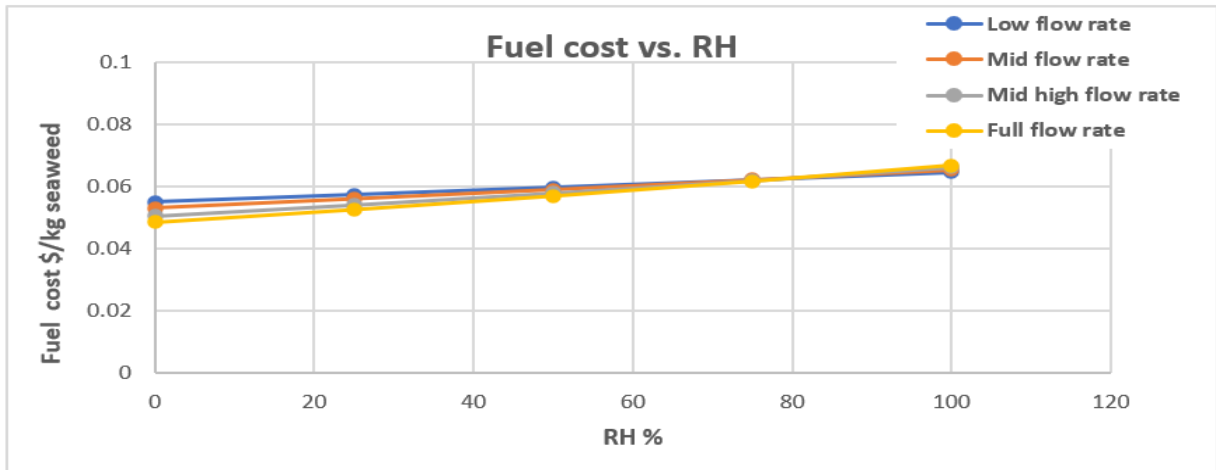


Figure A.12: Trends of energy costs (Fan electricity, heater fuel and combined) with respect to ambient air RH at ambient air temperature of 20°C.

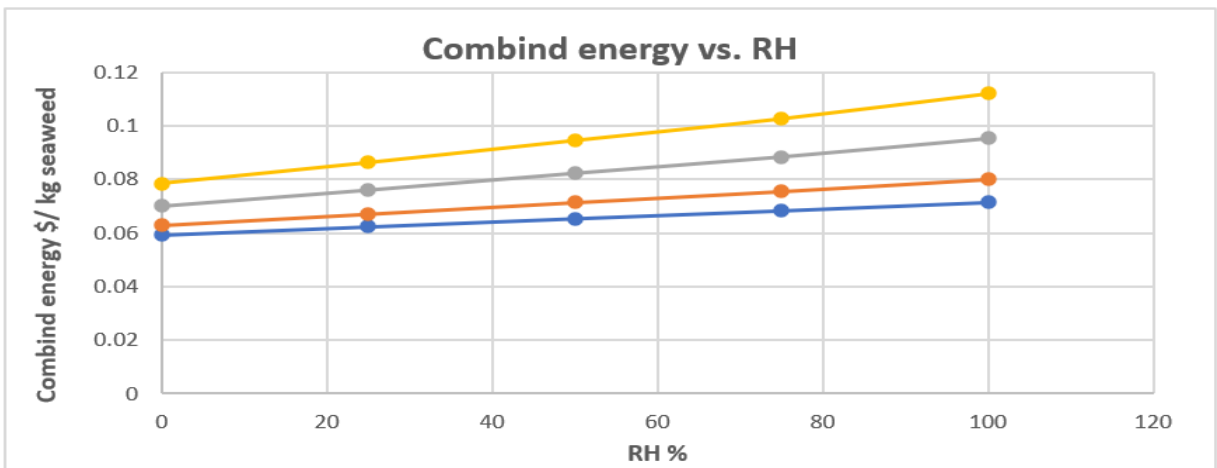
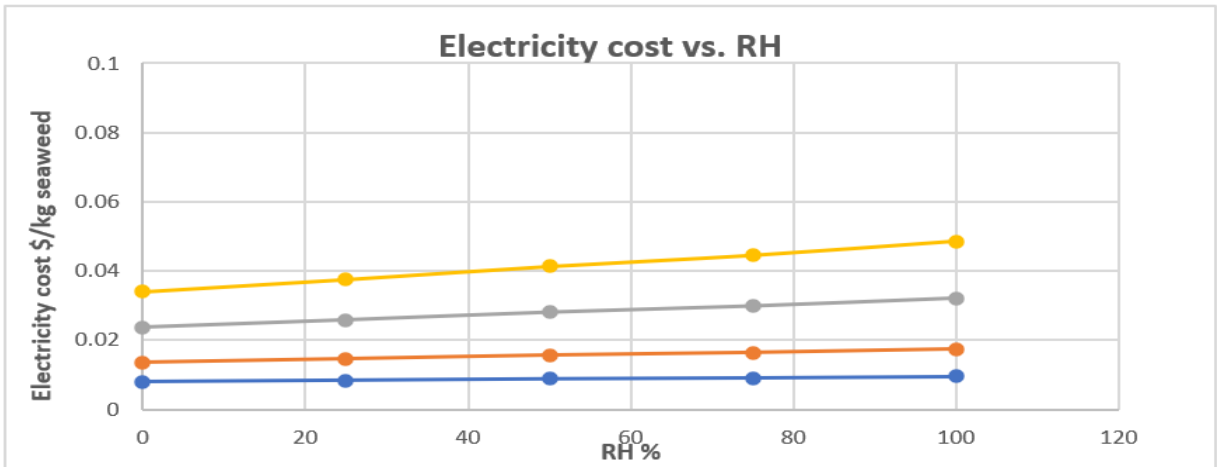
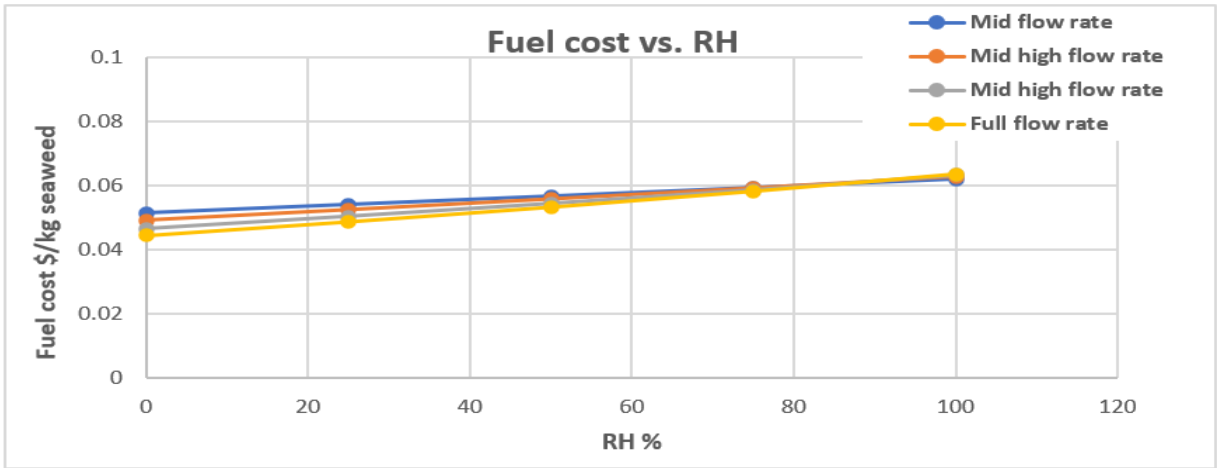


Figure A.13: Trends of energy costs (Fan electricity, heater fuel and combined) with respect to ambient air RH at ambient air temperature of 25°C.

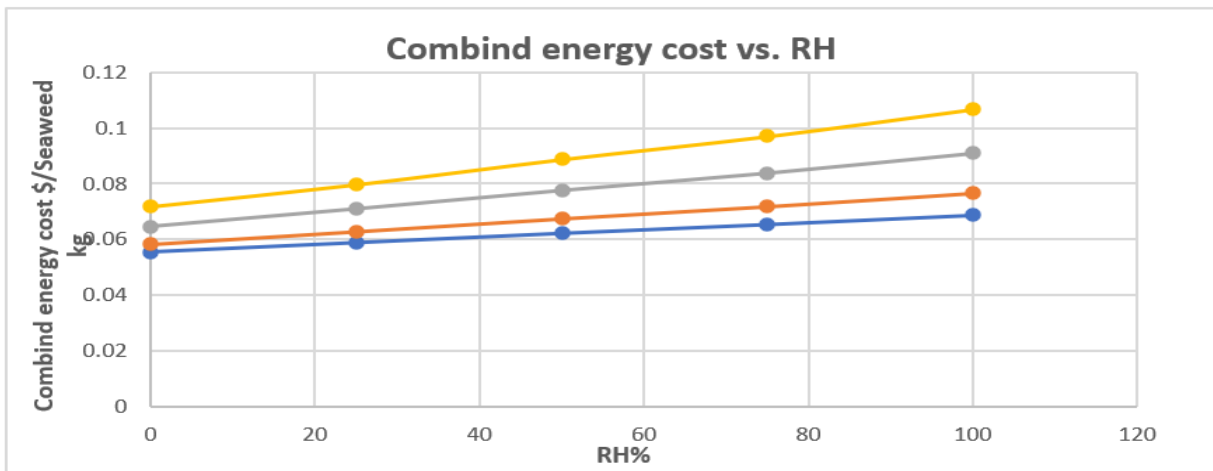
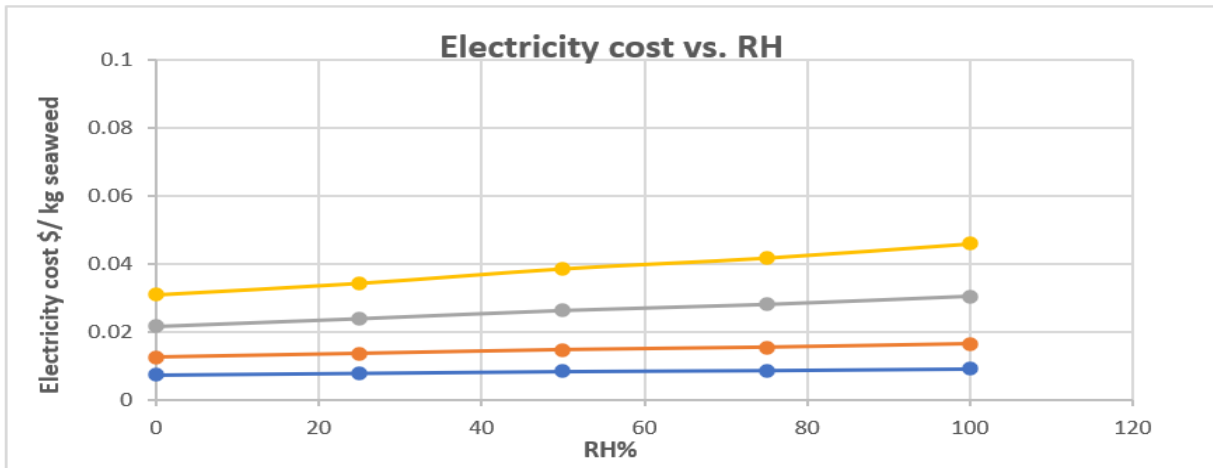
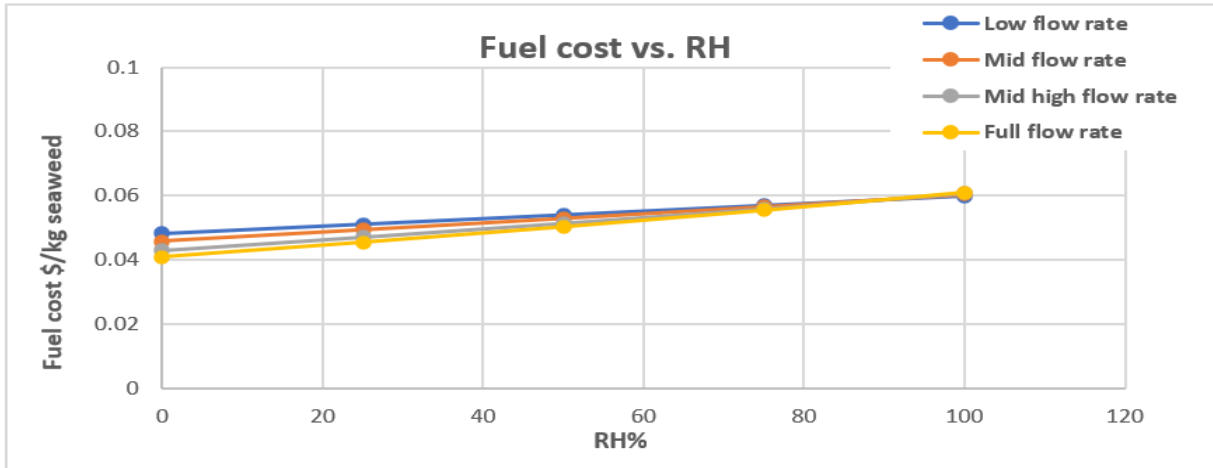


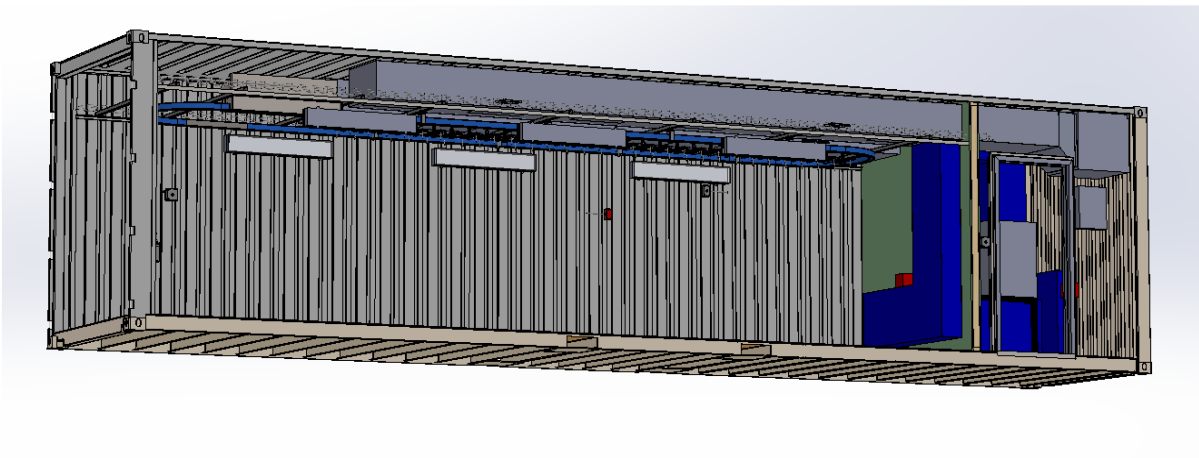
Figure A.14: Trends of energy costs (Fan electricity, heater fuel and combined) with respect to ambient air RH at ambient air temperature of 30°C.

Appendix B: Kelp Dryer Operations Guide

Machine Startup

Startup Procedure (4 Steps)

Loading



- a. Pre-Loading
- b. Loading
- c. Unloading

Interface

a. Screen User Interface (UI)

- i. System Status
- ii. Setup and Start
- iii. Temp and Humidity Monitor
- iv. Temperature Graph
- v. Relative Humidity Graph

b. Procedure

Data Log

Machine Startup

Start-up Procedure (4 Steps)

STEP 1 – Ensure the loading area is clear of any material from previous cycles.



Any dry materials in the loading area can potentially skew dry times and/or cause a fire hazard.

STEP 2 – Switch on the main breaker.



STEP 3 – Switch on emergency burner switch



STEP 4 – Using the control panel, set your desired default temperatures and humidity



Interface

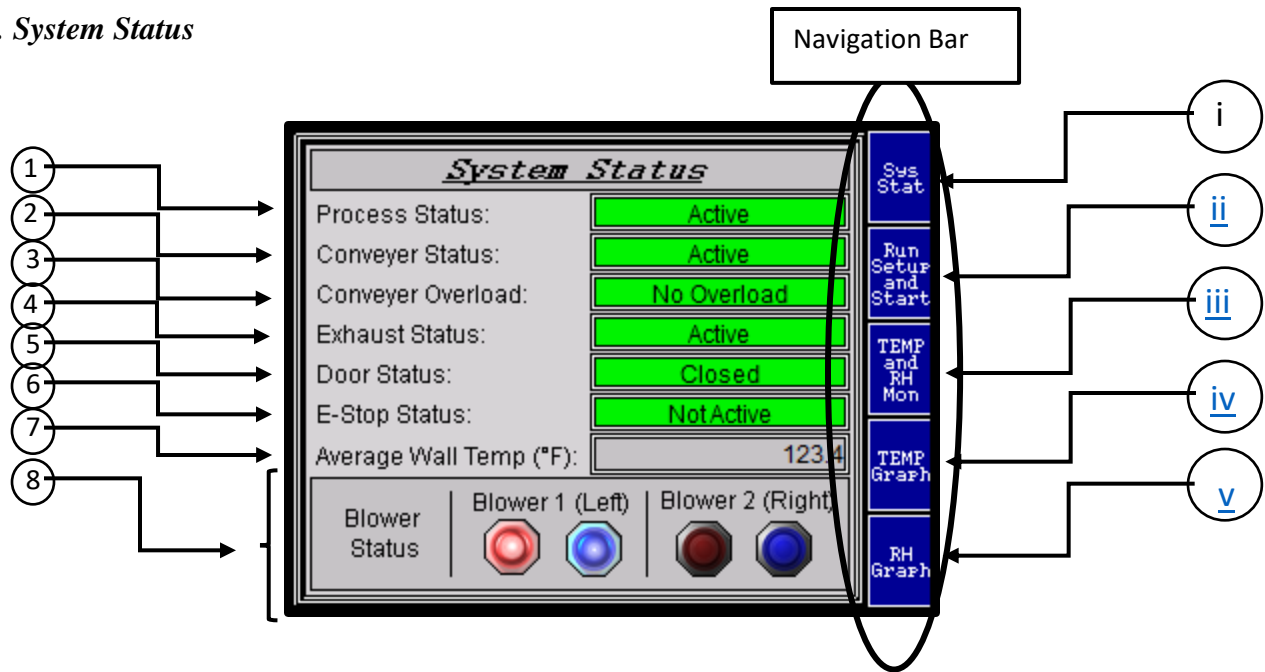
a. Screen User Interface (UI)

The control panel where the UI screens are located is left of the entryway. The E-Stop is located on the cabinet below the screen. The UI screen is what controls the autocycle.



NOTE: Screen values seen on some of the images in this section of manual are placeholders and not indicative of typical or nominal values.

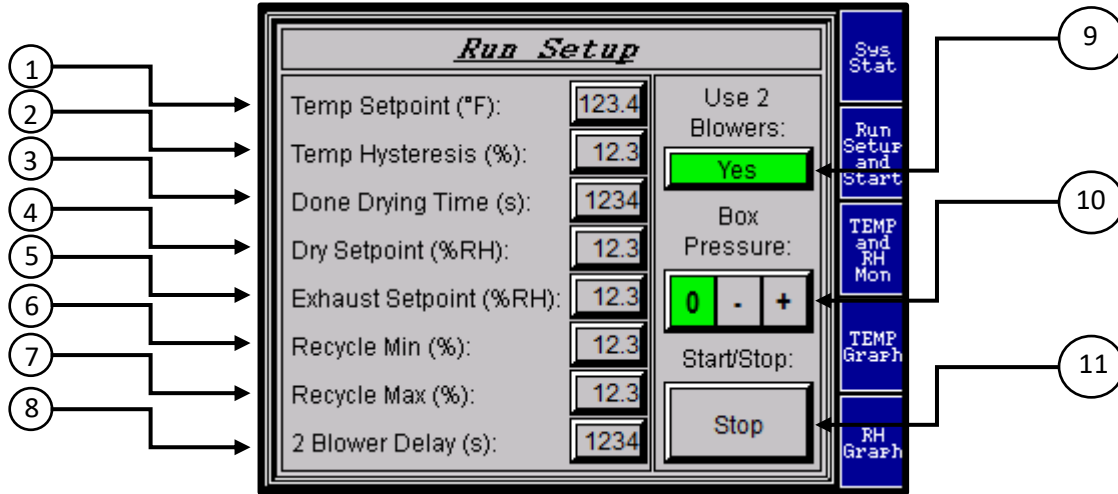
i. System Status



When switching between menus using the navigation bar, your current page is displayed by a light on an “F#” button.

Number	Callout	Description
1	Process Status	<i>Active</i> – Cycle in progress <i>Not Active</i> – Cycle not in progress
2	Conveyer Status	<i>Active</i> – Conveyer currently moving <i>Not Active</i> – Conveyer not moving
3	Conveyer Overload	<i>Overload</i> – Potential jam in the conveyer <i>No Overload</i> – System running normally
4	Exhaust Status	<i>Active</i> – Exhaust fan is active <i>Not Active</i> – Exhaust fan is not active
5	Door Status	<i>Open</i> – Door is open <i>Closed</i> – Door is closed
6	E-Stop Status	<i>Active</i> – E-Stop is enabled, machine function disabled <i>Not Active</i> – E-Stop is disabled, machine functions normally
7	Average Wall Temperature	Displays average temperature inside the dryer
8	Blower Status	Displays which blowers are active <i>Red light</i> indicates that particular furnace is on. <i>Blue light</i> indicates that particular fan is on.

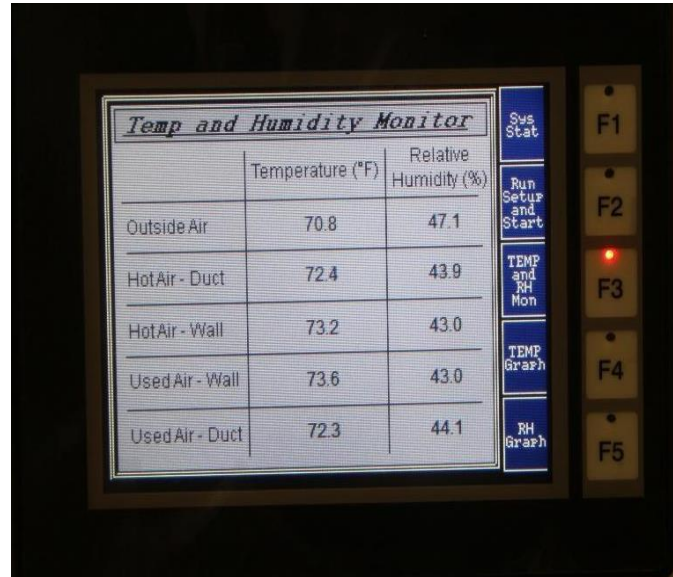
ii. Run Setup and Start



#	Callout	Description
1	Temp Setpoint	Sets the desired temperature inside the load area. Given in degrees Fahrenheit.
2	Temp Hysteresis	Sets the percentage limits for heater/fan on/off. Given in percentage.
3	Done Drying Time	Sets timer for drying. Given in seconds.
4	Dry Setpoint	Sets the desired dryness in the load area. Given in percent of relative humidity.
5	Exhaust Setpoint	Sets desired exhaust output. Given in percent of relative humidity
6	Recycle Min	Sets minimum ratio of recycled air. Given in percentage.
7	Recycle Max	Sets maximum ratio of recycled air. Given in percentage.
8	2 Blower Delay	Sets desired delay between two blowers. Given in seconds.
9	Use 2 Blowers	Option to use two blowers or one blower.
10	Box Pressure	Sets pressure in the load area; either neutral, slightly negative or slightly positive.
11	Start/Stop	Begins or ends the cycle.

iii. Temperature and Humidity Monitor

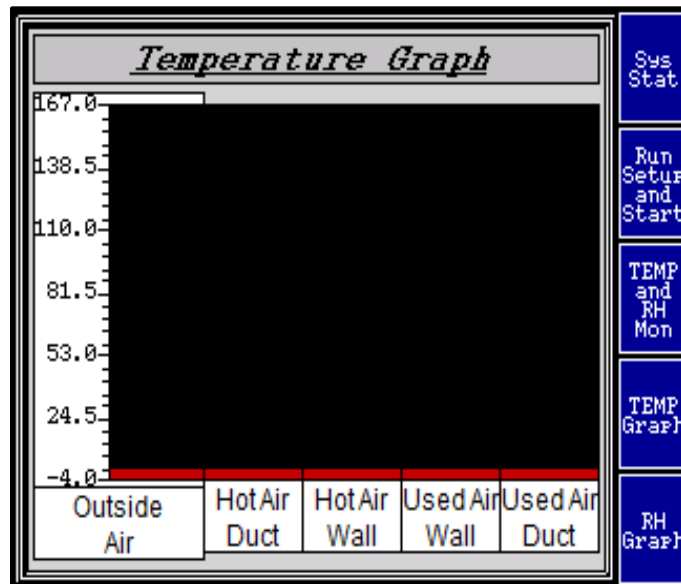
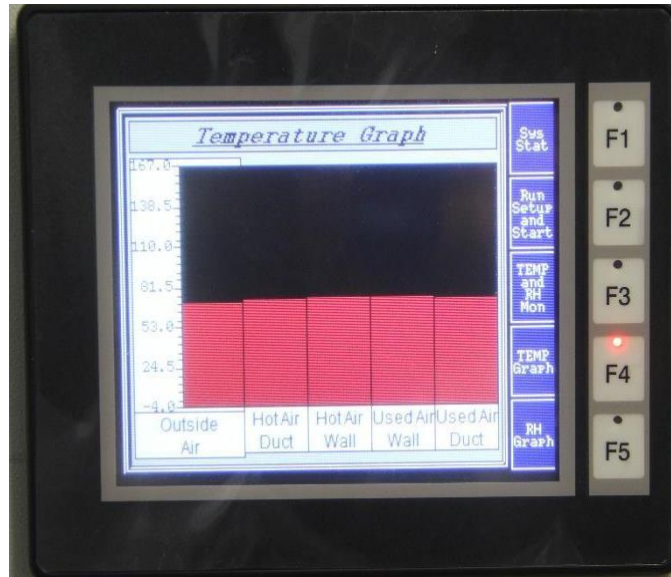
This screen displays the temperatures and relative humidity of each of the five sensor locations on the dryer. This is displaying typical values seen on the screen.



<i>Temp and Humidity Monitor</i>		
	Temperature (°F)	Relative Humidity (%)
Outside Air	123.4	123.4
HotAir - Duct	123.4	123.4
HotAir - Wall	123.4	123.4
Used Air - Wall	123.4	123.4
Used Air - Duct	123.4	123.4

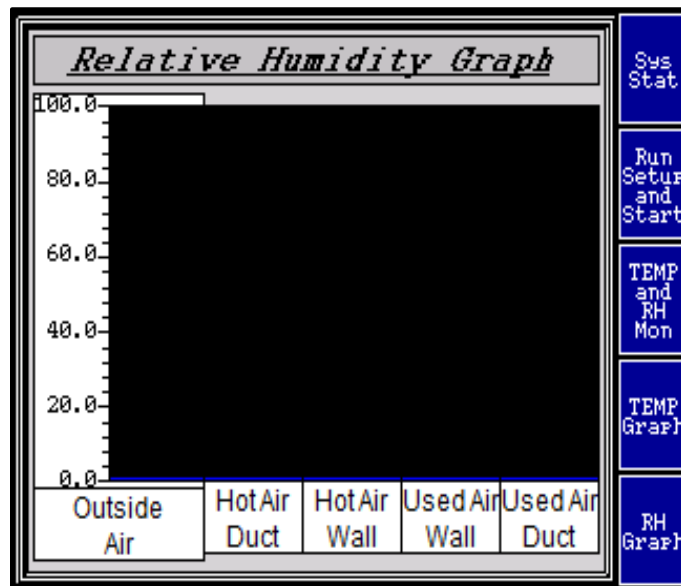
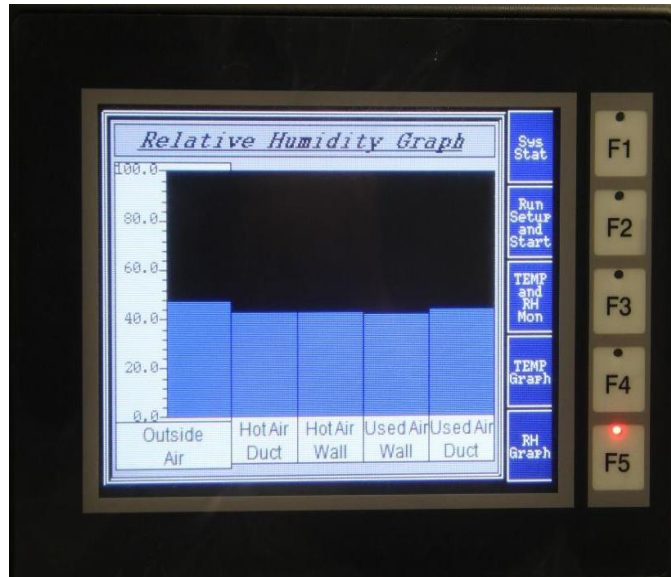
iv. Temperature Graph

Graphical method of viewing the temperature of each sensor location.

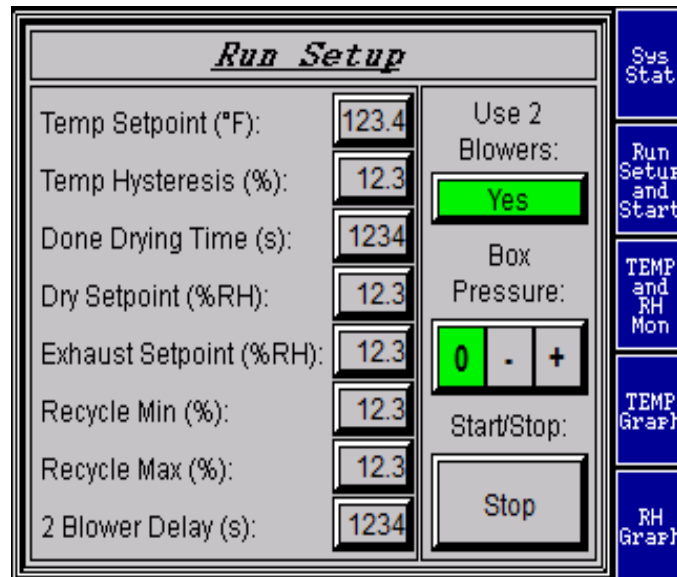


v. *Relative Humidity Graph*

Graphical method of view the relative humidity of each sensor location.



b. Procedure



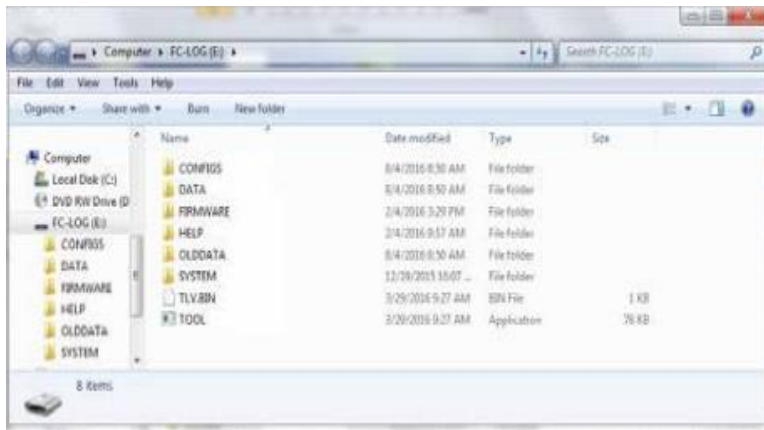
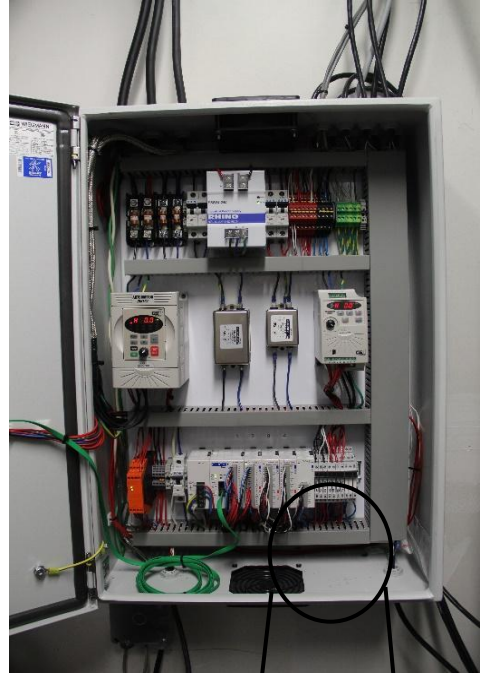
Once startup procedure is completed and material is properly loaded, press the “start” button in the screen UI.



In the event an interlock is triggered; for example, the conveyer overload, simply address the issue and press the reset button located on the control panel.

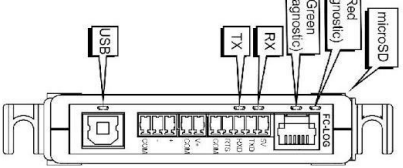
Data Logging

To access the data after completing the cycle, use a screwdriver on the side slots to open the control panel and access the data logger.



After accessing the data logger, connect a USB to the bottom FC LOG port and to a computer. Click on the “FC-LOG” drive in file explorer. To customize the settings, select the “TOOL.EXE” to open configuration settings of the logger. To access data, select the folder labeled “DATA”.

LED Status Indicators / Diagnostic LEDs



LED	Status	Description
Red (Diagnostic)	On	Diagnostic Indicator - see table below
Green (Diagnostic)	On	Diagnostic Indicator - see table below
Green (RX)	On	RS-232C/RS-485 activity - flashes when activity occurs on the RS-232C/RS-485 interface lines
Green (TX)	On	RS-232C/RS-485 activity - flashes when activity occurs on the RS-232C/RS-485 interface lines
Yellow (USB)	On	USB Not Connected
microSD (Follow)	On	The yellow LED Flashes whenever the SD card is being accessed. It may not appear to be on when the FC-106 is connected to a PC.

*Located at the top, center, on LEFT face of module.

LED	Cause	Solution
Green Fast Flashing	Normal operation in a messaging device. The message has been received successfully and the message card installed in the device.	Normal Operation - no solution required.
Green Slow Flashing	Normal operation as a Data Logger. The message the device has received is stored in the device and a valid configuration file.	Normal Operation - no solution required.
Red, Green Flashing (Repeating/Random Sequence)	Logger Critical Error	Check the FIRMWARE.TXT file in the root of the microSD card for error information.
Red Fast Flashing	The SD card or removable SD card in drive	Insert proper SD card into the holder and make sure it is seated properly.
Red/Green Fast Flashing	Firmware error	Boot loader across the firmware image in the memory is corrupted. Update firmware.

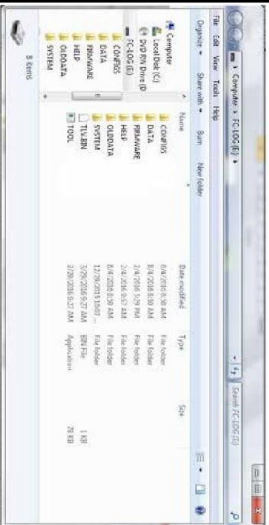
www.hiclogger.com

USB Mode - Connecting the Data Logger to a PC

1. Connect USB Type-A connector into PC USB Port.
2. Connect USB Type-B connector into FC-106 USB Port.

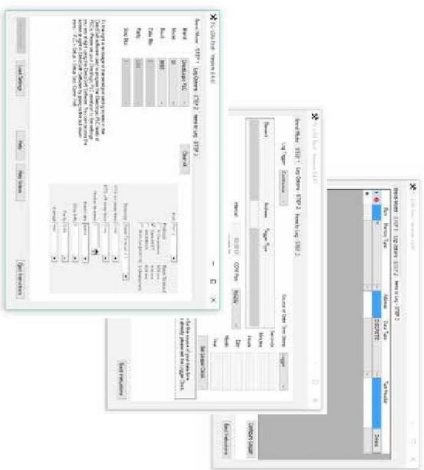


3. Use Windows Explorer to browse to removable disk drive labeled "FC-106".
4. Double click on "ICDL.exe" to run the configuration utility directly from the microSD card.



Configure the Data Logger

- The configuration tool is easy to use. As simple as 1, 2, 3.
1. Select the device you want to log into.
 2. Select how you want the logger to trigger.
 3. Select the locations from which you want to log data.



- To access the user manual included with the FC-106:
1. Connect the USB cable to the FC-106 and to your PC.
 2. Press the Windows Key + F to open Windows File Explorer.
 3. In the left pane, click on the drive labeled FC-106.
 4. In the right pane, double click the HELP folder.
 5. To view the user manual, double-click HELP.
 6. To view a tutorial showing how to configure the FC-106, in the main folder click Overview.

P.2

FC-10G USB Data Logger and Mass Storage Unit

Product Guide



Description:

The FC-10G is a low cost, user-configurable DIN-rail or side mount data logger. When connected to a PC through a USB cable, the FC-10G appears as a removable drive on the PC. When connected to a 24VDC supply or powered by the serial port of a PLC, the FC-10G will log data from the PLC and store the data in a standard CSV formatted file. Each item logged is date-time stamped in the CSV file. The files can be retrieved from the logger and imported into the software of your choosing. The logger data is stored on an internal 4GB microSD card and won't be lost in the event of a power failure.

The FC-10G currently supports DirectNET protocol for most AutomationDirect DirectLOGIC PLCs. It also supports Modbus protocol for some DirectLOGIC PLCs, Do-more PLCs, CLICK PLCs, Productivity PLCs and other Modbus devices.

Specifications (continued)

Terminal Block Specifications	
Field Wiring	Removable Screw Type Terminal Block
Number of Positions	20 (Pin#s: E2350-420, 3-0Pin#s: E2350-420)
Wire Range	26-16 AWG Solid or Stranded Conductor Wire Strain Relief Size: 6 (6.4 mm)
Screw Driver Size (Slotted)	0.4 (4.25mm mm) (Standard/Thread part number: TW-S0-VS-1)
Screw Torque	M2
	1.7 (Inch-pounds) (193mN)
Battery Specifications	
Battery Type	Coin, (Not Included)
Battery Voltage Rating	3.0VDC
Battery Current Rating	50mA
Replacement Part Number	CR2032 (Automated/Thread ID: BA1-1)
Battery Life	3 Years (at 100 samples per second) (Battery yield rate check with power is required. All uses & storage of the battery must be done in accordance with the manufacturer's instructions.)
Serial Communications Port Specifications	
Communication Standards	RS-232, RS-485 (single driver)
Communication Protocols	DirectNet Modbus RTU
Selectable Baud Rates	9600, 19200, 38400, 57600, 115200K
Cable Required	Manufacturer part number: Z-RUZ-251-2 (Automated/RTU connector) (Cable included)
Minimum Sample Rate	As fast as hardware will allow, 100 samples per second @ 115.2K
Log Data File Type	Common Spreadsheet Format: CSV CLICK RTU LOG: TUDS, RTU-242, RT-250, L102350, PL-240 DI-41K, DI-450, Productivity PLS, Do-more or any Modbus RTU capable PLC or device
Compatible PLCs	
USB Communications Port Specifications	
USB Mode	Mass storage device
USB Speed	Full speed, USB 2.0 compliant
Mass Storage Memory	4GB (microSD) (included) 8GB Max
Quiescent Current	1.10mA
User Configurable Logging Parameters	
Source of Date and Time	On board real time clock or RTU
Logging Data Trigger	Input (1 sensor terminal), PLC send, or continuous
Number of Samples Logged per Trigger	1 to 100
Create New Log File	Day, Week, Month, PLC Event
Log File Name	1001.06.CSV, 1002.07.CSV, etc.

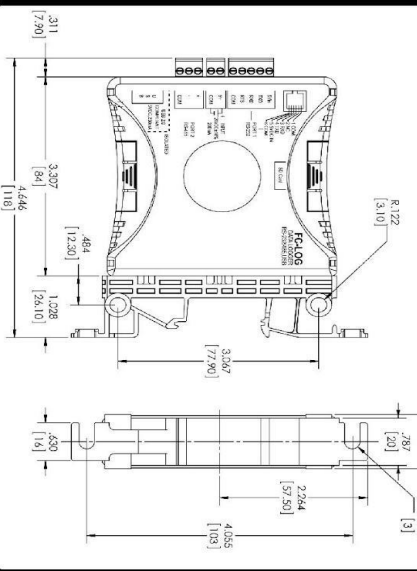
Specifications

Input Voltage (VIn)	USB: 5VDC ±10%, Vin terminal: 24VDC ±10%, FC-10G Pin: 5VDC ±10%
Input Current at Vin	20mA, 50mA, USB, 200mA (24VDC - terminal block), 150mA (5VDC - FC-10G)
Protection Type, Component	Pushbutton-type, polarity protection diode
General Specifications	
Mounting	35mm DIN Rail or panel mount (with no restriction)
Operating Temperature	0 to 80°C (32 to 176°F)
Storage Temperature	-20 to 70°C (-4 to 158°F)
Humidity	5 to 95% (non-condensing)
Environmental Air	No corrosive gases permitted (EN61131-2 pollution degree 1)
Vibration	IEC60068-2-6 (rail fit)
Shock	IEC 60068-2-27 (rail fit)
Communication Max Length	RS232: 50M (9.1 m) (Cable: 3.20M (10.00 m))
Weight	0.3 kg (1.09 lb)
Agency Approvals	UL 508 File E182507 Canada & USA CE EN61131-2

**Make sure and satisfy requirements See the D.C. for details.

FC-10G Insert 1st Edition 9-21-2016

Dimensions inch [mm]



Port and Terminal Block Specifications

RS-232 (RJ12)

Pin Number	Description
1	Common
2	Not used
3	RXD: Receive
4	TXD: Transmit
5	48VDC IN
6	Common

RS-485 Port 1 Terminal Block

Terminal Name	Signal
1	+ (A)
2	- (B)
3	Receive
4	Common

RS-232 Port 2 Terminal Block

Terminal Name	Signal
1	Transmit
2	Receive
3	Common
4	Common

Input Power

Terminal Name	Signal
V+	+24VDC, +18V, connection
COM	Common

USB Port

Pin Number	Signal
1	+5VDC IN
2	-Data
3	+Data
4	Common

*Do not connect if powered with 5VDC.

Appendix C: Calculations

Table C.1: Mass of seaweed calculations during drying process.

Mass of Seaweed Calculation June 17, 2021											
hanger no	hanger weight	hanger + wet seaweed	end cycle 1	end cycle 2	end cycle 3	end cycle 4	wet seaweed (g)	cycle 1 sw	cycle 2 sw	cycle 3 sw	cycle 4 sw
hanger 1	1058	1740	1488	1294	1264	1210	682	430	236	206	152
hanger 2	1058	1698	1440	1312	1232	1182	640	382	254	174	124
hanger 3	1052	1762	1498	1350	1254	1196	710	446	298	202	144
hanger 4	1060	1788	1534	1382	1268	1200	728	474	322	208	140
hanger 5	1054	2096	1790	1578	1436	1334	1042	736	524	382	280
hanger 6	1056	1828	1604	1442	1328	1252	772	548	386	272	196
hanger 7	1048	2210	1906	1690	1522	1408	1162	858	642	474	360
hanger 8	1054	2102	1788	1578	1442	1346	1048	734	524	388	292
hanger 9	1054	2010	1674	1456	1318	1234	956	620	402	264	180
sum			14722	13082	12064	11362	7740	5228	3588	2570	1868
1780 g (the total amount of dried seaweed from the 9 hangers after stopped the dryer and weighed the seaweed)									1.78		
902 g (net of dry seaweed from the 9 hangers after sun drying)											
Two boxes of dried seaweed were dried by sun to complete the drying Sun drying was done next day after done with the drying process											
1716 g (total dried seaweed from other hangers after dry them by sun # first box)											
2196 g (total dried seaweed from other hangers afer dry them in sun # second box)											
3912 g (total dried seaweed from other hangers (first + second) boxes that was dried by sun)											
4814 g (Total dried seaweed for the whole experiment(the 9 hanger)						4.8 kg	10.58 lb				
0.88 initial moisture content											
41309 g (total mass of start wet seaweed for the whole experiment)						41.3 kg	90 lb				
36495 g (total water mass that was evaporated at the end of the process)						36.5 kg	81 lb				

Table C.2: Calculation of the mass of water evaporated at each cycle.

No. of cycle	Moisture content	Whole mass (g)	remaining water g	Water evaporated g	Water evaporated kg
0	0.88	41309	36495	0	0
1	0.73	17710	12896	23599	24
2	0.66	14108	9294	3602	4
3	0.57	11225	6411	2883	3
4	0.46	8834	4020	2391	2
5 (sun drying)	0	4814	0	4020	4
					36.5

Table C.3: Calculation of the mass of water evaporated at each cycle after adding an imaginary cycle.

No. of cycle	Moisture content	Whole mass (g)	remaining water g	Water evaporated g	Water evaporated kg
0	0.88	41309	36495	0	0
0.1	0.82	26927	22113	14381	14
1	0.73	17927	13113	9000	9
2	0.66	14108	9294	3602	4
3	0.57	11225	6411	2883	3
4	0.46	8834	4020	2391	2
5 (sun drying)	0				4
					36.5

Table C.4: Calculation of fan energy by using energy balance.

1- Fan Energy Calculation by using Energy Balance - Seaweed Experiment - 6-17-2021

Cycle No.	Fan operating time (hr)	Energy of air coming in (kj/kg)	Energy of air coming out (kj/kg)	The difference of energy (KJ/kg)	Fan Flow Rate CFM
Experiment 1 cycle 1	1	40	80	40	2425.0
Experiment 1 cycle 2	1	43	74	31	2425.0
Experiment 1 cycle 3	1	43	66	23	2425.0
Experiment 1 cycle 4	1	41	62	21	2425.0
total time of operating	4.02	166.32	281.7		

FanFlow rate (m3/hr)	Flow in and out (m3/hr)	Air amount at each cycle m3	Specific volume (m3/kg)	Air mass (kg)	Energy loss of the fan(KJ)	fan energy loss (Btu)
4124.15	824.83	841.33	0.87	965.93	38907.7	36879.4
4124.15	824.83	824.83	0.87	945.91	29285.2	27758.5
4124.15	824.83	824.83	0.86	959.10	21915.5	20773.0
4124.15	824.83	824.83	0.86	956.88	20324.1	19264.6
				3827.82		104675

Table C.5: Temperatures of different location of the dryer.

T1 Fresh air T (°F)
T2 Used air wall T (°F)

Fresh air Temp °F	Fresh air T °C	Fresh air RH %	Used air duct Temp °F	Used air duct Temp °C	Used air duct RH %	used air wall T °F	used air wall T °C
72	22	42	98	37	42	91	33
79	26	31	100	38	33	94	34
79	26	31	99	37	28	94	34
77	25	32	98	37	25	92	33

Table C.6: Calculation of fan energy by using mass balance.

2- Fan Energy Calculation by using Mass Balance - Seaweed Experiment - 6-17-2021

Cycle No.	Fan operating Time	Fresh air T °C	Fresh air RH %	Used air duct T °C	Used air duct RH %	g water/ kg (d.a) in	g water/ kg (d.a) out	g water/ kg (d.a) changed
Cycle 1	1	22	42	37	42	6.922	16.69	9.8
Cycle 2	1	26	31	38	33	6.492	13.79	7.3
Cycle 3	1	26	31	37	28	6.492	11.03	4.5
Cycle 4	1	25	32	37	25	6.313	9.83	3.5

Water evaporated (end)	g/hr water changed	kg/hr dry air	flow rate L/s	flow rate CFM	20% full	Fraction
23599	23599	2416	586	1242	485	0.39
3602	3602	494	120	254		1.91
2883	2883	635	154	327		1.49
2391	2391	680	165	349		1.39

Table C.7: Calculation of energy loss.

Calculation of Energy loss									
Experiment and cycle No.	Operating Time (hr)	Energy delivered Btu/hr	Energy input (Btu)	Number of burners	T1 °F	T2 °F	T1 °C	T2 °C	water evaporated mass(kg)
cycle 1	0.5	129319.4	6460	1burner	72	91	22	33	900
cycle 2	0.3	129319.4	38796	1 burner	79	94	26	34	3602
cycle 3	0.4	129319.4	51728	1 burner	79	94	26	34	2883
cycle 4	0.6	129319.4	77592	1 burner	77	92	25	33	2391
1 Experiment 4 cycles	2		232775						

Cp of water KJ/kg.C	Seaweed mass kg	Cp seaweed KJ/kg C	Hv KJ/kg	Energy of evaporation (KJ)	Evaporation Energy Btu	Energy efficiency	Heat of combustion Btu/lb	Mass of Propane lb	Mass of Propane kg
4.186	6.75	3.42	2562	23056443	24324548	376.19	21500	3	1.4
4.186	6.75	3.42	2564	9233636	9741486	251.10	21500	2	0.8
4.186	6.75	3.42	2564	7390351	7796820	150.73	21500	2	1.1
4.186	6.75	3.42	2560	6121075	6457735	83.23	21500	4	1.6
								11	4.9

Energy input Btu/hr	Btu/gal Propane	Q purchased gal/hr	Propane Gallons	Propane Cost \$/gal	Propane Cost \$/hr	Propane density g/cm3	Propane density lb/ga	Gallons of Propane
129319	91502	1.41	0.71	2.8	4.0	0.49	4.09	0.74
129319	91502	1.41	0.42	2.8	4.0	0.49	4.09	0.44
129319	91502	1.41	0.57	2.8	4.0	0.49	4.09	0.59
129319	91502	1.41	0.85	2.8	4.0	0.49	4.09	0.88
			2.54					2.65

Calculation of specific heat capacity of seaweed
 There is another equation to estimate the specific heat capacity of seaweed from the book I Introduction to food engineering)

$$C_p = 0.837 + 3.349 X_w$$

X_w (the water content as a fraction)

X_w = **0.77**

C_p = **3.42** Specific heat capacity of seaweed KJ/kg K

Table C.8: Calculation of energy loss through the wall without insulation.

Cycle No.	Area (m2)	used wall temp °C	Outside Temp °C	convective heat transfer coeff. W/m °C	Q=h *A*(T2-T1) (watt)	Operating time (hr)	Heat loss (Btu/hr)	wall heat loss (Btu)
cycle 1	81.6	33	22	14.2	12231	1.02	41731.9	42567
cycle 2	81.6	34	26	14.2	9656	1.0	32946.3	32946
cycle 3	81.6	34	26	14.2	9656	1.0	32946.3	32946
cycle 4	81.6	33	25	14.2	9656	1.0	32946.3	32946
								141405

From the update calculation of the energy input	232775 Btu (total energy input from the burners)
	141405 Btu (total heat loss from the wall)
	0.61 %Energy loss through the wall
	61%

Table C.9: Calculation of energy loss through the wall.

If we used an insulation

R-value = **1.34** ft2 °F hr/Btu U-value = 1/R = 0.746269 Btu/ft2 F hr

1 Btu/ft2 F hr = 5.678 watt/m2 K

U-value = **4.237** watt/m2 K or W/m2 °C

Cycle No.	Area (m2)	used wall temp °C	Outside Temp °C	Overall heat transfer coeff. W/m °C	Q=h *A*(T2-T1) (watt)	Operating time (hr)	Heat loss (Btu/hr)	wall heat loss (Btu)
cycle 1	81.6	33	22	4.237	3803	1	12977.2	13237
cycle 2	81.6	34	26	4.237	2766	1	9438.0	9438
cycle 3	81.6	34	26	4.237	2766	1	9438.0	9438
cycle 4	81.6	33	25	4.237	2766	1	9438.0	9438
								41551

Calculation of energy saving after insulation

Energy input 232775 Btu

Wall heat loss after insulation 41551 Btu

Energy loss from the wall 18 %

Energy Saving after insulation 43 %

Table C.10: Calculation of energy loss through the wall without insulation.

Net Radiation Loss Rate		June 17,2021		Whr/m2/day	l/m2 day	W/m2
$q = \sigma \epsilon A (T_h^4 - T_c^4)$		Facing Directly South				
q (is the heat transfer per time Watt		Horizontal	5.49 kWhr/m2/day	5490	19764000	352
ϵ	0.79 emissivity coefficient	Vertical	2.57 kWhr/m2/day	2570	9252000	165
σ	5.6703E-08 (The Stefan-Boltzman constant)	Ver/Hor	0.47	http://www.solarelectricityhandbook.com/solar-irradiance.html		
T_h	Hot body absolute temp (K)	Th (Horizontal)		333.23 K		60.08 °C
T_c	Cold surrounding temp (K)	Th (Vertical)		318.11 K		44.96 °C 113 F
These temperatures are the same temperatures there were mentioned in sheet Fan and Burner converted from C to K		Horizontal				
Outside temp (K)	used air wall temp (K)	Q inside Horizontal		153.11 W/m2	0.77	0.44 Inside fraction
295.4	306	Q outside Horizontal		198.82 W/m2		
299.3	308	Vertical				
299.3	308	Q inside Vertical		59.52 W/m2	0.57	0.36
298.2	307	Q outside Vertical		105.23 W/m2		
298.05	307.25					
Average Temp of the first experiment		298.05 K (Outside temp of the first experiment at June 17,2021)		Daylength during June 17,2021		
		307.25 K (Used air wall temp of the first experiment at June 17,2021)		15:36:00 hr:min:sec		
				15.6 hr		
				4.02 hr (total running run)		
				81.6 m2 (Area of the box (container))		
		Btu	% energy loss			
Burner energy input		232775				
Solar Radiation energy		71623				
Total energy input		304398				
Fan Energy loss (convection)		104675	34 %			
Wall Energy loss (Conduction)		141405	46 %			
missing Energy		58317	19 %			

Dryer dimentions			
Length	945	cm	
Width	243	cm	
	270	cm	
		cm2	m2
Area of the roof	229635		22.9635
Area of one wall	255150		25.515

Calculate the solar radiation depend on weatherspark data

Average horizontal from 11:22 sunny to 16:45 mostly cloudy	0.63 kW/m2
Average horizontal	0.1 kW/m2
ratio: vertical/horizontal	0.47
Average vertical	0.17 kW/m2

Horizontal, facing south

1.47 kWhr/m2run	Total solar radiation (vertically and horizontaly during June 17)	
33.69 kWhr/run		
14.66 kWhr/run inside	71623 Btu	Total solar energy
50019 Btu	To calculate the total energy input	

Vertical facing south

0.687 kWhr/m2run
17.53 kWhr/run
6.33 kWhr/run inside
21604 Btu

Appendix D: Comparison between Praveen Cabinet and Tuqa Dryer

Praveen Cabinet:

Volume of one blade = $63.5 \text{ cm} \times 15.24 \text{ cm} \times 0.2 \text{ cm}$

Volume of 28 blades = $28 \times 193.55 \text{ cm}^3$

Volume of 28 blades = 5419.34 cm^3

Mass of seaweed = $1 \text{ g/cm}^3 \times 5419.34 \text{ cm}^3$

Mass of seaweed = 5419.34 g

Volume of the cabinet = $76.2 \text{ cm} \times 76.2 \text{ cm} \times 127 \text{ cm}$

Volume of the cabinet = 737417.9 cm^3

Density of the cabinet = $5419.34/737417.9 = 0.0073 \text{ g/cm}^3$

Density of the cabinet = 7.3 kg/m^3

Tuqa Dryer:

Volume of the chamber = $33' \times 8' \times 9' = 2376 \text{ ft}^3 = 67.3 \text{ m}^3$

Mass of wet seaweed = 57.9 kg

Density of the chamber = $57.9/67.3 = 0.86 \text{ kg/m}^3$

From the calculation we can notice that the cabinet has more density than the chamber.

BIOGRAPHY OF THE AUTHOR

Tuqa was born in Basrah, Iraq on March 5, 1986. She was raised in Basrah, Iraq. She attended the University of Basrah and graduated in 2008 with a Bachelor's degree in Materials Science and Engineering. She was accepted in the graduate program for Master's degree of Materials Science and Engineering at the University of Basrah in 2009. In 2010, Tuqa offered a job as an assistant engineer in Basrah Oil Company (formerly South Oil Company). In 2012, Tuqa left the Basrah Oil Company and accompanied her husband who awarded a scholarship to study PhD in Physics at the University of Maine. Tuqa entered the Chemical Engineering graduate program at the University of Maine in the summer of 2018. In 2020, Tuqa awarded the University of Maine Trustee scholarship. In 2021, Tuqa received the third place in Graduate Student Government student innovation commercialization award for research that shows promise to develop into a commercial product or service at the University of Maine. Tuqa is a candidate for the Master of Science degree in Chemical Engineering from the University of Maine in December 2022.